Robust estimation methods of velocity vectors based on a new voting method for rigid motion objects in occluded and brightness changed scenes, and its application to fluid objects

by

Hiroki IMAMURA

submitted to
Japan Advanced Institute of Science and Technology
in partial fulfillment of the requirements
for the degree of
Doctor of Philosophy

Supervisor: Associate Professor Kazunori Kotani

School of Information Science
Japan Advanced Institute of Science and Technology

Abstract

Estimation method of optical flow is an effective method for analysis image sequences. However, there are important problems that have to be solved to precisely estimate optical flow such as occlusion, brightness change and fluid analysis using image sequences.

As purpose of this research, in actual image sequences, I aim at solving these important problems in optical flow estimation. In order to solve the problems, I attempt to use velocity vector constraint equations for estimating velocity vectors, which mean "actual motions of objects", in each problem. In actual image sequence, there is a case that parameters including velocity vectors in the constraint equations are scattered in the parameter space, since differential coefficients of the parameters in the constraint equations are affected by noise and so on. In such the situation, we can not uniquely determine parameters of velocity vectors. In order to estimate the parameters of velocity vectors in such the situation, I use a voting process with a weighting function which is based on an non-liner approach to estimate parameters in the constraint equations. Since each problem has a particular problem, based on the voting method, I solve each problem by using each particular approach such as

·**Occlusion:** In estimating velocity vectors, in order to exclude effectiveness of constraint equations effected by noise and in occlusion regions, I use an method of optical flow estimation via voting process with a weighting function. To separate different motions in regions of different motions, in the voting process, I set a condition to separate constraint equations in different motions. In occlusion regions, there is a limit of precision of optical flow estimation by using the voting process with a weighting function. Thus, I use extrapolation of velocity vectors in occlusion regions from estimated velocity vectors in assigned regions of the occlusion regions.

·**Brightness change:** A velocity vector constraint equation considered brightness change includes three parameters such as velocity vector parameters and temporal change of intensity. In order to estimate the most likelihood parameter in a parameter space, I expand the parameter space to a 3-dimensional parameter space. I then estimate the parameters in the constraint equation by using a voting process with a weighting function in a 3-dimensional voting space.

·**Fluid analysis using image sequences:** In order to deal with the problem of fluid analysis using by image sequences as a problem of estimating of the most likelihood in a parameter space, I derive an optical flow constraint equation considering physical constraints of fluid. The constraint equation includes three parameters such as velocity vector parameters and spatial change of pressure. In order to estimate the most likelihood parameter in a parameter space, expand the parameter space to a 3-dimensional parameter space. I then estimate the parameters in the constraint equation by using a voting process with a weighting function in a 3-dimensional voting space.

In this thesis, I describe the proposed methods for each problem in detail and show its effectiveness.

Acknowledgments

Contents

Chapter 1

Introduction

1.1 Motivation

Based on the computational vision proposed by Marr[1], computation vision algorithms based on 2-dimensional images information such as shape from X (X: shading, texture, contour or motion) have been studied. The field of studies of the computation vision algorithms has been called as "Computer Vision". In recent years, computer vision not only aims at estimating shape information using the technique of shape from X but also aims at composition, estimation or generation of variety information including shape information. As information for composition, estimation or generation of variety information, motion information is one of the most important information in computer vision. Since we can, based on motion information, compose, generate or estimate variety information. For example, there are plenty of applications that compose, estimate or generate the variety information based on motion information such as

· **Image composition[9][10]**
Calculating parameters of a position or a direction in a camera using motion information, this method inserts computer graphics image into image frames based on the calculated parameters.

· **Super resolution[11]∼[14]**
Super resolution is a problem such that solves an inverse problem of estimating x from an observation value y in $y = Hx + b$ (H: linear degradation operator, b: noise). There are many methods to solve the inverse problem. Among them, there is a method based on motion information.

· **Motion compensation[15]∼[19]**
Analyzing motion in a region of an image sequence, a side of transmission transmits the motion information in the region. A side of receiver receives the motion information, and then, assigns the motion information to the region of an image sequence. In a side of receiver, it is possible to reduce quantity of information by this process.

· **Robot control[20]∼[22]**
In the field of robot control, there are methods using motion information estimated by techniques of computer vision to obtain a position and a direction of the robots in actual

environment.

· **Objects tracking[23]∼[26]** For the sake of doubtful parson tracking or observation of the volume of traffic, this method tracks motion objects in an image sequence using motion information.

· **Gesture recognition[27][28]**
Analyzing of parson's motion, this method recognizes gestures of parsons based on the motion information.

· **Facial expression analysis[29]∼[32]**
Extracting of motion on a face in an image sequence, the method analyzes facial expression based on the extracted facial motion.

· **Structure estimation[33]∼[39]**
3-dimensional positions are constrained by motion, inner and outer parameters of a camera. Using this constraint. This method estimates 3-dimensional positions in a situation that inner and outer parameters in a camera are known and motion information has already estimated.

Table 1.1: Motion estimation ability

	Properties	
	Each pixel	Each object
Background subtraction	×	o
Active contour model	×	o
Optical flow estimation	o	o

In order to obtain the motion information by using techniques of computer vision, some methods such as

·Background subtraction [3][4]

·Active contour model [5][6]

·Optical flow estimation [7][8]

have been proposed.

The methods of background subtraction extract motion regions in an image frame by subtraction of temporally continuous frames. If there are motion regions in an image frame, the motion regions are left by subtracting of temporally continuous frames since intensity on a pixel included in motion regions in a previous frame is expected to differ from intensity on the pixel in the next frame (Figure 1.1).

The methods of active contour model extract an interest object in an image frame using an energy function. By trucking of an interest object extracted using by the active contour model, we can obtain motion information of the interest object (Figure 1.2).

The methods of optical flow estimation estimate motion vector on each pixel in an image frame by being based on information of temporal and spatial intensity (Figure 1.3).

2

An object

Frame 1   Frame 2

A subtructed motion region
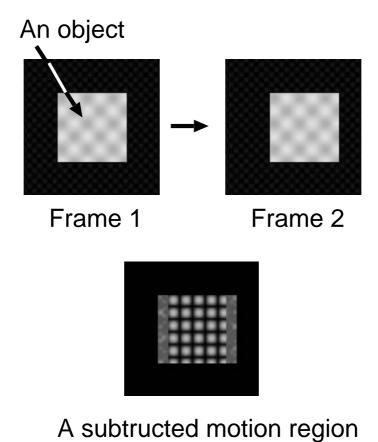
Figure 1.1: An example of background subtraction. The lower figure shows a subtracted region extracted by subtraction the frame1 and the frame2. The subtracted region denotes the motion region between the frame1 and the frame2.

An object   Active contour model

Time 1   Time 2   Time 3
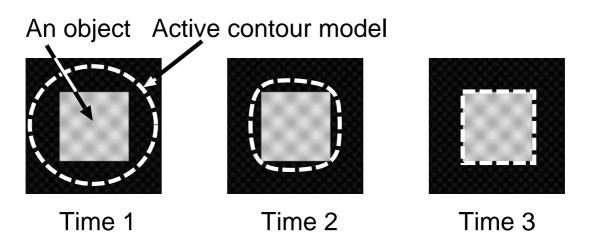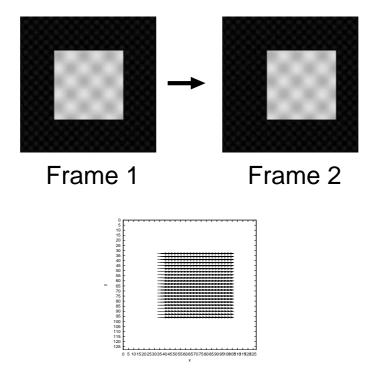
Figure 1.2: An example of active contour model. In figure of time 1, the dot string denotes initial position of the active contour model. As time goes by, the active contour model converges at the object in the image.

Figure 1.3: An example of optical flow estimation. Based on information of spatial and temporal intensity in a frame 1 and a frame 2, optical flow estimation estimates motion vectors in each pixel.

The methods for obtaining of the motion information have each ability. Table 1.1 shows the ability of motion estimation in each method.

The methods except optical flow estimation estimate global motion information on each object in an image sequence. Thus, the methods except optical flow estimation can not obtain local motion information on each pixel in an image sequence. On the contrary, estimation methods of optical flow estimate motion vectors in each pixel based on the following property of image sequences with respect to intensity.

· Temporal-spatial correlation of intensity in an image sequence is high

For instance, spatial autocorrelation coefficients of general image frames is about 0.9. From the property, it is expected that following conditions are held.

· Intensities in corresponding points between frames are equivalent

· Temporal and spatial changes of intensity are smooth

These conditions are called as optical flow realizable conditions. If the optical flow realizable conditions are held, motion vectors in a pixel satisfying the conditions are constrained by temporal-spatial differential coefficients of intensity. The constraint can be expressed by an optical flow constraint equation[7] such as

$$I_x u + I_y v + I_t = 0, \qquad (1.1)$$

4

where I_x and I_y respectively denote spatial differential coefficients of intensity for x axis and y axis in image space, I_t denotes a temporal differential coefficient of intensity, u and v denote components of a motion vector in a pixel. Since I_x, I_y and I_t can be determined from image sequences, we can estimate motion vectors by solving the optical flow equation with respect to u and v. In order to estimate motion vectors using the optical flow constraint equation, we consider the following property of image sequences with respect to motions.

· Motions in a local region of an image sequence are approximately equivalent

Based on the property, we assume that the following assumption holds.

· Motion vectors in a local region of an image sequence are equivalent

Based on the assumption, estimation methods of optical flow estimate motion vectors in each pixel by least mean square using the constraint equations in a local region of an image sequence. Since the estimation methods of optical flow estimate motion vectors in each pixel, estimation methods of optical flow can estimate local motion information on each pixel in an image sequence. By using segmentation based on motion vectors extracted by optical flow estimation, we can expect to estimate global motion information on each object. Thus, estimation methods of optical flow have high flexibility in motion analysis. Therefore, estimation methods of optical flow have been mainly used in motion analysis of image sequences.

Optical flow estimation methods have effectiveness for motion analysis such as being able to flexibly estimate motion information. However, there are problems in optical flow estimation [2] such as

· Occlusion

· Brightness change

· Fluid analysis by using image sequences

· Determination of camera parameters

· Aperture problem etc.

Among them, since occlusion and brightness change often occur in image sequences and fluid analysis by using image sequence are needed in field of fluid measurement, it is important to solve occlusion, brightness change problems and the fluid analysis problem by using image sequences. Thus, I focus on the following important problems.

· Occlusion

· Brightness change

· Fluid analysis by using image sequences

The cause of occurring these problems is not to satisfy the optical flow realizable conditions to estimate "appearance motions". If the realizable conditions are not held or insufficient, precision of optical flow estimation decreases. Following two cases do not satisfy the realizable conditions.

·Occlusion

Occlusion regions
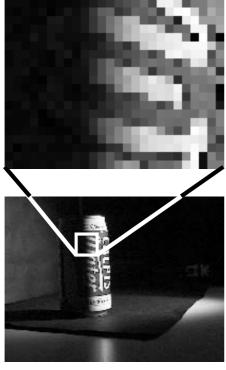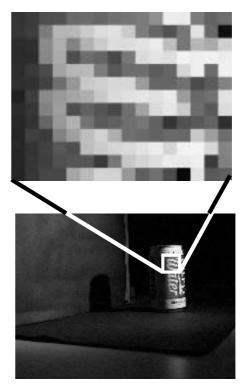
Frame1   Frame2

Figure 1.4: An example of occlusion. The car in left side moves to right side, the car in right side moves to left side. Occlusion occurs inside the ellipse regions.

Frame1   Frame2

Figure 1.5: An example of brightness change. A can moves to the depth right under a point light source (lower, Frame1, Frame2), intensity in a region on the can is changed by changing of shading (upper, expanded figures).

Frame1   Frame2

Figure 1.6: An example of incompressible viscous fluid. The figures show flow of incompressible viscous fluid behind a cylinder in the frame 1 and the frame 2.

Occlusion occurs when an object moves on another object, or an object moves on a background. In this case, the optical flow realizable conditions are not satisfied by appearance and disappearance of corresponding points between frames, therefore, optical flow is not estimated precisely (Figure 1.4).

·**Brightness change**

Brightness change occurs when intensity of a light source changes temporally or shading change on an object occurs by motion of the object under a point light source. In this case, the optical flow realizable conditions are not satisfied by difference of intensity in corresponding points between frames (Figure 1.5)

Even though in case of satisfying the optical flow realizable conditions, there is a case that precision of optical flow estimation decreases such as

·**Fluid analysis by using image sequences**

In case of analysis of fluid objects by using image sequences, optical flow realizable conditions are insufficient to estimate optical flow. To precisely estimate optical flow, we have to consider physical constraint conditions to precisely estimate velocity vectors in the analysis of fluid object by using image sequences (Figure 1.6).

1.2　Purpose of this research and approaches

As purpose of this research, I aim at solving the following important problems

·Occlusion

·Brightness change

·Fluid analysis by using image sequences

in actual image sequences, since the applications using optical flow information aim at applying to actual image sequences.

I consider that the essence of these problems is to estimate optical flow as "appearance motions" which mean motion vectors in case of assuming that optical flow realizable conditions hold, I attempt to solve the problems using velocity vector constraint equations that can be applied to estimation of velocity vectors[52][54] which mean "actual motions of objects". In each pixel in an image frame, I assume that constraint equations which can be applied to estimate velocity vectors of objects in each problem could be formularized as

$$a_1 u + a_2 v + a_3 = 0, \tag{1.2}$$

where u and v denote components of a velocity vector for x-axis and y-axis in image space respectively, a_1 and a_2 denote coefficients of u and v, a_3 denotes a constant term. We can obtain the constraint equation (1.2) in each pixel. However, in each pixel, we cannot determine the parameters u and v since the constraint equation includes plural parameters. To determine the parameters, I set an assumption such as

Assumption: Parameters of constraint equations in an interest pixel and its neighboring pixels are equivalent.

If this assumption holds, we can uniquely determine the parameters by solving si-

Parameter space u-v
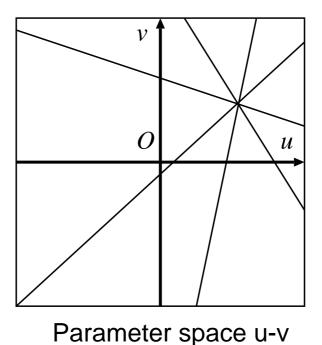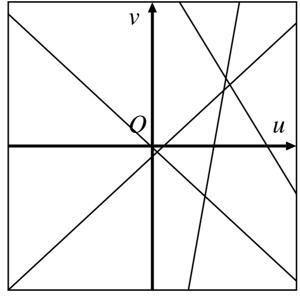
Figure 1.7: An intersection of constraint equation in parameter space u-v.

multaneous equation of the constraint equations in an interest pixel and its neighboring pixels. This means intersections of constraint equation converge into a point in parameter space u-v (Figure 1.7). However, If the assumption is not held, intersections of the constraint equations are scattered in the parameter space u-v. In this situation, we can not determine the parameters uniquely. Since the constraint equation includes differential coefficients, the constraint equation effected in the regions where realizable conditions of

Parameter space u-v

Figure 1.8: Scattered intersections of constraint equation in parameter space u-v.

the constraint equation are not held or where noise is added. Therefore in the regions, intersections of the constraint equations are further scattered in the parameter space u-v (Figure 1.8).

In this situation, we need a method that can estimate the most likelihood parameter from the scattered intersections in the parameter space.

There are some methods based on a concept of integral approach to estimate the most likelihood parameter from the scattered intersections in the parameter space. These are called "Robust estimation". As robust estimation methods, following methods have been proposed.

· M-estimation [64]

· LMedS estimation [65]

· Voting process with a weighting function [66]

Among them, the voting process with a weighting function has been corroborated its effectiveness in studies of hough transformation[40]~[43], and it has effective properties such as

· It can estimate the optimum parameter excluding local minimum

· It can reduce calculation times keeping a property of estimating the most likelihood parameter

I adopt a voting process with a weighting function method that has the effective properties to estimate the most likelihood parameter from the scattered intersections in the parameter space.

Since each problem has a peculiar problem, I attempt to solve the peculiar problem by following different approaches.

9

·Occlusion

In estimating velocity vectors, in order to exclude effectiveness of constraint equations effected by noise and in occlusion regions, I use a method of velocity vector estimation via voting process with a weighting function. To separate different motions in regions of different motions, in the voting process, I set a condition to separate constraint equations in different motions. In occlusion regions, there is a limit of precision of velocity vectors estimation by using the voting process with a weighting function. Thus, I use extrapolation of velocity vectors in occlusion regions from estimated optical flow in assigned regions of the occlusion regions.

·Brightness change

An velocity vector constraint equation considered brightness change includes three parameters such as velocity vector parameters and temporal change of intensity. In order to estimate the most likelihood parameter in the parameter space, I expand the parameter space to a 3-dimensional parameter space. I then estimate the parameters in the constraint equation by using a voting process with a weighting function in a 3-dimensional voting space.

·Fluid analysis by using image sequences

In order to deal with the problem of fluid analysis using by image sequences as a problem of estimating of the most likelihood in a parameter space, I derive an velocity vector constraint equation considering physical constraints of fluid. The constraint equation includes three parameters such as velocity vector parameters and spatial change of pressure. In order to estimate the most likelihood parameter in a parameter space, I expand the parameter space to a 3-dimensional parameter space. I then estimate the parameters in the constraint equation by using a voting process with a weighting function in a 3-dimensional voting space.

1.3 Overview of this thesis

This thesis consists of 6 chapters. The following terms present outlines of each chapter.

Chapter 2: The basic theory of optical flow estimation

This chapter presents the basic theory of optical flow estimation such as concepts of optical flow estimation and methods of estimating optical flow based on the concepts.

Chapter 3: A new method of optical flow estimation for occlusion

This chapter presents a new method of velocity vector estimation for occlusion and shows the results of experiments for evaluation of velocity vector estimation precision in conventional methods and a new proposed method.

Chapter 4: A new method of optical flow estimation for brightness change

This chapter presents a new method of velocity vector estimation for brightness change and shows the results of experiments for evaluation of velocity vector estimation precision in conventional methods and a new proposed method.

Chapter 5: A new method of optical flow estimation for incompressible viscous fluid

This chapter presents a new method of velocity vector estimation for fluid analysis and shows the results of experiments for evaluation of velocity vector estimation precision in conventional methods and a new proposed method.

Chapter 6: Conclusions

This chapter presents conclusion and future works.

Chapter 2

The basic theory of optical flow estimation

Optical flow has been mainly used in motion analysis of image sequences since optical flow estimation has high flexibility in motion analysis. Methods of optical flow estimation estimate optical flow vectors as "appearance motion". In order to estimate actual motion vectors of objects in occlusion, brighness change or fluid analysis using image sequences, we have to improve the methods of optical flow estimation. In advance of showing estimation methods of motion vectors in occlusoin, brightness change or fluid analysis using image sequences, this section presents the basic theory of the optical flow estimation.

Methods of optical flow estimation are broadly classified into

- · Block matching methods

- · Gradient methods

The following sections present block matching methods and gradient methods respectively.

2.1 Block matching methods

Block matching methods[44][45] estimate optical flow based on similarity of regions between a previous image frame and a next frame image. The following evaluation functions are mainly used to estimate optical flow in block matching methods.

2.1.1 SAD evaluation function

A block matching method using the following evaluation function is called as sum of absolute differences (SAD).

$$B_{SAD}(u, v) = \sum_{x_w, y_w \in W} |I(x, y, t) - I(x + u + x_w, y + v + y_w, t + dt)|, \qquad (2.1)$$

where u and v are components of optical flow on coordinates x and y in image space, $B_{SAD}(u, v)$ is an evaluation function of sum of absolute differences with respect to u and v, W is a matching region for estimating u and v. $I(x, y, t)$ is intensity on a pixel (x, y) at time t, $I(x + u + x_w, y + v + y_w, t + dt)$ is intensity on a pixel $(x + u + x_w, y + v + y_w)$ at time $t + dt$. The block matching method using the SAD evaluation function estimates u and v

getting the maximum evaluation value in the SAD evaluation function to be optical flow components.

2.1.2 SSD evaluation function

A block matching method using the following evaluation function is called as sum of squared differences (SSD).

$$B_{SSD}(u,v) = \sum_{x_w,y_w \in W} \{I(x,y,t) - I(x+u+x_w, y+v+y_w, t+dt)\}^2, \qquad (2.2)$$

where $B_{SSD}(u,v)$ is an evaluation function of sum of squared differences with respect to u and v. The block matching method using the SSD evaluation function estimates u and v getting the maximum evaluation value in the SSD evaluation function to be optical flow components.

2.1.3 CC evaluation function

A block matching method using the following function is called as cross correlation (CC).

$$B_{CC} = \sum_{u,v \in W} (I(x,y,t) \times I(x+u+x_w, y+v+y_w, t+dt)), \qquad (2.3)$$

where $B_{CC}(u,v)$ is an evaluation function of cross correlation with respect to u and v. The block matching method using the CC evaluation function estimates u and v getting the maximum evaluation value in the CC evaluation function to be optical flow components.

2.2 Gradient methods

Gradient methods[7][8] estimate optical flow based on an optical flow constraint equation that constraints optical flow with respect to temporal and spatial gradient of intensity on an image sequence. The following sections present the optical flow constraint equation and general methods to solve the optical flow constraint equation.

2.2.1 Optical flow constraint equation

Let $I(x,y,t)$ be the intensity at time t at the image point (x,y). Then, if $u(x,y)$ and $v(x,y)$ are the x and y components of the optical flow vector at that point, we expect that the intensity will be the same at time t+dt at the point $(x+\delta x, y+\delta y)$, where $\delta x = u\delta t$ and $\delta y = v\delta t$. That is,

$$I(x+u\delta t, y+v\delta t, t+\delta t) = I(x,y,t) \qquad (2.4)$$

for a small time interval dt. This single constraint is not sufficient to determine both u and v uniquely. It is also clear that we can take advantage of the fact that the motion field is continuous almost everywhere. If brightness varies smoothly with x, y and t, we can expand the left-hand side of the equation above in a Taylor series and so obtain

$$I(x, y, t) + dx\frac{\partial I}{\partial x} + dy\frac{\partial I}{\partial y} + dt\frac{\partial I}{\partial t} + e = I(x, y, t). \tag{2.5}$$

Where e contains second- and higher-order terms in dx, dy and dt. Canceling $I(x, y, t)$, dividing through by dt and taking the limit as $dt{\to}0$, we obtain

$$\frac{\partial I}{\partial x}\frac{dx}{dt} + \frac{\partial I}{\partial y}\frac{dy}{dt} + \frac{\partial I}{\partial t} = 0, \tag{2.6}$$

which is actually just the expansion of the equation

$$\frac{dI}{dt} = 0 \tag{2.7}$$

in the total derivative of I with respect to time. Using the abbreviations $u = \frac{dx}{dt}$, $v = \frac{dy}{dt}$, $I_x = \frac{\partial I}{\partial x}$, $I_y = \frac{\partial I}{\partial y}$, $I_t = \frac{\partial I}{\partial t}$, we obtain

$$I_x u + I_y v + I_t = 0. \tag{2.8}$$

The derivatives I_x, I_y and I_t are estimated from the image. The above equation is called the optical flow constraint equation [7], since it expresses a constraint on the components u and v of the optical flow. Consider a two-dimensional space with axes u and v, which we shall call velocity space (figure 3). Values of (u, v) satisfying the constraint equation lie on a straight line in velocity space. All that a local measurement can do is to identify this constraint line. We can rewrite the constraint equation in the form

$$(I_x, I_y){\cdot}(u, v) = -I_t. \tag{2.9}$$

The component of optical flow in the direction of the brightness gradient $(I_x, I_y)^T$ is thus

$$\frac{I_t}{\sqrt{I_x^2 + I_y^2}}. \tag{2.10}$$

We cannot, however, determine the component of the optical flow at right angles to this direction, that is, along the isobrightness contour. This ambiguity is also known as the aperture problem.

2.2.2 General methods to solve the optical flow constraint equation

There are mainly two methods to solve the optical flow constraint equation [46] such as

· Global method [7]

· Local method [8]

the next section present details about each method.

14

Global method

Horn and Schunck [7] proposed the method using the following an evaluation functions for determination of u and v in equation 2.8. First, they defined an evaluation function e_s for evaluation of smoothness in u and v with respect to x and y,

$$e_s = \int \int ((u_x^2 + u_y^2) + (v_x^2 + v_y^2))dxdy \tag{2.11}$$

where u_x, u_y, v_x and v_y mean $\partial u/\partial x$, $\partial u/\partial y$, $\partial v/\partial x$ and $\partial v/\partial y$ respectively. Second, They defined an evaluation function e_c for evaluation of satisfaction of equation 2.8 with respect to x and y,

$$e_c = \int \int (I_x u + I_y v + I_t)^2 dxdy, \tag{2.12}$$

Finally, They estimated u and v by minimizing the evaluation function,

$$e_a = e_s + \lambda e_c, \tag{2.13}$$

where λ is a parameter that weights the error in the image motion equation relative to the departure from smoothness. This parameter will be large if brightness measurements are accurate and small if they are noisy. Minimizing an integral of the form

$$\int \int F(u, v, u_x, u_y, v_x, v_y) dxdy \tag{2.14}$$

is a problem in the calculus of variations. The corresponding Euler equations are

$$F_u - \frac{\partial}{\partial x} F_{u_x} - \frac{\partial}{\partial y} F_{u_y} = 0, \tag{2.15}$$

$$F_v - \frac{\partial}{\partial x} F_{v_x} - \frac{\partial}{\partial y} F_{v_y} = 0. \tag{2.16}$$

In this case,
$$F = (u_x^2 + u_y^2) + (v_x^2 + v_y^2) + \lambda(I_x u + I_y v + I_t)^2, \tag{2.17}$$

so the Euler equation yield

$$\nabla^2 u = \lambda(I_x u + I_y v + I_t)I_x, \tag{2.18}$$

$$\nabla^2 v = \lambda(I_x u + I_y v + I_t)I_y, \tag{2.19}$$

where

$$\nabla^2 = \frac{\partial^2}{\partial x^2} + \frac{\partial^2}{\partial y^2} \tag{2.20}$$

is the Laplacian operator. This coupled pair of elliptic second-order partial differential equations can be solved using iterative methods.

Local method

Lucas and Kanade [8] use a local constant model for u and v which is solved as a weighted least-squares solution to equation 2.8. Velocity estimates are computed by minimizing

$$\sum_{x,y\in\Omega} W(x,y)^2(\nabla I(x,y,t){\cdot}(u,v) + I_t(x,y,t))^2, \tag{2.21}$$

where W(x) denotes a window function and R is a spatial neighborhood, Ω denotes a support region for estimating u and v. The solution of the equation 2.21 represented as

$$\boldsymbol{A}^T\boldsymbol{W}^2\boldsymbol{A}\boldsymbol{v} = \boldsymbol{A}^T\boldsymbol{W}^2\boldsymbol{b}, \tag{2.22}$$

where

$$\boldsymbol{A} = [\nabla I(x_1, y_1, t), \cdots, \nabla I(x_n, y_n, t)]^T, \tag{2.23}$$

$$\boldsymbol{W} = diag[W(x_1, y_1, t), \cdots, W(x_n, y_n, t)], \tag{2.24}$$

$$\boldsymbol{b} = -(I_t(x_1, y_1, t), \cdots, I_t(x_n, y_n, t))^T, \tag{2.25}$$

with respect to points $(x_i, y_i, t){\in}\Omega$ $(i = 1, \cdots, n)$. In case of $\boldsymbol{A}^T\boldsymbol{W}^2\boldsymbol{A}$ has regularity, we can obtain

$$\boldsymbol{v} = [\boldsymbol{A}^T\boldsymbol{W}^2\boldsymbol{A}]^{-1}\boldsymbol{A}^T\boldsymbol{W}^2\boldsymbol{b}. \tag{2.26}$$

This method decides $\boldsymbol{v}$ as estimated optical flow in the Ω.

Chapter 3

A new method of velocity vector estimation for solving the occlusion problem

3.1   Introduction

When an object moves in front of a background or another object, occluded or appearance regions occur. These regions are called occlusion regions. In occlusion regions and its neighboring regions, There are optical flow constraint equations that do not satisfy optical flow realizable conditions by appearance/disappearance of intensity and constraint equations in regions of different motions and, in case of actual image sequences, constraint equations effected by noise. Conventional optical flow estimation methods [7][8] estimate velocity vectors including such constraint equations effected by noise, constraint equations in occlusion region and constraint equations in regions of different motions. Thus, velocity vectors are not precisely estimated in case of occurring occlusion in actual image sequences. In estimating velocity vectors, in order to exclude effectiveness of constraint equations effected by noise and in occlusion regions, I use an method of velocity vector estimation via voting process with a weighting function. To separate different motions in regions of different motions, in the voting process, I set a condition to separate constraint equations in different motions. In occlusion regions, there is a limit of precision of velocity vector estimation in the method of velocity vector estimation via voting process with a weighting function. For estimating velocity vectors in occlusion regions, I use extrapolation from estimated velocity vectors in assigned regions of occlusion regions.

In an object tracking system such as observation system of invasion for plural objects, we have to separate each object to track each object in case of overlapping each object. Therefore, we can expect to apply the proposed method to the object tracking system for plural objects. In a human gesture recognition system to help communication with each other person through computers, we have to separate each part of body to recognize meaning of gesture in case of overlapping each part of body. Thus, we can expect to apply the proposed method to the human gesture recognition system.

3.2　An approach for solving the occlusion problem

3.2.1　Velocity vector estimation via a voting process with a weighting function

In occlusion regions and its neighboring regions, conventional methods [7][8] estimate optical flow including constraint equations that do not satisfy optical flow realizable conditions by appearance/disappearance of intensity and constraint equations in regions of different motions and, in case of actual image sequences, constraint equations effected by noise. Thus, in whole pixels in case of global method [7], in a region where includes those constraint equations in case of local method [8], velocity vectors in not sufficiently estimated because estimated velocity vectors using the conventional methods include effectiveness of those constraint equations.

In estimating velocity vectors, in order to exclude the constraint equations that do not satisfy optical flow realizable conditions by appearance/disappearance of intensity and constraint equations effected by noise, I use a method of velocity vector estimation via voting process with a weighting function. To separate different motions in regions of different motions, in the voting process, I set a condition to separate constraint equations in different motions. We can expect to precisely estimate velocity vectors in case of occurring occlusion in actual image sequences. However, there is a limit of velocity vector estimation precision in occlusion regions in the method of velocity vector estimation via voting process with a weighting function.

3.2.2　A limit of velocity vector estimation precision in occlusion regions in the method via the voting process

If an object in an image sequence is a rigid object, a motion of the object is described as isotropic motion. In a region of the rigid object in an image sequence, a velocity vector holds the following theorem [66].

Theorem *A velocity vector (u, v) in a region holds the following inequality*

$$u_{min} \leq u \leq u_{max}, \tag{3.1}$$

$$v_{min} \leq v \leq v_{max}, \tag{3.2}$$

where u_{min} and v_{min} denote the minimum values of velocity vector components in a region respectively, u_{max} and v_{max} denote the maximum values of velocity vector components in a region respectively. Equation (3.1) and (3.2) denote range of velocity vectors can be estimated in a region (Figure 3.1).

Let us consider the situation shown in Figure 3.2. In case of estimating velocity vectors in a occlusion region using constraint equations in a region except a occlusion region, velocity vectors in a occlusion region must be estimated within the range of velocity vectors in a region except a occlusion region. However, velocity vectors in occlusion regions gets over the range of velocity vectors in a region except a occlusion region since a isotropic motion is a spatial monotone increasing or decreasing (Figure 3.3).

Since the method via voting process with a weighting function excludes constraint equations in occlusion regions, the method estimates velocity vectors in occlusion regions

Range of velocity vectors
can be estimated in the region

Velocity vectors in a region   Parameter space
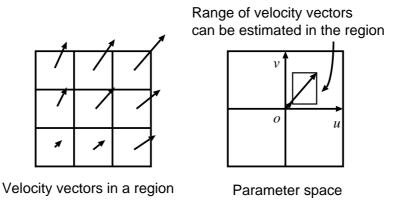
Figure 3.1: Velocity vectors in a region and its range of velocity vectors in parameter space.

Occlusoin regions

Velocity vectors in a region
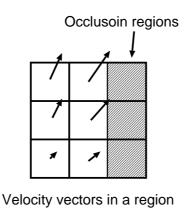
Figure 3.2: Estimating of velocity vectors in occlusion regions using velocity vectors in regions except occlusion regions.

Range of velocity vectors
can be estimated in the region

An actual velocity vector
in an occlusion region

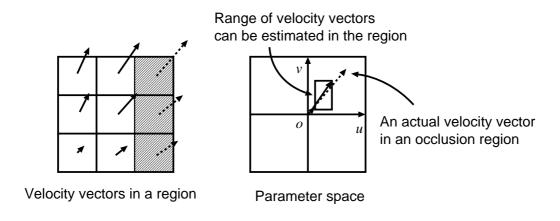Velocity vectors in a region   Parameter space

Figure 3.3: Getting over of a velocity vector in an occlusion region from the range of a velocity vector in a region except a occlusion region.

using constraint equations in neighboring regions of occlusion regions. Thus, in case of the situation such as shown in Figure 3.2, we can not sufficiently estimate velocity vectors in a occlusion region.

3.2.3 Velocity vector estimation in occlusion regions using extrapolation

We can not sufficiently estimate velocity vectors in occlusion regions using only the method of velocity vector estimation via a voting process with a weighting function (Figure 3.4). In regions except occlusion regions, we can expect to precisely estimate velocity vectors by using the voting process with a weighting function. Therefore, I estimate velocity vectors in occlusion regions using extrapolation from estimated velocity vectors in assigned regions of occlusion regions (Figure 3.5). For the extrapolation, I execute the following process.

1. Extraction of occluded/appearance regions

2. Decision of assigned regions of occluded/appearance regions

3. Extrapolation of velocity vectors in occluded/appearance regions from estimated velocity vectors in its assigned regions

To realize the extrapolation process, we need a method of velocity vector estimation that can precisely estimate velocity vectors in whole pixels. Using the method of velocity vector estimation via a voting process with a weighting function, we can expect to precisely estimate velocity vectors in regions except occlusion regions. Assuming that precision of velocity vectors in occlusion regions estimated by the voting process with a weighting function is sufficient to be able to be used to the extrapolation process, in estimation of velocity vectors in occlusion regions, I use the method of velocity vector estimation via a voting process with a weighting function for the extrapolation process.

3.3 Estimation of velocity vectors for occlusion using extrapolation

For the extrapolation process, I execute the following process.

1. Extraction of occluded/appearance regions

2. Decision of assigned regions of occluded/appearance regions

3. Extrapolation of velocity vectors in occluded/appearance regions from estimated velocity vectors in its assigned regions

To realize the extrapolation process, I execute the following process consists of 5 steps. (Figure 3.6).

Step 1. Estimation of velocity vectors

Step 2. Segmentation based on motion continuity

Step 3. Extraction of occluded and appearance regions

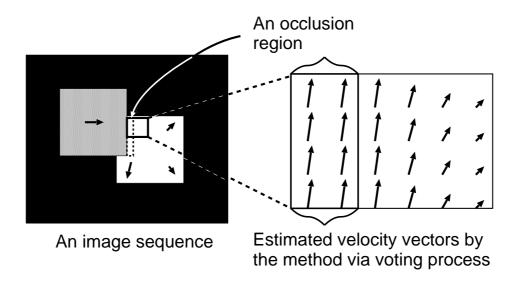Step 4. Decision of assigned regions of occluded and appearance regions

Figure 3.4: Velocity vectors estimated by the method via voting process.
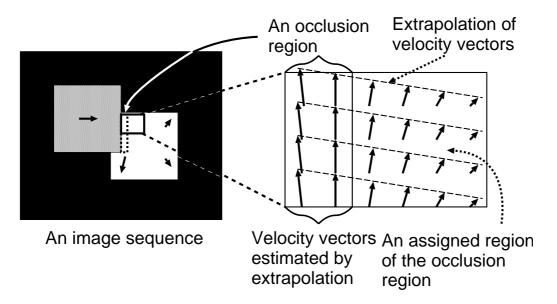

Figure 3.5: Velocity vectors estimated by extrapolation from estimated velocity vectors in assigned regions of the occlusion regions.
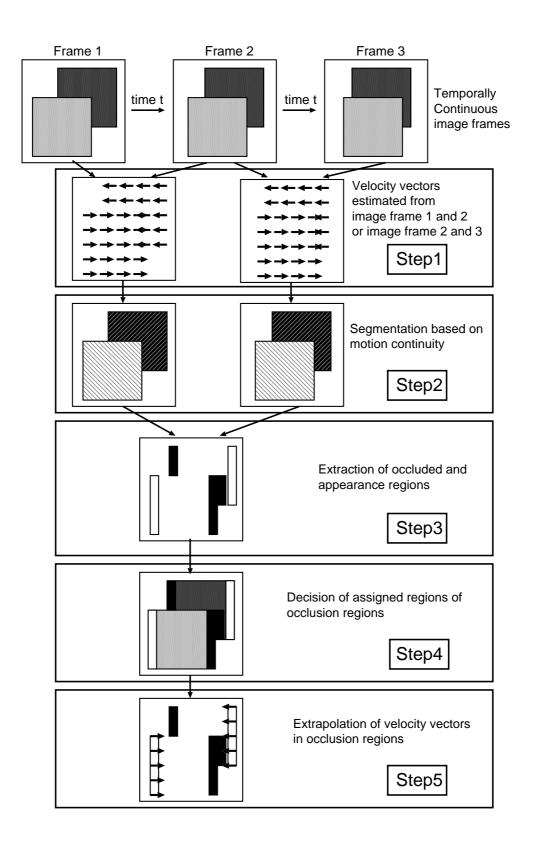
Figure 3.6: The process of extrapolation for estimating velocity vectors in occluded/appearance regions.
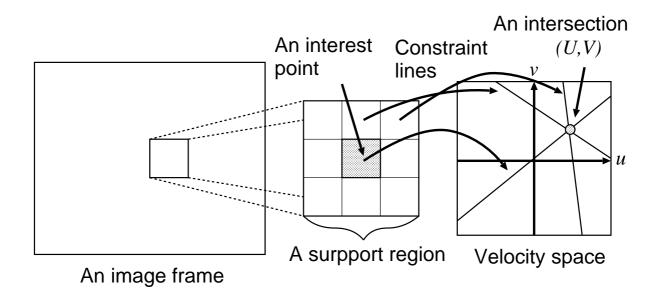
Figure 3.7: A support region and constraint lines in velocity space.

Step 5. Extrapolation of velocity vectors in occlusion regions
The 5 steps are minutely presented in following section.

3.3.1 Estimation of velocity vectors (Step1)

Using the method via voting process with a weighting function, this step estimates velocity vectors in whole pixels. This step estimates velocity vectors in the 1st frame and the 2nd frame or the 2nd frame and 3rd frame for letter steps.

A method of velocity vector estimation via voting process with a weighting function

Let intensity on a pixel (x, y) at time t in an image sequence be $I(x, y, t)$. An intensity constraint of velocity vectors with respect to velocity vector components u and v for x axis and y axis is represented as [7]

$$I_x u + I_y v + I_t = 0, \tag{3.3}$$

where I_x, I_y and I_t denote partial differential coefficients of $I(x, y, t)$ with respect to x, y and t respectively. Equation (3.3) represents a line in parameter space u and v called velocity space. We call the line "a constraint line". Since the constraint line contains two parameters u and v, we cannot determine the parameter u and v of a constraint line on a pixel. To determine the parameters u and v in a constraint line, we assume that velocity vector components u and v on an interest pixel are equivalent to u and v on neighboring pixels of the interest pixel in a support region. If the assumption is satisfied, in a support region, constraint lines on a interest pixel and the neighboring pixels have equivalent values of U and V as values of u and v, intersections of constraint lines on a interest pixel and the neighboring pixels converge into a coordinate (U, V) in parameter space u and v. In this case, we can determine the coordinate (U, V) as estimated parameters of u and v on the interest pixel (Figure 3.7).

However, In case of following situations, the constraint lines have different intersections from U and V.

(A) Fluctuation of intersections of constraint equation by influence of motions

I consider in isotropic motion. Isotropic motions in a point on the coordinate (x, y) is expressed as

$$\begin{pmatrix} x' \\ y' \end{pmatrix} = \boldsymbol{AB} \begin{pmatrix} x \\ y \end{pmatrix} + \begin{pmatrix} \alpha \\ \beta \end{pmatrix}, \tag{3.4}$$

where

$$\boldsymbol{A} = \begin{pmatrix} a & 0 \\ 0 & b \end{pmatrix}, \boldsymbol{B} = \begin{pmatrix} \cos\theta & -\sin\theta \\ \sin\theta & \cos\theta \end{pmatrix},$$

x' and y' are values after moving of x and y respectively, a and b are parameters of a rate of expansion/contraction respectively, θ is an angle of rotation, α and β are parameters of translation along x-axis and y-axis respectively. I express parameters of a velocity vector as

$$\begin{pmatrix} u \\ v \end{pmatrix} = \begin{pmatrix} x' \\ y' \end{pmatrix} - \begin{pmatrix} x \\ y \end{pmatrix}. \tag{3.5}$$

Then equation (3.5) is expressed as

$$\begin{pmatrix} u \\ v \end{pmatrix} = \boldsymbol{AB} \begin{pmatrix} x \\ y \end{pmatrix} + \begin{pmatrix} \alpha \\ \beta \end{pmatrix} - \begin{pmatrix} x \\ y \end{pmatrix}. \tag{3.6}$$

Similarly, isotropic motions of a point on a coordinate $(x + \Delta x, y + \Delta y)$ is expressed as

$$\begin{pmatrix} u' \\ v' \end{pmatrix} = \boldsymbol{AB} \begin{pmatrix} x + \Delta x \\ y + \Delta y \end{pmatrix} + \begin{pmatrix} \alpha \\ \beta \end{pmatrix} - \begin{pmatrix} x + \Delta x \\ y + \Delta y \end{pmatrix}, \tag{3.7}$$

where u',v' are parameters of a velocity vector on the coordinate $(x + \Delta x, y + \Delta y)$. From (3.6) and (3.7), we define spatial changes of velocity vectors as

$$\begin{pmatrix} \Delta u \\ \Delta v \end{pmatrix} = \begin{pmatrix} u' \\ v' \end{pmatrix} - \begin{pmatrix} u \\ v \end{pmatrix}. \tag{3.8}$$

From (3.6) and (3.7), equation (3.8) is expressed as

$$\begin{pmatrix} \Delta u \\ \Delta v \end{pmatrix} = \boldsymbol{AB} \begin{pmatrix} x + \Delta x \\ y + \Delta y \end{pmatrix} + \begin{pmatrix} \alpha \\ \beta \end{pmatrix} - \begin{pmatrix} x + \Delta x \\ y + \Delta y \end{pmatrix} - \left\{ \boldsymbol{AB} \begin{pmatrix} x \\ y \end{pmatrix} + \begin{pmatrix} \alpha \\ \beta \end{pmatrix} - \begin{pmatrix} x \\ y \end{pmatrix} \right\}. \tag{3.9}$$

Moreover, equation (3.9) is expressed as

$$\begin{pmatrix} \Delta u \\ \Delta v \end{pmatrix} = \{\boldsymbol{AB} - \boldsymbol{E}\} \left\{ \begin{pmatrix} x + \Delta x \\ y + \Delta y \end{pmatrix} - \begin{pmatrix} x \\ y \end{pmatrix} \right\} \tag{3.10}$$

$$= \{\boldsymbol{AB} - \boldsymbol{E}\} \begin{pmatrix} \Delta x \\ \Delta y \end{pmatrix} \tag{3.11}$$

where

$$E = \begin{pmatrix} 1 & 0 \\ 0 & 1 \end{pmatrix}. \tag{3.12}$$

From (3.11), in translation, a value of each Δu or Δv is zero. The meaning is that spatial change of velocity vectors is nothing. On the other hand, in motions except translation, intersections are scattered in velocity space because a value of each Δu or Δv is not zero. Moreover, a value of each Δu or Δv depends on a value of each Δx or Δy. Therefore, in the motions except translation, the more a value of each Δx or Δy gets enough large, the more fluctuation of intersection in velocity space gets large.

(B) Fluctuation of intersections of constraint equation by influence of intersections of constraint equations in occlusion regions or constraint equations effected by noise

I consider two constraint equations (3.3) that satisfy optical flow realizable conditions in a support region. The equations are expressed by

$$I_x^{(1)} u + I_y^{(1)} v + I_t^{(1)} = 0, \tag{3.13}$$

$$I_x^{(2)} u + I_y^{(2)} v + I_t^{(2)} = 0, \tag{3.14}$$

where $I_x^{(1)}$, $I_y^{(1)}$ or $I_t^{(1)}$ denote partial differential coefficients of $I(x, y, t)$ with respect to x, y and t on a pixel in a support region respectively, $I_x^{(2)}$, $I_y^{(2)}$ or $I_t^{(2)}$ denote partial differential coefficients of $I(x, y, t)$ with respect to x, y and t on another pixel in a support region respectively. An intersection $(u, v)^\top$ of these constraint equations is expressed as

$$\begin{pmatrix} u \\ v \end{pmatrix} = \begin{pmatrix} \frac{I_y^{(1)} I_t^{(2)} - I_t^{(1)} I_y^{(2)}}{I_x^{(1)} I_y^{(2)} - I_x^{(2)} I_y^{(1)}} \\ \frac{I_x^{(1)} I_t^{(2)} - I_t^{(1)} I_x^{(2)}}{I_x^{(2)} I_y^{(1)} - I_x^{(1)} I_y^{(2)}} \end{pmatrix}. \tag{3.15}$$

If the equation (3.13) is a constraint equation that does not satisfy optical flow realizable conditions by factors such that spatial/temporal intensity change is intense by occlusion or a constraint equations effected by noise, the spatial/temporal gradients in the image are changed intensely. Thus, (3.13) is replaced by

$$I_x^{(1)'} u + I_y^{(1)'} v + I_t^{(1)'} = 0, \tag{3.16}$$

where $I_x^{(1)'}$, $I_y^{(1)'}$ or $I_t^{(1)'}$ are coefficients of equation (3.13) in case of not satisfying optical flow realizable conditions respectively. Therefore the intersection $(u, v)^\top$ of the constraint equations is changed to

$$\begin{pmatrix} u' \\ v' \end{pmatrix} = \begin{pmatrix} \frac{I_y^{(1)'} I_t^{(2)} - I_t^{(1)'} I_y^{(2)}}{I_x^{(1)'} I_y^{(2)} - I_x^{(2)} I_y^{(1)'}} \\ \frac{I_x^{(1)'} I_t^{(2)} - I_t^{(1)'} I_x^{(2)}}{I_x^{(2)} I_y^{(1')} - I_x^{(1)'} I_y^{(2)}} \end{pmatrix}. \tag{3.17}$$

Then, I define a difference vector $(\Delta u, \Delta v)^\top$ as

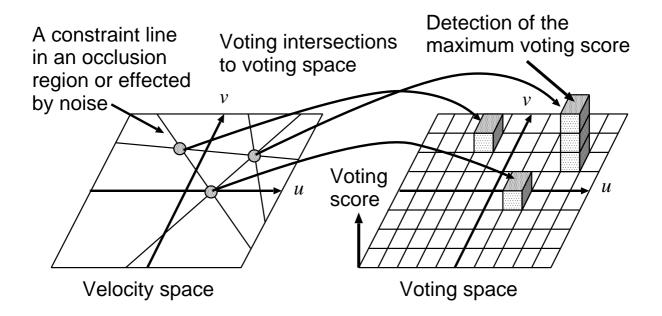$$\begin{pmatrix} \Delta u \\ \Delta v \end{pmatrix} = \begin{pmatrix} u - u' \\ v - v' \end{pmatrix}. \tag{3.18}$$

Figure 3.8: Voting of intersections to voting space.

From equation (3.15) and (3.17), $(\Delta u, \Delta v)^\top$ is expressed as

$$
\begin{pmatrix} \Delta u \\ \Delta v \end{pmatrix} = \begin{pmatrix} \dfrac{(I_x^{(1)'}I_y^{(2)}-I_x^{(2)}I_y^{(1)'})(I_y^{(1)}I_t^{(2)}-I_t^{(1)}I_y^{(2)})-(I_x^{(1)}I_y^{(2)}-I_x^{(2)}I_y^{(1)})(I_y^{(1)'}I_t^{(2)}-I_t^{(1)'}I_y^{(2)})}{(I_x^{(1)}I_y^{(2)}-I_x^{(2)}I_y^{(1)})(I_x^{(1)'}I_y^{(2)}-I_x^{(2)}I_y^{(1)'})} \\[2ex] \dfrac{(I_x^{(2)}I_y^{(1')}-I_x^{(1)'}I_y^{(2)})(I_x^{(1)}I_t^{(2)}-I_t^{(1)}I_x^{(2)})-(I_x^{(2)}I_y^{(1)}-I_x^{(1)}I_y^{(2)})(I_x^{(1)'}I_t^{(2)}-I_t^{(1)'}I_x^{(2)})}{(I_x^{(2)}I_y^{(1)}-I_x^{(1)}I_y^{(2)})(I_x^{(2)}I_y^{(1)'}-I_x^{(1)'}I_y^{(2)})} \end{pmatrix}. \quad (3.19)
$$

Since $I_x^{(1)} \neq I_x^{(1)'}$, $I_y^{(1)} \neq I_y^{(1)'}$, $I_t^{(1)} \neq I_t^{(1)'}$, the difference vector $(\Delta u, \Delta v)^\top$ is not zero vector. This means, if there is a constraint equation that does not satisfy optical flow realizable conditions or a constraint equation effected by noise in a support region, intersections of constraint equation are scattered.

I use voting process to estimate values of estimation parameter from scattered intersections of constraint lines by the factors of $(\mathbf{A})$, excluding intersections of constraint lines by the factors of $(\mathbf{B})$. By voting of intersections in the parameter space u and v to the voting space, if intersections of constraint lines by the factors of $(\mathbf{A})$ converge into a cell in voting space, the voting score in the cell will be the maximum voting score. Then we decide the coordinate of the maximum voting score as estimated parameters u and v. By this process, we can expect to precisely estimate estimated parameters u and v excluding the intersections of constraint lines by the factors of $(\mathbf{B})$ (Figure 3.8).

In order to separate different motions from an interest pixel, we use constraint lines that satisfy the following constraint lines such as

· Constraint lines on pixels of the same object as on an interest pixel.

We assume that intensity of an interest pixel and the neighboring pixels are almost equivalent, if they are in a same object. If the assumption holds, The condition is formularize as

$$
|I(x, y, t) - I(a, b, t)| \leq Th_o, \quad (3.20)
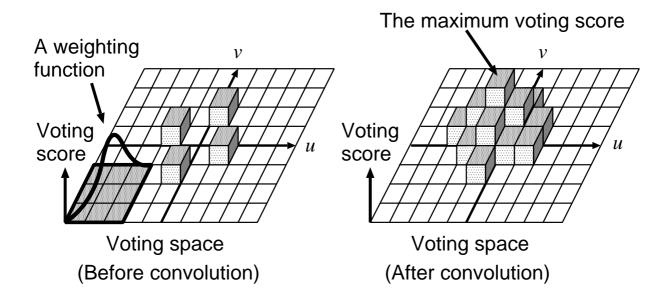$$

Figure 3.9: Effective of voting process with a weighting function.

where $I(a, b, t)$ is intensity of an interest pixel (a, b) at time t, $I(x, y, t)$ is intensity of neighboring pixels of the interest pixel at time t, Th_o is a threshold in the condition. We adopt constraint equations that satisfy the above equations to voting process. In case that intersections of constraint lines do not converge into a cell in voting space, There is a case that we cannot obtain the maximum voting score by distribution of voting scores. To obtain the reasonable maximum voting score in case of distribution of voting scores, a method of voting process with a weighting function has been proposed. This method detects the reasonable maximum voting score (u_{med}, v_{med}) in $f'(u_\alpha, v_\alpha)$ convoluting voting score $f(u, v)$ by a weighting function $w(u - u_\alpha, v - v_\alpha; \sigma)$. The $f'(u_\alpha, v_\alpha)$ is expressed as

$$f'(u_\alpha, v_\alpha) = \sum_{u=-V/2}^{V/2} \sum_{v=-V/2}^{V/2} w(u - u_\alpha, v - v_\alpha; \sigma) f(u, v), \qquad (3.21)$$

where V denotes axis size of each u and v in the voting space, u_α, v_α denote interest coordinates in voting space. We use Gaussian function as a weighting function

$$w(u - u_\alpha, v - v_\alpha; \sigma) = \frac{1}{\sqrt{2\pi}\sigma} \exp\left\{-\frac{(u - u_\alpha)^2 + (v - v_\alpha)^2}{2\sigma^2}\right\}, \qquad (3.22)$$

where σ denotes a variance parameter. Then the method decides (u_{med}, v_{med}) as estimated value of velocity vector components u and v in the interest pixel (Figure 3.9).

3.3.2 Segmentation based on motion continuity (Step2)

This step executes segmentation based on motion continuity of the velocity vectors obtained in the Step1. Two adjacent pixels are given by (x_1, y_1) and (x_2, y_2) respectively, and velocity vector components on the pixels are given by (u_1, v_1) and (u_2, v_2) respectively. The combination condition of these pixels is expressed by

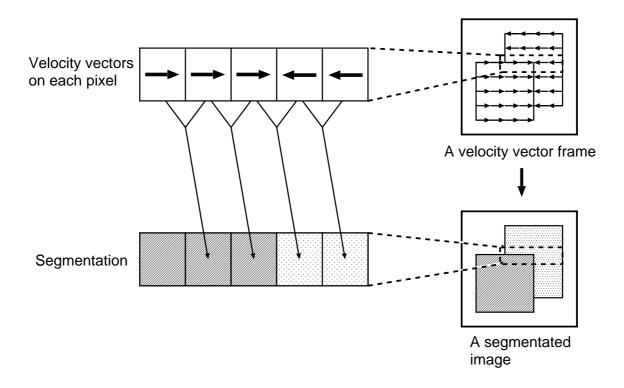$$|u_1 - u_2|^2 + |v_1 - v_2|^2 < Th_R, \qquad (3.23)$$

27

Figure 3.10: Segmentation based on motion continuity.

where Th_R is a threshold. If adjacent pixels satisfy the condition, they are assigned to be in a same region. If not, they are assigned to be in different regions. After segmentation, each region is labeled (Figure 3.10). This step generates segmented image 1 based on velocity vectors in image frame 1 and 2, and segmented image 2 based on velocity vectors in image frame2 and 3.

3.3.3   Extraction of occluded and appearance regions (Step3)

This step extracts occluded and appearance regions. In order to apply the method of extraction of occluded and appearance regions to actual image sequence containing more than two objects, I use a method of extraction of occluded and appearance regions based on properties of occluded and appearance regions.

Occlusion regions have a following property.

·A property of occlusion regions: A region on a pixel at time t is different from a region on the pixel after moving at time t.

The property of occlusion regions is expressed by

$$a(x, y, t) \neq a(x + u, y + v, t), \tag{3.24}$$

where $a(x, y, t)$ is a label of a pixel on (x, y, t). u and v denote $u = u(x, y, t)$ and $v = (x, y, t)$ respectively. The label $a(x, y, t)$ of segmented image 1 is determined in Step2. This step determines a region on $a(x + u, y + v, t)$ as an occluded region (Figure 3.11).

Appearance regions have a following property.

·A property of appearance regions: A region on a pixel at time $t + \Delta t$ is different from a region on a pixel before moving at time $t + \Delta t$.
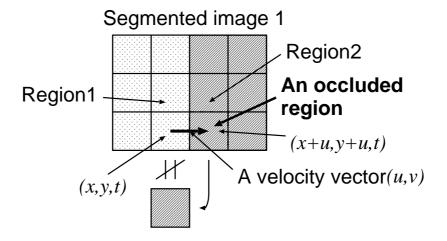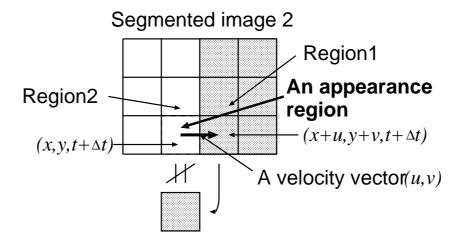
28

Figure 3.11: The property of occluded regions.

Figure 3.12: The property of appearance regions.

The property of appearance regions is expressed by

$$a(x + u, y + v, t + \Delta t) \neq a(x, y, t + \Delta t), \qquad (3.25)$$

where $a(x, y, t + \Delta t)$ is a label of a pixel on $(x, y, t + \Delta t)$. The label $a(x, y, t + \Delta t)$ of segmented image 2 is determined in Step2. This step determines a region on $a(x, y, t + \Delta t)$ as an appearance region (Figure 3.12).

3.3.4 Decision of assigned regions of occluded and appearance regions (Step4)

This step decides assigned regions of occluded and appearance regions for extrapolating of velocity vectors in occlusion regions. In the segmented image 1, this step decides a region on occlusion region as an assigned region of the occlusion region (Figure 3.13) and decides a region on appearance region as an assigned region of the appearance region (Figure 3.14).
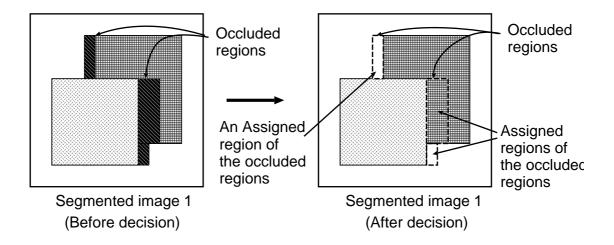
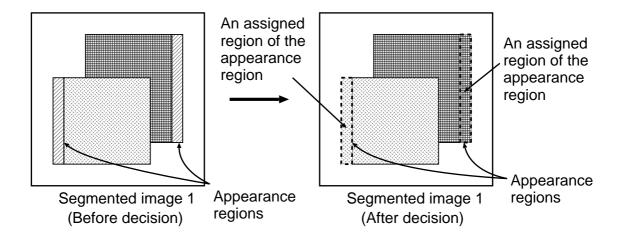Figure 3.13: Decision of assigned region of occluded regions.

Figure 3.14: Decision of assigned regions of appearance regions.

3.3.5 Extrapolation of velocity vectors in occlusion regions (Step5)

This step extrapolates velocity vectors in occlusion regions regarding velocity vector components u and v as a function $u(x, y)$ and $v(x, y)$ with respect to x and y. There are some methods to interpolate unknown values of a function,

- · Lagrange's interpolation method
- · Newton's interpolation method
- · Spline function interpolation method

As a extrapolation method, since Newton's interpolation method is easy to expand to extrapolation method and velocity vector components $u(x, y)$ and $v(x, y)$ are 2-dimensional function, I use Newton's interpolation method expanded to 2-dimension.

Expansion of Newton's interpolation method to 2-dimension

Differential in 1-dimension discrete space is defined as

$$\Delta_h f(x) = f(x+h) - f(x),\tag{3.26}$$

where h is a interval of x in $f(x)$. Then, n order differential is defined as

$$\Delta_h^{(n)} f(x) = \sum_{i=0}^{n} (-1)^i ({}_nC_i) f(x + (n-i)h)\tag{3.27}$$

where ${}_nC_i$ is binomial coefficients, ${}_nC_i$ means $n!/i!(n-i)!$. Then, 1-dimensional Newton's interpolation is expressed as

$$f(x+h) = f(x) + \sum_{i=1}^{n} \frac{1}{i!} \{\Delta_h^{(i)} f(x)\}(h)^i\tag{3.28}$$

Next, I expand the 1-dimensional Newton's interpolation to 2-dimension. Partial differential in 2-dimensional discrete space is defined as

$$\Delta_{h_x} f(x,y) = f(x+h_x, y) - f(x,y),\tag{3.29}$$

$$\Delta_{h_y} f(x,y) = f(x, y+h_y) - f(x,y),\tag{3.30}$$

where h_x and h_y denote interval of x and y in $f(x,y)$ respectively. Then, n order partial differential is defined as

$$\Delta_{h_x}^{(n)} f(x,y) = \sum_{i=0}^{n} (-1)^i ({}_nC_i) f(x + (n-i)h_x, y)\tag{3.31}$$

$$\Delta_{h_y}^{(n)} f(x,y) = \sum_{i=0}^{n} (-1)^i ({}_nC_i) f(x, y + (n-i)h_y)\tag{3.32}$$

By above equations, 2-dimensional Newton's interpolation is expressed as

$$f(x+h_x, y+h_y) = f(x,y) + \sum_{i=1}^{n} \frac{1}{i!} \{\Delta_{h_x}^{(i)} f(x,y)(h_x) + \Delta_{h_y}^{(i)} f(x,y)(h_y)\}^i\tag{3.33}$$

An extrapolation method of velocity vectors in occlusion regions

Based on the 2-dimensional Newton's extrapolation method expressed in equation (3.33), This step extrapolates velocity vectors in occluded/appearance regions using

$$u(X,Y) = u(x_0, y_0) + \sum_{i=1}^{n} \frac{1}{i!} \{\Delta_{h_x}^{(i)} u(x_0, y_0)(h_x) + \Delta_{h_y}^{(i)} u(x_0, y_0)(h_y)\}^i\tag{3.34}$$

$$v(X,Y) = v(x_0, y_0) + \sum_{i=1}^{n} \frac{1}{i!} \{\Delta_{h_x}^{(i)} v(x_0, y_0)(h_x) + \Delta_{h_y}^{(i)} v(x_0, y_0)(h_y)\}^i\tag{3.35}$$

where $X = x_0 + h_x$ and $Y = y_0 + h_y$, (X,Y) denotes coordinates on a pixel that is extrapolated respectively (Figure 3.15).

The pixels that satisfy the following conditions such as

An assigned region

An velocity vector frame

Velocity vectors
on the assiged
region

An occluded or
An appearance
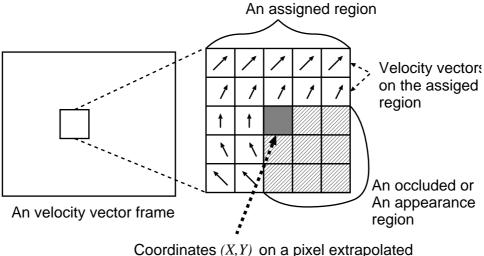region

Coordinates *(X,Y)* on a pixel extrapolated

Figure 3.15: Extrapolation of velocity vectors from assigned regions.

· a pixel in assigned regions of occluded and appearance regions

· a pixel satisfies the definition of 2-dimensional Newton's interpolation

are used to extrapolate velocity vectors in occluded/appearance regions.

The second condition will be different by definition of differential. There are some definitions of differential such as

· Central differential : $1/2\{f(x+h) - f(x-h)\}$

· Forward differential : $f(x+h) - f(x)$

· Backward differential : $f(x) - f(x-h)$

Ideally, I would like to use the central differential that has confidences. However, the central differential needs a lot of pixels to extrapolate velocity vectors in occluded/appearance regions. In case of not satisfying the condition of central differential, this step uses the forward differential or backward differential (Figure 3.16). If there is no pixel that do not satisfy the definition of the above differentials, this step assigns velocity vectors estimated by the voting method to occluded/appearance regions.
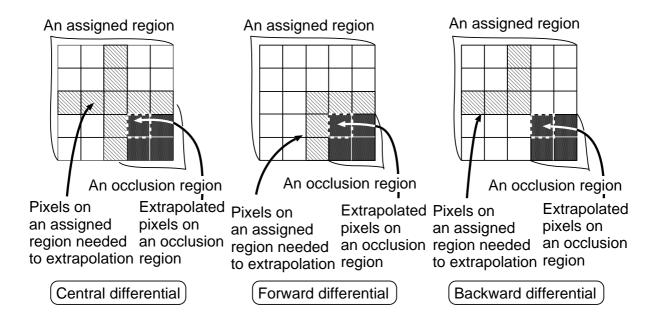
An assigned region   An assigned region   An assigned region

An occlusion region   An occlusion region   An occlusion region

Pixels on an assigned region needed to extrapolation   Extrapolated pixels on an occlusion region   Pixels on an assigned region needed to extrapolation   Extrapolated pixels on an occlusion region   Pixels on an assigned region needed to extrapolation   Extrapolated pixels on an occlusion region

Central differential   Forward differential   Backward differential

Figure 3.16: Pixels for extrapolation in each differential calculation.

3.4 Experiments for evaluation of effectiveness of the proposed method

In order to evaluate effectiveness in the proposed method, I experiment on evaluating of effectiveness of the proposed method in synthetic image sequences, noisy synthetic image sequences or actual image sequences. As conventional methods to compare precision of velocity vector estimation to the method using voting process with a weighting function, I adopt following major methods such as

    · Local method (Lucas-Kanade's method)[8]
    · Global method (Horn's method)[7]

3.4.1 Experiments in synthetic image sequences

(Experiment:1-A) Experiments of comparison of velocity vector estimation precision in conventional methods and the method using the voting process with a weighting function

In order to quantitatively evaluate of effectiveness of the method using the voting process with a weighting function, in whole pixels in an image frame, I experiment on comparison of velocity vector estimation precision in conventional method and the method using the voting process with a weighting function. In this experiments, I use synthetic image sequences having properties such as

    · There are occluded/appearance regions between frames.
    · There is sufficient difference of intensity between objects.

    · Intensity on an object and a background in a frame smoothly changes spatially and temporally.

    I use the image frame shown in Figure 3.17 as a first image frame and, as a second or a third image frame, I respectively use an image that objects in the first image frame are transformed by affine transform of translation, expansion, contraction or rotation whose parameters are shown in from Table 3.5 through Table 3.8 on condition that parameters in Table 3.5 are defined right direction as positive direction, parameters in Table 3.8 are defined counterclockwise as positive direction. Parameters of image frames used in this experiments are shown in Table 3.1.

Table 3.1: Parameters of image frames used in this experiments.

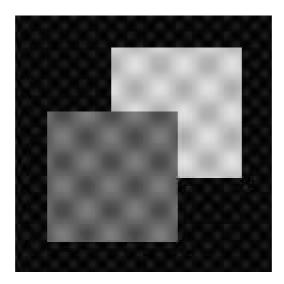|	
Frequency of a sine (Texture)	0.12[Hz]
Amplitude of a sine (Texture)	25[intensity]
Bias of intensity (Background)	25[intensity]
Bias of intensity (left lower object)	100[intensity]
Bias of intensity (right upper object)	200[intensity]
Resolution	128×128[pixels]

Figure 3.17: A synthetic image frame used in this experiments.

Parameters, determined in this experiment, in conventional methods and the proposed method are shown in Table 3.17, 3.18 and 3.19 respectively.

Table 3.2: Parameters in local method.

The size of the support region	10×10[pixels]

Table 3.3: Parameters in global method.

Weighting coefficient of evaluation terms of smoothness	3
Repetition calculation times	200[times]

Table 3.4: Parameters in the method using voting process with a weighting function.

The threshold in the voting possible condition 1	30[intensity]
The threshold in the voting possible condition 2	10[intensity]
The threshold in the voting possible condition 3	5[intensity]
The threshold in segmentation based on motion continuity	0.02
The size of the support region	30×30[pixels]
The size of a cell in the voting space	1.0×10^{-2}
The variance parameter in the weighting function	4

To quantitatively evaluate precision of velocity vector estimation in whole pixels in an image frame, I define the mean of errors $\bar{e}$

$$\bar{e} = \frac{1}{M} \sum_{x,y\in R_o} ||\boldsymbol{f}_c(x,y) - \boldsymbol{f}_e(x,y)||, \qquad (3.36)$$

where M is number of pixels in an image frame, R_o is an image regions, $\boldsymbol{f}_e(x,y)$ is an estimated velocity vector in a coordinate of an image (x,y). $\boldsymbol{f}_c(x,y)$ is a correct velocity vector.

Table 3.5: Parameters in image sequences containing translation motions.

Names of each image sequence	Parameters of translation motions [pixel/frame]	
	The left lower object	The right upper object
Tran1	0.5	-0.5
Tran2	1.0	-1.0
Tran3	1.5	-1.5
Tran4	2.0	-2.0
Tran5	2.5	-2.5
Tran6	3.0	-3.0
Tran7	3.5	-3.5
Tran8	4.0	-4.0
Tran9	4.5	-4.5
Tran10	5.0	-5.0

Table 3.6: Parameters in image sequences containing expansion motions.

Names of each image sequence	Parameters in expansion motions [times/frame]	
	The left lower object	The right upper object
Exp1	1.01	1.01
Exp2	1.02	1.02
Exp3	1.03	1.03
Exp4	1.04	1.04
Exp5	1.05	1.05
Exp6	1.06	1.06
Exp7	1.07	1.07
Exp8	1.08	1.08
Exp9	1.09	1.09
Exp10	1.10	1.10

The results in the mean of errors of conventional methods and the method using voting process with a weighting function in each image sequence are shown in Figure 3.18, 3.19, 3.20 and 3.21 respectively.

In the results of the mean of errors, I obtained well results of precision of velocity vector estimation by using the method using the voting process with a weighting function. The factor is supposed to get rid of effectiveness of intersections of constraint equation in occluded/appearance regions and separating different motions by using a condition of constraint equation for voting. the precision of each methods decreased as motions get large. The cause of this is supposed to be not satisfying an optical flow realizable condition such that motions are infinitesimal by enlargement of motion.

As an example, a correct velocity vector field and velocity vector fields estimated by conventional methods and the method using voting process with a weighting function in Trans2 are shown in Figure 3.22, Figure 3.23, Figure 3.24 and Figure 3.25 respectively.

Table 3.7: Parameters in image sequences containing contraction motions.

Names of each image sequence	Parameters in contraction motions [times/frame]	
	The left lower object	The right upper object
Cont1	0.99	0.99
Cont2	0.98	0.98
Cont3	0.97	0.97
Cont4	0.96	0.96
Cont5	0.95	0.95
Cont6	0.94	0.94
Cont7	0.93	0.93
Cont8	0.92	0.92
Cont9	0.91	0.91
Cont10	0.90	0.90

Table 3.8: Parameters in image sequences containing rotation motions.

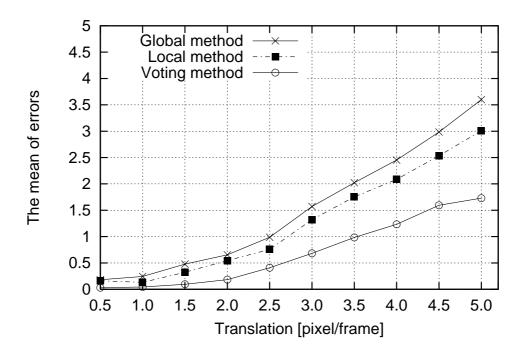| Names of each image sequence	Parameters in rotation motions [degree/frame]	
	The left lower object	The right upper object
Rot1	0.5	0.5
Rot2	1.0	1.0
Rot3	1.5	1.5
Rot4	2.0	2.0
Rot5	2.5	2.5
Rot6	3.0	3.0
Rot7	3.5	3.5
Rot8	4.0	4.0
Rot9	4.5	4.5
Rot10	5.0	5.0

Figure 3.18: The mean of errors $\bar{e}$ of conventional methods and the method using voting process with a weighting function in translation motions.
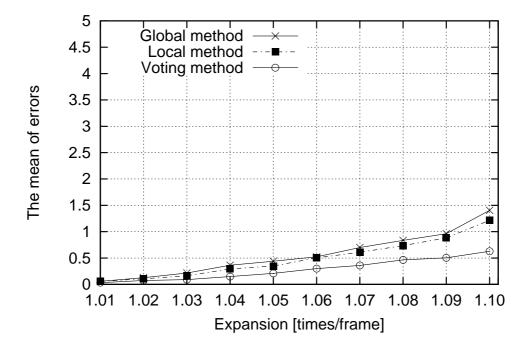

Figure 3.19: The mean of errors $\bar{e}$ of conventional methods and the method using voting process with a weighting function in expansion motions.
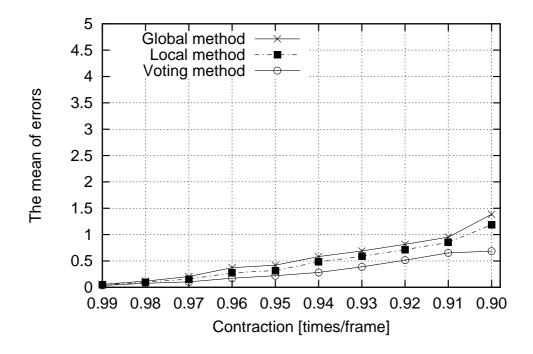
Figure 3.20: The mean of errors $\bar{e}$ of conventional methods and the method using voting process with a weighting function in contraction motions.
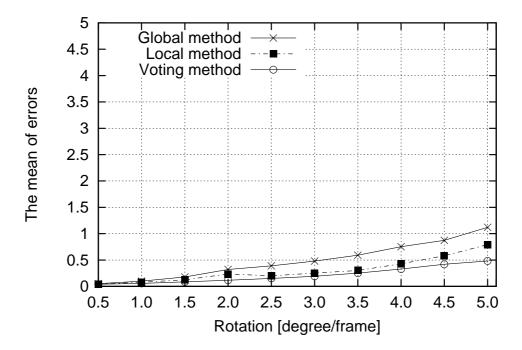

Figure 3.21: The mean of errors $\bar{e}$ of conventional methods and the method using voting process with a weighting function in rotation motions.
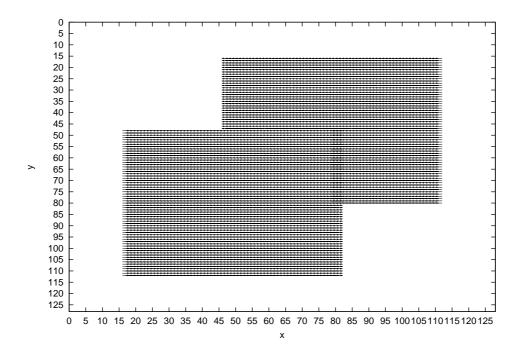
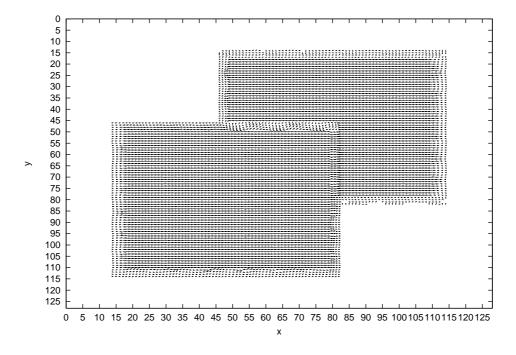Figure 3.22: A correct velocity vector field in Trans2.

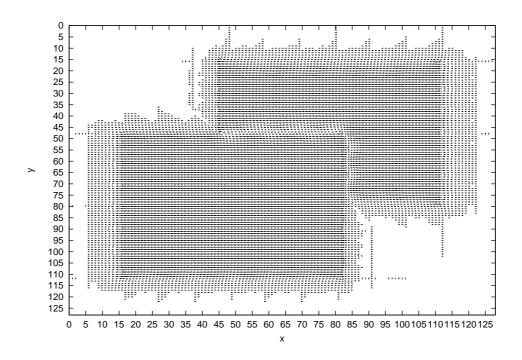Figure 3.23: Estimated velocity vector field by local method in Trans2.

Figure 3.24: Estimated velocity vector field by global method in Trans2.
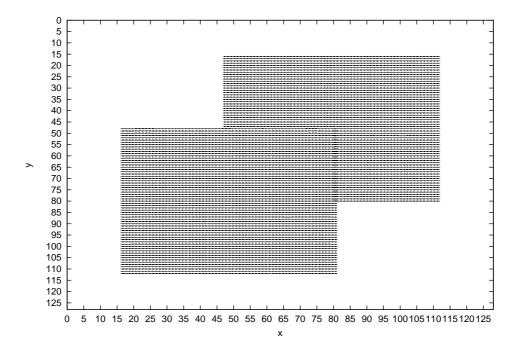

Figure 3.25: Estimated velocity vector field by the method using voting process with a weighting function in Trans2.

41

(Experiment:1-B) Experiments of comparison of velocity vector estimation precision in the method using the voting process with a weighting function and in case of applying extrapolation

In order to quantitatively evaluate of effectiveness in case of applying extrapolation in synthetic image sequences, in occlusion regions, I experiment on comparison of velocity vector estimation precision in the method using the voting process with a weighting function and in case of applying extrapolation.

I use the image sequences used in the previous experiment and the same parameters of the method using voting process with a weighting function as the parameters used in the previous experiment.

To quantitatively evaluate precision of velocity vector estimation in occlusion regions, I use the mean of errors $\bar{e}$ in occlusion regions such as

$$\bar{e} = \frac{1}{M} \sum_{x,y \in R_o} ||\boldsymbol{f}_c(x,y) - \boldsymbol{f}_e(x,y)||, \tag{3.37}$$

where M is number of pixels in occluded/appearance regions, R_o is occluded/appearance regions, $\boldsymbol{f}_e(x,y)$ is an estimated velocity vector of a coordinate of an image (x,y) in occluded/appearance regions. $\boldsymbol{f}_c(x,y)$ is a correct velocity vector in occluded/appearance regions.

The results in the mean of errors of the method using voting process with a weighting function and in case of applying extrapolation in occlusion regions of each image sequence are shown in Table 3.9, Table 3.10, Table 3.11 and 3.12 respectively.

To quantitatively evaluate improvement in the mean of errors, I define the improved rate of the mean of errors

$$\Delta \bar{e} = 100 \times \frac{\bar{e}_{vote} - \bar{e}_{ext}}{\bar{e}_{vote}}[\%], \tag{3.38}$$

where $\bar{e}_{vote}$ is the mean of errors $\bar{e}$ in occluded/appearance regions obtained by velocity vector estimation via voting process with a weighting function. $\bar{e}_{ext}$ is the mean of errors $\bar{e}$ in occluded/appearance regions obtained by extrapolation.

The results of the improved rate of the mean of errors are shown in Figure 3.26, 3.27, 3.28 and 3.29 respectively.

From the results, I obtained well results of precision of velocity vector estimation by applying extrapolation. The factor is supposed to extrapolate velocity vectors in occlusion regions from estimated velocity vectors in assigned regions that has reliability.

As an example, a correct velocity vector field and velocity vector fields estimated by the method using voting process with a weighting function and in case of applying extrapolation in Exp3 are shown in Figure 3.31, Figure 3.32 and its expanded figure 3.33 of rectangle regions in the correct velocity vector field, Figure 3.31 and 3.32 respectively.

Table 3.9: The mean of errors $\bar{e}$ of (A) the method using voting process with a weighting function and (B) in case of applying extrapolation in occluded/appearance regions of translation motions.

Names of each image sequence	The mean of errors $\bar{e}$	
	(A)	(B)
Trans1	1.32×10^{-3}	1.30×10^{-3}
Trans2	4.79×10^{-3}	4.76×10^{-3}
Trans3	1.55×10^{-2}	1.54×10^{-2}
Trans4	5.22×10^{-2}	5.22×10^{-2}
Trans5	5.15×10^{-1}	5.15×10^{-1}
Trans6	1.49	1.49
Trans7	3.33	3.33
Trans8	4.99	4.99
Trans9	9.21	9.21
Trans10	1.47×10	14.7×10

Table 3.10: The mean of errors $\bar{e}$ of (A) the method using voting process with a weighting function and (B) in case of applying extrapolation in occluded/appearance regions of expansion motions.

Names of each image sequence	The mean of errors $\bar{e}$	
	(A)	(B)
Exp1	-	-
Exp2	1.17×10^{-1}	0.99×10^{-1}
Exp3	2.13×10^{-1}	1.89×10^{-1}
Exp4	2.99×10^{-1}	2.75×10^{-1}
Exp5	6.29×10^{-1}	5.98×10^{-1}
Exp6	1.08	1.04
Exp7	2.00	1.96
Exp8	2.93	2.90
Exp9	4.31	4.30
Exp10	1.47×10	14.7×10

Table 3.11: The mean of errors $\bar{e}$ of (A) the method using voting process with a weighting function and (B) in case of applying extrapolation in occluded/appearance regions of contraction motions.

Names of each image sequence	The mean of errors $\bar{e}$	
	(A)	(B)
Cont1	-	-
Cont2	-	-
Cont3	1.01×10^{-1}	0.92×10^{-1}
Cont4	1.84×10^{-1}	1.73×10^{-1}
Cont5	3.15×10^{-1}	3.05×10^{-1}
Cont6	5.99×10^{-1}	5.87×10^{-1}
Cont7	9.56×10^{-1}	9.46×10^{-1}
Cont8	1.62	1.61
Cont9	2.87	2.87
Cont10	3.89	3.89

Table 3.12: The mean of errors $\bar{e}$ of (A) the method using voting process with a weighting function and (B) in case of applying extrapolation in occluded/appearance regions of rotation motions.

Names of each image sequence	The mean of errors $\bar{e}$	
	(A)	(B)
Rot1	-	-
Rot2	2.88×10^{-2}	2.68×10^{-2}
Rot3	9.12×10^{-2}	8.84×10^{-2}
Rot4	1.54×10^{-1}	1.53×10^{-1}
Rot5	2.42×10^{-1}	2.36×10^{-1}
Rot6	4.13×10^{-1}	4.12×10^{-1}
Rot7	7.15×10^{-1}	7.06×10^{-1}
Rot8	1.24	1.23
Rot9	2.09	2.08
Rot10	3.38	3.36
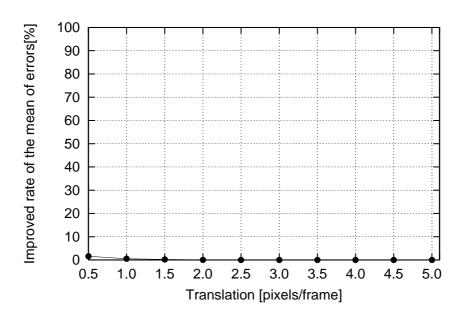
Figure 3.26: Improved rate of the mean of errors $\Delta\bar{e}$ in translation motions.
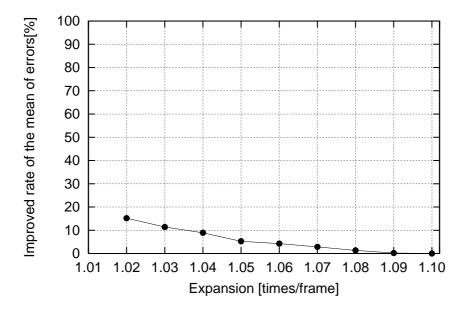
Figure 3.27: Improved rate of the mean of errors $\Delta\bar{e}$ in expansion motions.
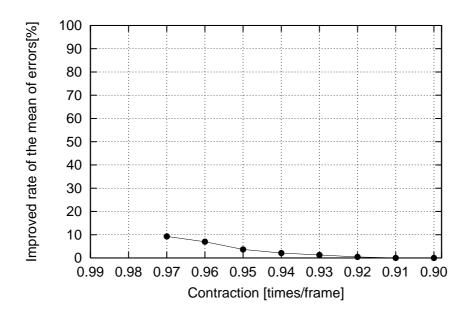
Figure 3.28: Improved rate of the mean of errors $\Delta\bar{e}$ in contraction motions.
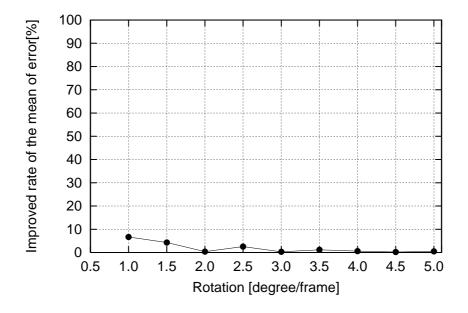
Figure 3.29: Improved rate of the mean of errors $\Delta\bar{e}$ in rotation motions.
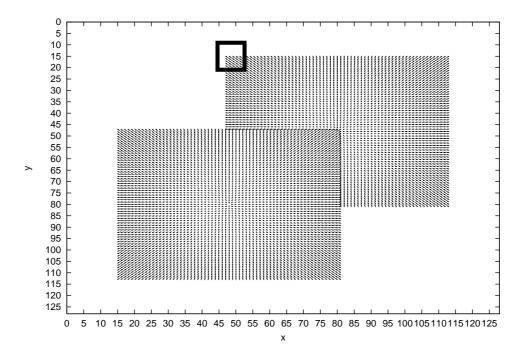
Figure 3.30: A correct velocity vector field in Exp3.
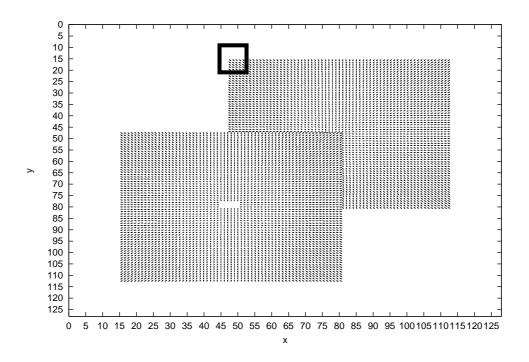
Figure 3.31: A velocity vector field estimated by the method using voting process with a weighting function in Exp3.
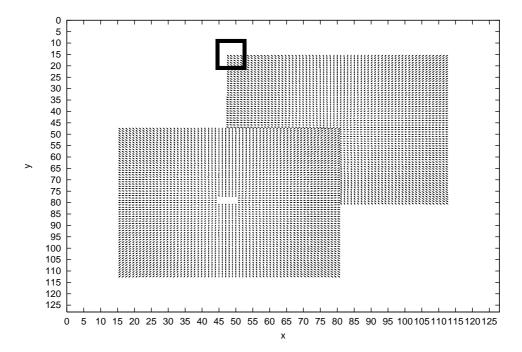
Figure 3.32: A velocity vector field estimated by in case of applying extrapolation in Exp3.
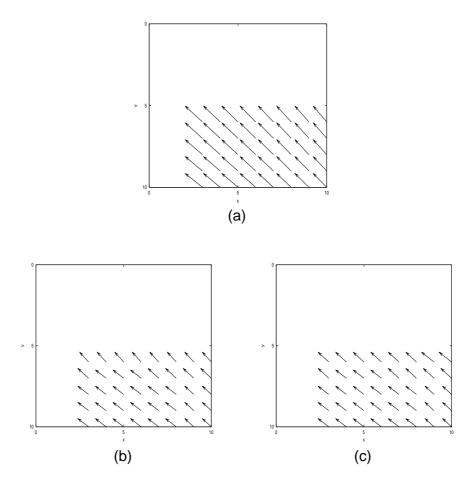
Figure 3.33: Expanded figures of the rectangle regions in (a):a correct velocity vector field, (b):Figure 3.31 and (c):Figure 3.32.

3.4.2 Experiments in noisy synthetic image sequences

(Experiment:2-A) Experiments of comparison of velocity vector estimation precision in conventional methods and the method using the voting process with a weighting function

In order to quantitatively evaluate of effectiveness of conventional methods and the method using the voting process with a weighting function, in noisy synthetic image sequences, I experiment on comparison of velocity vector estimation precision in conventional method and the method using the voting process with a weighting function. In this experiment, I use

$$PSNR[dB] = 20 \log \frac{255}{\sigma} \tag{3.39}$$

as a evaluation scale of quantity of noise. Synthetic images used in this experiments are synthetic images $I'(x, y, t)$ expressed as

$$I'(x, y, t) = I(x, y, t) + n \tag{3.40}$$

where n denotes Gaussian noise expressed as

$$P(n) = \frac{1}{\sqrt{2\pi}\sigma} \exp^{-\frac{n^2}{2\sigma^2}}, \tag{3.41}$$

$I(x, y, t)$ denotes a synthetic image used in previous experiments. As examples, I use image sequences Trans6, Exp3, Cont6 or Rot8 that are added Gaussian noise.

Parameters, determined in this experiment, in conventional methods and the proposed method are shown in Table 3.17, 3.18 and 3.19 respectively.

To quantitatively evaluate precision of velocity vector estimation in occlusion regions, I use the mean of errors $\bar{e}$ used in the experiment:1-A.

The results in the mean of errors of conventional methods and the method using voting process with a weighting function in each image sequence are shown in Figure 3.34, 3.35, 3.36 and 3.37 respectively.

In the results of the mean of errors, I obtained well results of precision of velocity vector estimation by using the method using the voting process with a weighting function. The factor is supposed to get rid of effectiveness of intersections of constraint equation in occluded/appearance regions and separating different motions by using a voting possible condition, in addition to getting rid of effectiveness of noise.

As an example, a correct velocity vector field and velocity vector fields estimated by conventional methods and the method using voting process with a weighting function in Trans6 of $PSNR$=35.4[dB] are shown in Figure 3.38, Figure 3.39, Figure 3.40 and Figure 3.41 respectively.
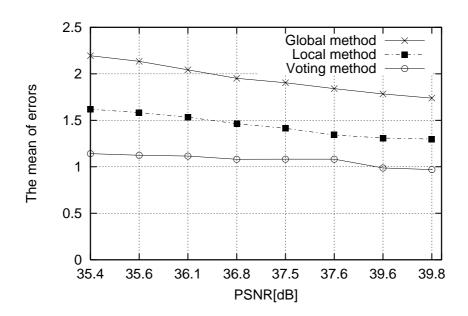
Figure 3.34: The mean of errors $\bar{e}$ of conventional methods and the method using voting process with a weighting function in Trans6 (3.0[pixel/frame]).
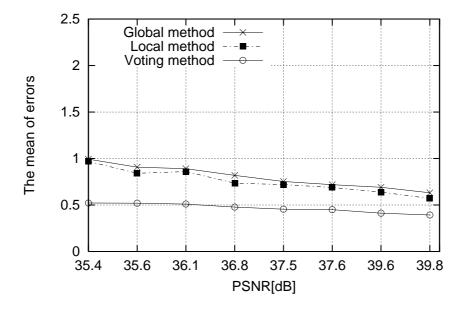
Figure 3.35: The mean of errors $\bar{e}$ of conventional methods and the method using voting process with a weighting function in Exp6 (1.06[times/frame]).
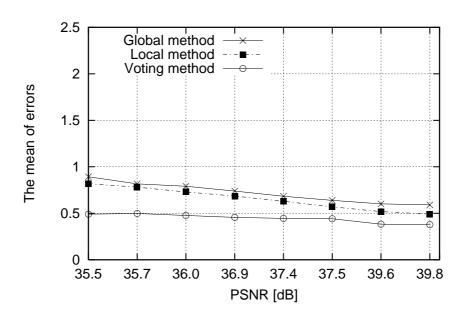
Figure 3.36: The mean of errors $\bar{e}$ of conventional methods and the method using voting process with a weighting function in Cont6 (0.94[times/frame]).
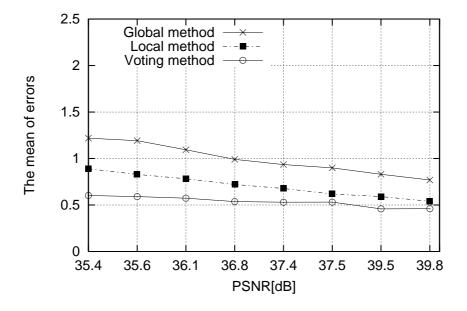
Figure 3.37: The mean of errors $\bar{e}$ of conventional methods and the method using voting process with a weighting function in Rot8 (4.0[degree/frame]).
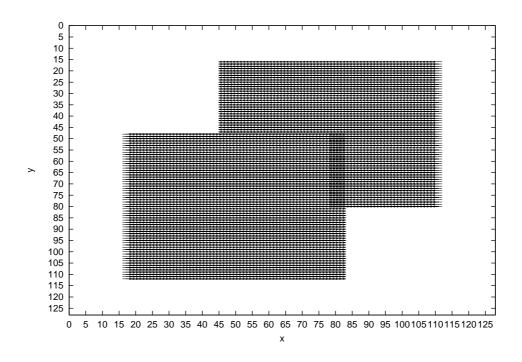
Figure 3.38: A correct velocity vector field in Trans6 of $PSNR$=35.4[dB].
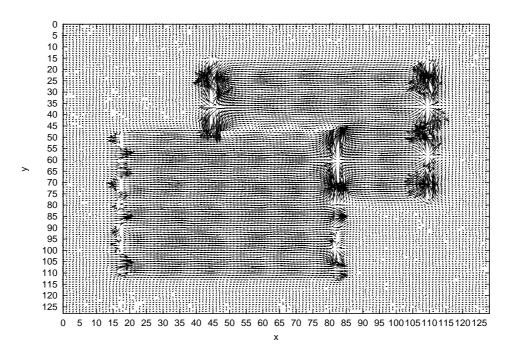
Figure 3.39: Estimated velocity vector field by local method in Trans6 $PSNR$=35.4[dB].
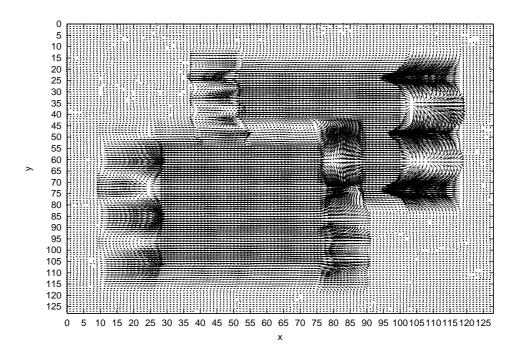
Figure 3.40: Estimated velocity vector field by global method in Trans6 $PSNR$=35.4[dB].
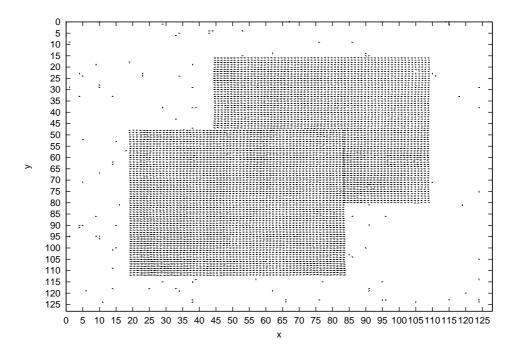
Figure 3.41: Estimated velocity vector field by the method using voting process with a weighting function in Trans6 $PSNR$=35.4[dB].

54

(Experiment:2-B) Experiments of comparison of velocity vector estimation precision in the method using the voting process with a weighting function and in case of applying extrapolation

In order to quantitatively evaluate of effectiveness in case of applying extrapolation in noisy synthetic image sequences, in occlusion regions, I experiment on comparison of velocity vector estimation precision in the method using the voting process with a weighting function and in case of applying extrapolation.

I use the image sequences used in the previous experiment and the same parameters of the method using voting process with a weighting function as the parameters used in the previous experiment.

To quantitatively evaluate precision of velocity vector estimation in occlusion regions, I use the mean of errors $\bar{e}$ used in experiment:1-B.

The results in the mean of errors of the method using voting process with a weighting function and in case of applying extrapolation in occlusion regions of each image sequence are shown in Table 3.13, Table 3.14, Table 3.15 and Table 3.16 respectively. These results are 10 times average with respect to adding Gaussian noise in 3 samples of each motion.

To quantitatively evaluate improvement in the mean of errors, I use the improved rate of the mean of errors $\Delta\bar{e}$ used in experiment:1-B.

The results of the improved rate of the mean of errors are shown in Figure 3.42, 3.43, 3.44 and 3.45 respectively. These results are 10 times average with respect to adding Gaussian noise in 3 samples of each motion. From the results, even though in noisy image sequences, I obtained well results of precision of velocity vector estimation by applying extrapolation. The mean of errors intends to decrease as quantity of noise increases. Since precision of velocity vector estimation in occluded/appearance regions depends on precision of velocity vector estimation in assigned regions of occluded/appearance regions, the factor is supposed that precision of velocity vector estimation in assigned regions of occluded/appearance regions decrease as quantity of noise increases. I obtained well results of the improved rate of the mean of errors as motions get small. the factor is supposed that effectiveness of extrapolation decreases since precition of velocity vector estimation in occluded/appearance region and its assigned region decreases as motions get large.

As an example, a correct velocity vector field and velocity vector fields estimated by the method using voting process with a weighting function and in case of applying extrapolation in Rot8 of $PSNR$=36.8[dB] are shown in Figure 3.46, Figure 3.47, Figure 3.48 and its expanded figure 3.49 of the rectangle regions in a correct velocity vector field, Figure 3.47 and Figure 3.48 respectively.

Table 3.13: The mean of errors $\bar{e}$ of (A) the method using voting process with a weighting function and (B) in case of applying extrapolation in occluded/appearance regions of noisy translation image sequences.

| $PSNR$[dB] | The mean of errors $\bar{e}$ | | | | | |
| | 2.5[pixel/frame] | | 3.0[pixel/frame] | | 3.5[pixel/frame] | |
	(A)	(B)	(A)	(B)	(A)	(B)
39.8	5.23	5.23	6.15	6.14	7.36	7.36
39.6	5.42	5.42	6.15	6.14	7.38	7.38
37.5	5.48	5.48	6.15	6.14	7.46	7.46
37.4	5.51	5.51	6.15	6.14	7.52	7.52
36.9	5.58	5.58	6.15	6.14	7.56	7.56
36.0	5.61	5.61	6.15	6.14	7.73	7.73
35.7	5.82	5.81	6.15	6.14	7.91	7.91
35.4	5.96	5.95	6.15	6.14	8.02	8.02

Table 3.14: The mean of errors $\bar{e}$ of (A) the method using voting process with a weighting function and (B) in case of applying extrapolation in occluded/appearance regions of noisy expansion image sequences.

| $PSNR$[dB] | The mean of errors $\bar{e}$ | | | | | |
| | 1.05[times/frame] | | 1.06[times/frame] | | 1.07[times/frame] | |
	(A)	(B)	(A)	(B)	(A)	(B)
39.8	0.92	0.92	1.15	1.14	1.52	1.52
39.5	0.98	0.98	1.31	1.29	1.68	1.68
37.5	1.01	1.00	1.58	1.57	1.78	1.78
37.4	1.24	1.23	1.73	1.72	1.86	1.85
36.8	1.25	1.24	1.84	1.83	2.19	2.18
36.1	1.36	1.34	1.95	1.94	2.30	2.29
35.6	1.42	1.39	2.10	2.10	2.42	2.40
35.4	1.53	1.50	2.21	2.21	2.63	2.61

Table 3.15: The mean of errors $\bar{e}$ of (A) the method using voting process with a weighting function and (B) in case of applying extrapolation in occluded/appearance regions of noisy contraction image sequences.

| $PSNR$[dB] | The mean of errors $\bar{e}$ | | | | | |
| | 0.95[times/frame] | | 0.94[times/frame] | | 0.93[times/frame] | |
	(A)	(B)	(A)	(B)	(A)	(B)
39.8	0.82	0.82	1.17	1.15	1.61	1.61
39.6	0.96	0.96	1.28	1.26	1.68	1.68
37.5	1.11	1.11	1.49	1.48	1.72	1.72
37.4	1.26	1.25	1.68	1.67	1.83	1.82
36.9	1.38	1.37	1.86	1.85	1.96	1.95
36.0	1.41	1.39	2.04	1.04	2.15	2.14
35.7	1.45	1.42	2.14	2.14	2.32	2.29
35.4	1.63	1.60	2.23	2.23	2.48	2.45

Table 3.16: The mean of errors $\bar{e}$ of (A) the method using voting process with a weighting function and (B) in case of applying extrapolation in occluded/appearance regions of noisy rotation image sequences.

| $PSNR$[dB] | The mean of errors $\bar{e}$ | | | | | |
| | 3.5[degree/frame] | | 4.0[degree/frame] | | 4.5[degree/frame] | |
	(A)	(B)	(A)	(B)	(A)	(B)
39.8	2.14	2.14	2.48	2.42	2.86	2.86
39.5	2.26	2.25	2.61	2.57	2.98	2.97
37.5	2.42	2.42	2.85	2.80	3.18	3.18
37.4	2.56	2.54	2.91	2.86	3.32	3.31
36.8	2.58	3.54	3.15	3.11	3.45	3.43
36.1	2.85	3.78	3.32	3.31	3.52	3.49
35.6	2.96	3.87	3.51	3.49	3.81	3.76
35.4	3.02	2.94	3.62	3.62	3.93	3.89
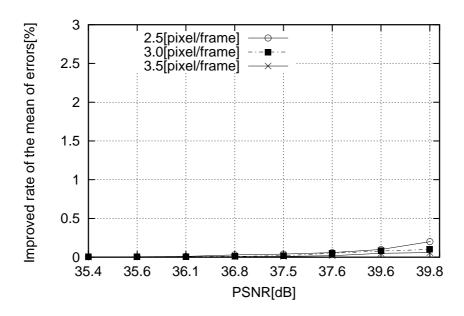
Figure 3.42: Improved rate of the mean of errors $\Delta\bar{e}$ in noisy image sequences of translation.
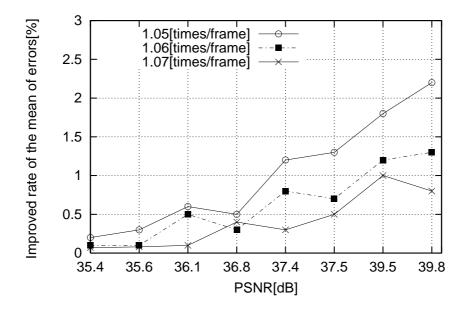
Figure 3.43: Improved rate of the mean of errors $\Delta\bar{e}$ in noisy image sequences of expansion.

58
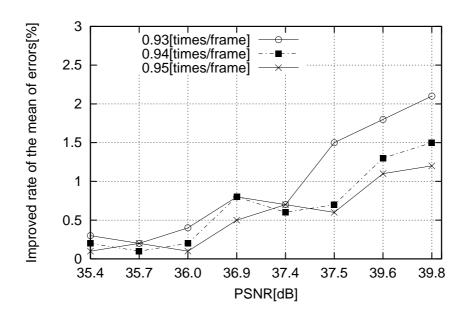
Figure 3.44: Improved rate of the mean of errors $\Delta\bar{e}$ in noisy image sequences of contraction.
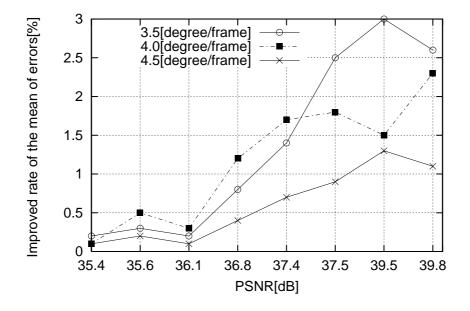
Figure 3.45: Improved rate of the mean of errors $\Delta\bar{e}$ in noisy image sequences of rotation.
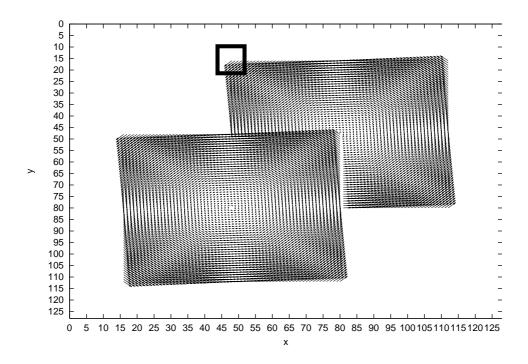
Figure 3.46: A correct velocity vector field in Rot8 of $PSNR$=36.8[dB].
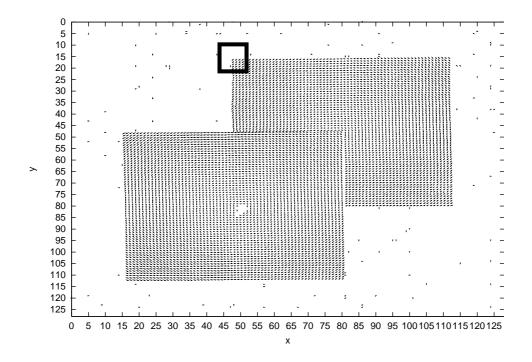
Figure 3.47: A velocity vector field estimated by the method via voting process with a weighting function in Rot8 of $PSNR$=36.8[dB].
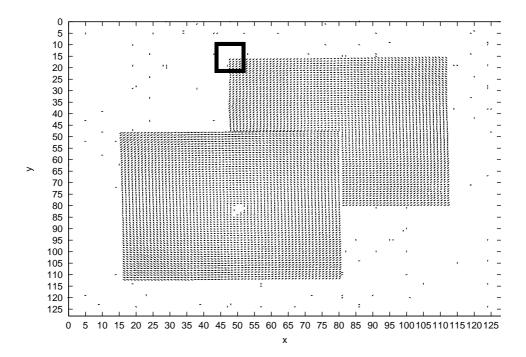
Figure 3.48: A velocity vector field applied extrapolation in Rot8 of $PSNR$=36.8[dB].
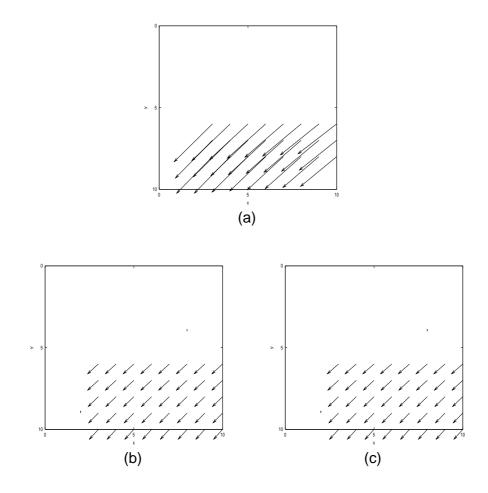
Figure 3.49: Expanded figures of the rectangle regions in (a):a correct velocity vector field, (b):Figure 3.47 and (c):Figure 3.48

3.4.3 Experiments in actual image sequences

(Experiment:3-A) Comparison of precision of velocity vector estimation in conventional methods and the method via voting process with a weighting g function

In order to evaluate effectiveness of the method via voting process with a weighting function, I experiment on applying the conventional methods and the method via voting process with a weighting function to actual image sequences including following motions

- · Translation

- · Expansion/Contraction

- · Rotation

In this experiments, I determine the parameters in the proposed methods and the method via voting process with a weighting function to the values shown in Table 3.17, Table 3.18 and Table 3.19 respectively.

Table 3.17: Parameters in local method.

The size of the support region	15×15[pixels]

Table 3.18: Parameters in global method.

Weighting coefficient of evaluation terms of smoothness	4.2
Repetition calculation times	120[times]

Table 3.19: The values in determined parameters of the method via voting process with a weighting function for actual image sequences.

The threshold in the voting possible condition 1	11[intensity]
The threshold in the voting possible condition 2	6[intensity]
The threshold in the voting possible condition 3	3[intensity]
The threshold in segmentation based on motion continuity	0.05
The size of the support region	35×35[pixels]
The size of each cell in the voting space	1.0×10^{-2}
The variance parameter in the weighting function	2
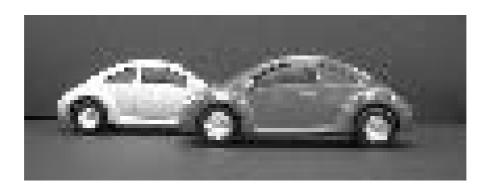
3 frames of each image sequence used in this experiments are shown in Figure 3.50,Figure 3.51 or Figure 3.52 respectively. The resolution of each image sequence are 106×41[pixels], 96×61[pixels] or 86×61[pixels] respectively.

The velocity vector fields estimated by conventional methods and the method via voting process with a weighting function in an actual image sequence including a translation motion are shown in Figure 3.53, Figure 3.54 and Figure 3.55 respectively. The velocity vector fields estimated by conventional methods and the method via voting process with a weighting function in an actual image sequence including expansion/contraction motions are shown in Figure 3.56, Figure 3.57 and Figure 3.58 respectively. The velocity vector fields estimated by conventional methods and the method via voting process with a weighting function in an actual image sequence including a rotation motion are shown in Figure 3.59, Figure 3.60 and Figure 3.61 respectively.
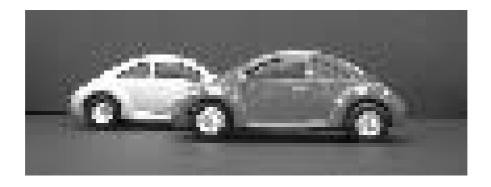
From the results, we see that we could precisely estimate by using the method via voting process with a weighting function. The factor is supposed to get rid of effectiveness of constraint equations that do not satisfy optical flow realizable conditions in occlusion regions and that are effected by noise, in addition to separating different motions.

Frame1

Frame2
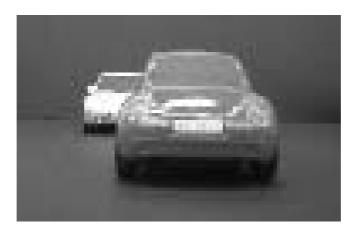
Frame3

Figure 3.50: The actual image sequence used in this experiments including a translation motion.

Frame1

Frame2

Frame3

Figure 3.51: The actual image sequence used in the experiments including a expansion/contraction motion.

Frame1

Frame2

Frame3

Figure 3.52: The actual image sequence used in this experiments including a rotation motion.
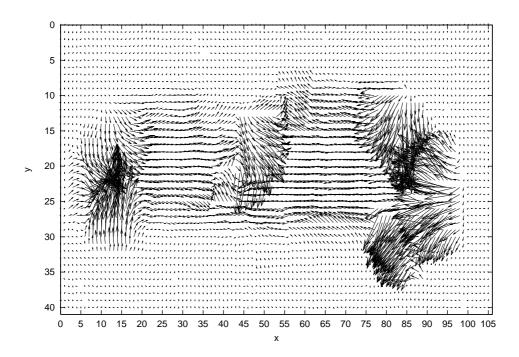
Figure 3.53: A velocity vector field estimated by local method n an actual image sequence including a translation motion.
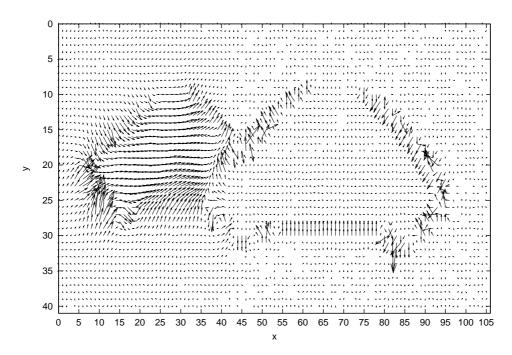
Figure 3.54: A velocity vector field estimated by global method in an actual image sequence including a translation motion.
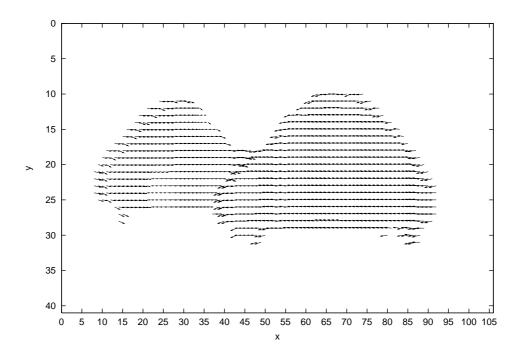
Figure 3.55: A velocity vector field estimated by the method via voting process with a weighting function in an actual image sequence including a translation motion.
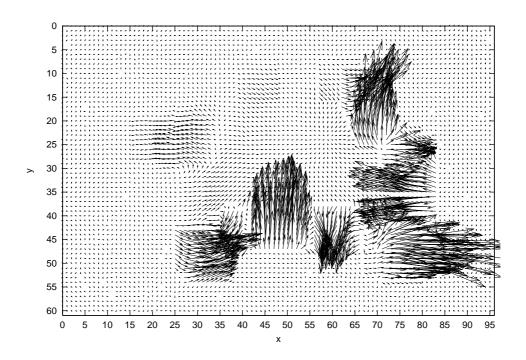
Figure 3.56: A velocity vector field estimated by local method n an actual image sequence including expansion/contraction motions.
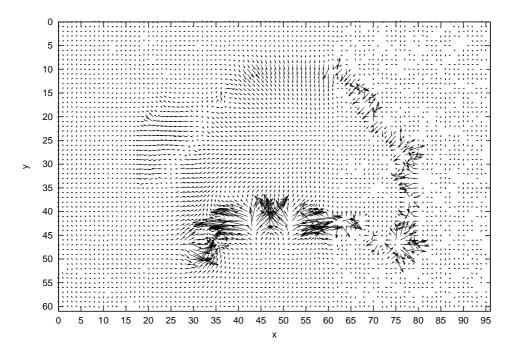
Figure 3.57: A velocity vector field estimated by global method in an actual image sequence including expansion/contraction motions.
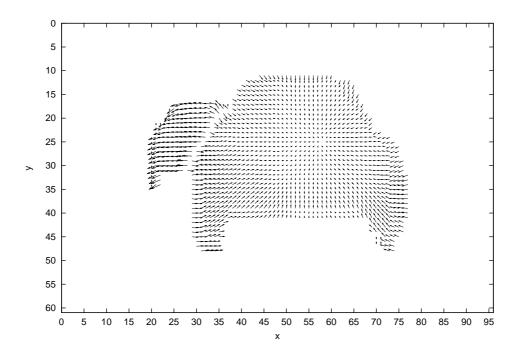
Figure 3.58: A velocity vector field estimated by the method via voting process with a weighting function in an actual image sequence including expansion/contraction motions.
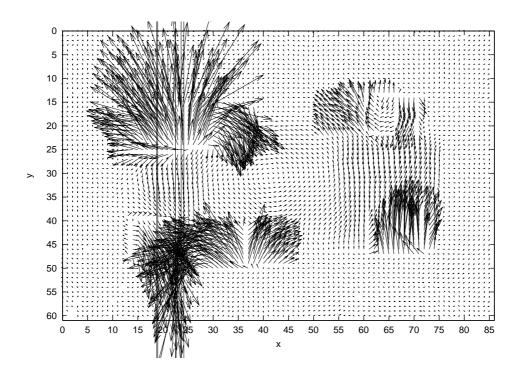
Figure 3.59: A velocity vector field estimated by local method n an actual image sequence including a rotation motion.
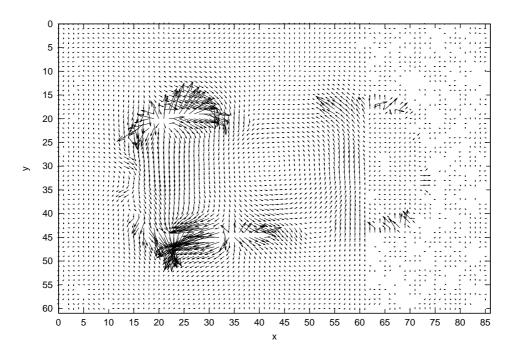
Figure 3.60: A velocity vector field estimated by global method in an actual image sequence including a rotation motion.
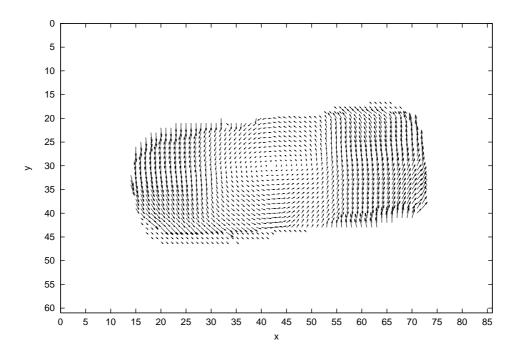
Figure 3.61: A velocity vector field estimated by the method via voting process with a weighting function in an actual image sequence including a rotation motion.

(Experiment:3-B) Comparison of precision of velocity vector estimation in conventional methods and the method via voting process with a weighting g function

In order to evaluate effectiveness of extrapolation, I experiment on comparison of velocity vector estimation precision of the method via voting process with a weighting function and in case of applying extrapolation in actual image sequences.

In this experiments, I determine the same parameters in the method via voting process with a weighting function as the parameters used in the previous experiment. I use the same image sequences used in the previous experiment.

The results of the experiments in an actual image sequence including translation motion are shown in Figure 3.62 and Figure 3.63. The expanded figure in rectangle regions in Figure 3.62 and Figure 3.63 is shown in Figure 3.64. The results of the experiments in an actual image sequence including expansion/contraction motion are shown in Figure 3.65 and Figure 3.66. The expanded figure in rectangle regions in Figure 3.65 and Figure 3.66 is shown in Figure 3.67. The results of the experiments in an actual image sequence including rotation motion are shown in Figure 3.68 and Figure 3.69. The expanded figure in rectangle regions in Figure 3.68 and Figure 3.69 is shown in Figure 3.70.

From the results, we see that precision of velocity vector estimation in occlusion regions was improved by applying extrapolation in each image sequence.
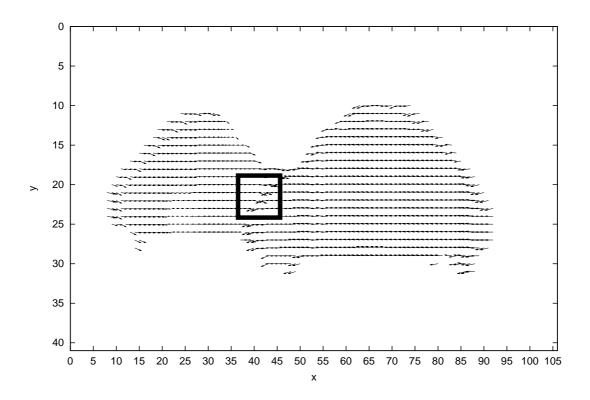
Figure 3.62: A velocity vector field estimated by the method via voting process with a weighting function.
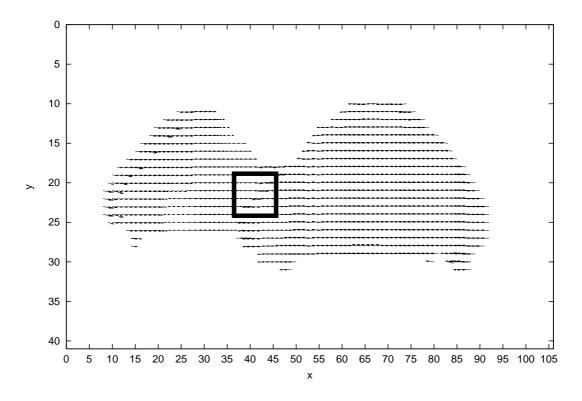
Figure 3.63: A velocity vector field applied extrapolation.

75

(a)

(b)
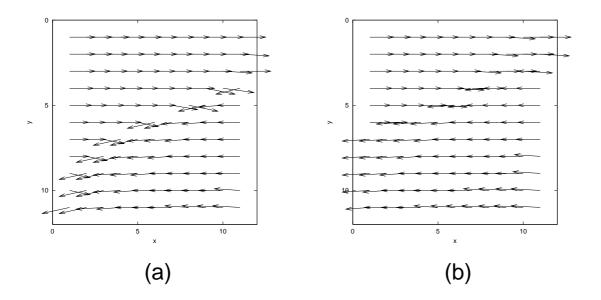
Figure 3.64: Expanded figures of rectangle regions in Figure 3.62 (a) and Figure 3.63 (b).
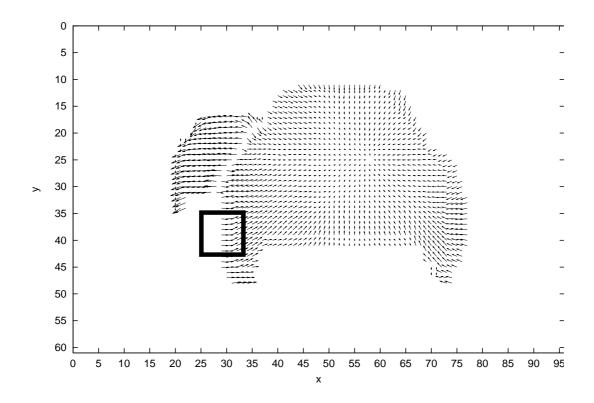
Figure 3.65: A velocity vector field estimated by the method via voting process with a weighting function.
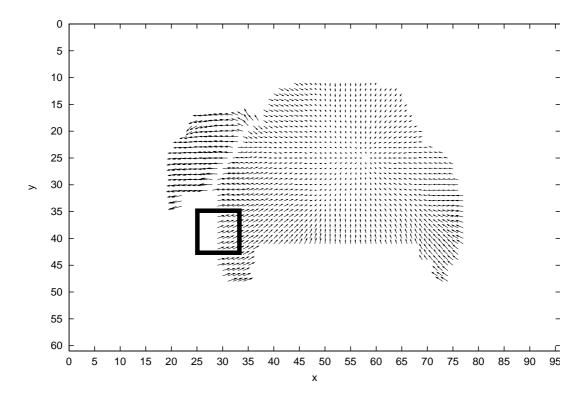
Figure 3.66: A velocity vector field applied extrapolation.

(a)   (b)
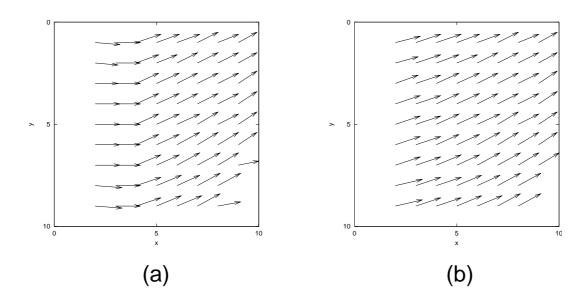
Figure 3.67: Expanded figures of rectangle regions in Figure 3.65 (a) and Figure 3.66 (b).
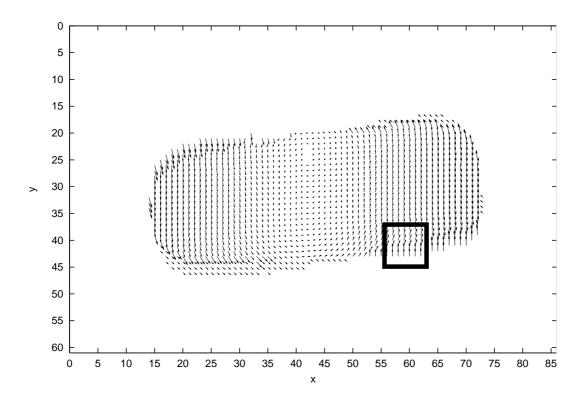
Figure 3.68: A velocity vector field estimated by the method via voting process with a weighting function.
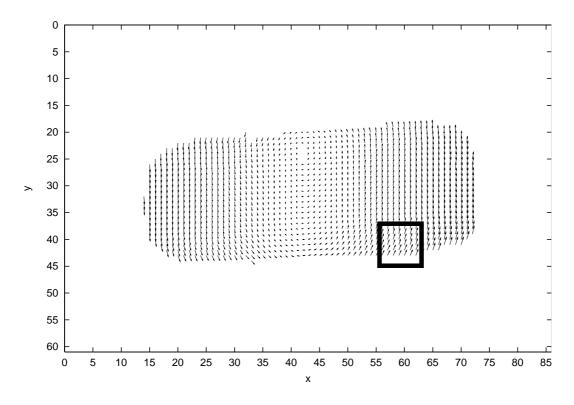
Figure 3.69: A velocity vector field applied extrapolation.

79
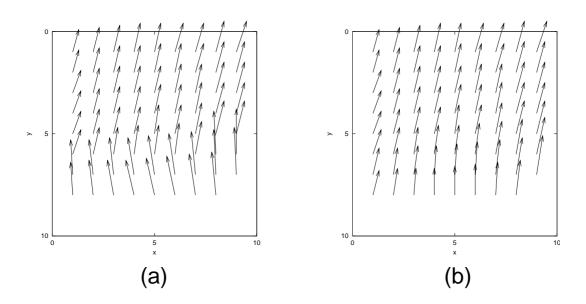
Figure 3.70: Expanded figures of rectangle regions in Figure 3.68 (a) and Figure 3.69 (b).

3.5 Summary

In order to precisely estimate velocity vectors in situation of occurring occlusion in actual image sequences, I proposed a method of velocity vector estimation based on voting process with a weighting function using extrapolation.

To evaluate effectiveness of the proposed method, I experimented on comparison of velocity vector estimation precision in conventional method and the method via voting process with a weighting function in synthesis image sequences and noisy synthesis image sequences. From the results of the experiment, by using the method via the voting process, I obtained approximately 40% higher precision of velocity vector estimation in the maximum than precision of velocity vector estimation in conventional methods. The factor is supposed to get rid of effectiveness of intersections of constraint equations in occlusion regions and separate different motions in regions including different motions, in addition to getting rid of effectiveness of noise. In order to moreover obtain precise estimation results in the estimation of velocity vectors using the voting process, primarily, we have to investigate the optimum weighting function for each application in velocity vector estimation considering occlusion.

I experimented on comparison of velocity vector estimation precision in the method via voting process with a weighting function and in case of applying extrapolation in synthesis image sequences and noisy synthesis image sequences. From the results of the experiment, by applying extrapolation, I obtained approximately 15% higher precision of velocity vector estimation in the maximum than precision of velocity vector estimation in the method using the voting process. The factor is supposed to extrapolate velocity vectors in occlusion regions from estimated velocity vectors in assigned regions of occlusion regions that has reliability. In order to moreover obtain precise estimation results in the estimation of velocity vectors using extrapolation, we have to improve the method using the voting method since extrapolation depends on the results of velocity vector estimation by the method using the voting method.

Finally, I experimented on comparison of velocity vector estimation precision in conventional method and the method via voting process with a weighting function in actual image sequences. By using the method via the voting process, I obtained well results of velocity vector estimation precision in comparison with the conventional methods. Similarly, I experimented on comparison of velocity vector estimation precision in the method via voting process with a weighting function and in case of applying extrapolation in actual image sequences. By applying extrapolation, I obtained well results of velocity vector estimation precision in comparison with the method via the voting process.

Chapter 4

A new method of velocity vector estimation for solving the brightness change problem

4.1 Introduction

Estimation of optical flow is an available method for motion analysis in image sequence. However, there is a problem such that estimation precision of velocity vectors declines in a situation of brightness change.

In case of dealing with physical phenomena such as metrology or fluid analysis, there are cases not avoiding to brightness change[51]. For instance, in the field of metrology, they analyze cloud motion using image sequences taken in enough time intervals because of infinitesimal cloud motion in actual time rates of camera. In case of analysis of cloud motion using image sequence taken by satellites, the image sequences taken by satellites in enough time intervals occur brightness change by shading effect caused by rotation of the earth. Moreover, in case of taking image sequences of cloud in enough time intervals from the ground, brightness change occurs in the image sequences of cloud by changing of an angle of incidence of the sun by rotation of the earth. In 3-dimensional high-speed motion objects such as fluid, in normal NTSC video frame rates, brightness change occurs by shading, shadowing or high speeding of object motion. In these situations, we have to consider brightness change for precision estimation of velocity vectors.

To precisely estimate velocity vectors in these situations, following method considering brightness change have been proposed. The methods are classified into

- · Methods considering intensity change with respect to time[51][52]
- · Methods considering intensity change with respect to time and space[53][54]

These methods have effective properties for estimating velocity vectors in the situation of brightness change in actual image sequence.

By dealing with estimating velocity vectors in a situation of occurring brightness change as estimating the most likelihood parameter of constraint equations considering brightness change in a parameter space, I propose a method that has all effective properties in the conventional methods considering brightness change and an effective property which has not obtained by the conventional methods. In order to estimate the most likelihood parameter in a parameter space, I expand the parameter space to a 3-dimensional

parameter space since a constraint equation considering brightness change has three parameters. I then estimate the parameters in the constraint equation by using a voting process with a weighting function in a 3-dimensional voting space.

In object tracking systems such as an observation system of invasion or observation system of traffic considering a situation that an object moves into a region of shade or moves out from a region of shade, we have to consider the brightness change on the object. Thus, we can expect to apply the proposed method to the object tracking systems. In an robot control using visual servo such as guard robots considering a situation that robot moves across different lighting environments, we have to consider the different lighting environments in the visual servo, Therefore, we can apply the method to the robot control using visual servo.

4.2 Extension of a velocity vector constraint equation

In this section, I derive a velocity vector constraint equation which is taken account of intensity change between corresponding points.

Let $I(x, y, t)$ be an intensity of a pixel (x, y) in an image at the time of t, and let $I(x + \Delta x, y + \Delta y, t + \Delta t)$ be an intensity of the corresponding pixel $(x + \Delta x, y + \Delta y)$ in an image at the time of $t + \Delta t$. Let W be a quantity of intensity change. The relation between $I(x, y, t)$ and $I(x + \Delta x, y + \Delta y, t + \Delta t)$ is expressed by

$$I(x + \Delta x, y + \Delta y, t + \Delta t) - I(x, y, t) = W. \tag{4.1}$$

We can expand the left side of (4.1) in a Taylor series and obtain

$$\frac{\partial I}{\partial x}\Delta x + \frac{\partial I}{\partial y}\Delta y + \frac{\partial I}{\partial t}\Delta t + e = W, \tag{4.2}$$

where e contains second- and high order terms in Δx, Δy and Δt. Because we consider that e is sufficiently small, we ignore e. We can divide both sides of (4.2) by Δt. We take the limits as $\Delta t \to 0$, we obtain

$$\frac{\partial I}{\partial x}\frac{dx}{dt} + \frac{\partial I}{\partial y}\frac{dy}{dt} + \frac{\partial I}{\partial t} = \frac{W}{dt}. \tag{4.3}$$

Using the abbreviations $I_x = \frac{\partial I}{\partial x}, I_y = \frac{\partial I}{\partial y}, I_t = \frac{\partial I}{\partial t}$, $u = \frac{dx}{dt}, v = \frac{dy}{dt}, w = \frac{W}{dt}$. We obtain

$$I_x u + I_y v + I_t = w. \tag{4.4}$$

Equation (4.4) is a velocity vector constraint equation which is taken account of intensity change between corresponding points. Equation (4.4) is used in conventional methods. However, interpretation of the constraint equation in conventional methods differs from our interpretation of the constraint equation.

4.3 Properties of conventional methods

The methods of velocity vector estimation to apply for brightness change have been proposed by Nomura[51], Cornelius[52], Mukawa[53] and Negahdaripour[54]. The conventional methods are classified into two categories.

First, there are the methods which use temporal constraint (Equation (4.4)) of intensity change. The methods have been proposed by Nomura [51] and Cornelius [52]. Nomura derived the Equation (4.4) which based on the theorem of influx-efflux intensity. The method determines parameters in equation (4.4) by using a constraint condition that object motions and intensity change are constant in at least three frames. Cornelius derived the constraint equation (Equation (4.4)) which is assumed that w only depends on diffuse reflection component in a reflection model [67].

On the other hand, the methods which use temporal and spatial constraints have been proposed by Mukawa[53] and Negahrdairpour [54]. Mukawa derived the constraint equations such as

$$w_x = cI_x, \tag{4.5}$$

$$w_y = cI_y, \tag{4.6}$$

where c is a constant, w_x and w_y are differentials of w with respect to x and y, I_x and I_y are differentials of intensity I with respect to x and y, respectively. Equation (4.5) and (4.6) represent the relations between quantity of intensity change in a pixel and quantity of spatial intensity change. Negahdaripour extended the Mukawa's method to apply to the situation that light source intensity changes temporally. These methods can be applied to the situation that a reflection rate of an object changes spatially.

The properties of conventional methods are shown in Table 4.1. The sign o in the table expresses that the method has the property is specified in their research paper. The sign × in the table expresses that the method does not have the property is specified in their research paper. The sign − in the table expresses that the method has the property is not specified in their research paper.

Table 4.1: Properties of each method (1=the parameters in a constraint equation can be estimated in 2 frames, 2=the reflection rate on the surface of an object is not necessary to be constant, 3=change of intensity by effectiveness of shading is considered, 4=change of intensity by changing of a light source intensity is considered, 5=the method has robustness against noise, 6=the method has robustness in the region where pattern changes intensely).

	Properties					
	1	2	3	4	5	6
Nomura[51]	×	-	-	o	o	-
Cornelius[52]	o	×	o	-	-	-
Mukawa[53]	o	o	o	×	-	-
Negahdaripour[54]	o	o	o	o	-	-

4.4 An estimation method of velocity vectors for brightness change using 3-dimensional voting space

The conventional methods have effective properties for estimating velocity vectors in the situation of brightness change in actual image sequence.

By dealing with estimating velocity vectors in a situation of occurring brightness change as estimating the most likelihood parameter of constraint equations considering brightness change in a parameter space, I propose a method that has all effective properties in the conventional methods considering brightness change. In order to realize the method, we first use an assumption for velocity vector estimation for obtaining the property 1. Second, since a constraint equation considering brightness change has three parameters, I estimate the parameters in the constraint equation by using a voting process with a weighting function in a 3-dimensional voting space and a condition of constraint equations for voting for obtaining properties from 2 through 6.

4.4.1   An assumption for velocity vector estimation in the situation of brightness change
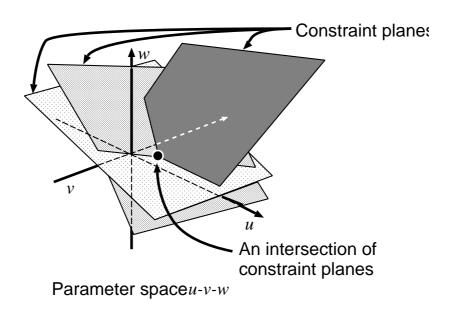
Figure 4.1: Constraint planes on u-v-w space and an intersection point

Equation (4.4) contains three parameters u, v and w. In parameter space u-v-w, equation (4.4) expresses a plane. Thus, we call equation (4.4) a constraint plane. A constraint plane is obtained in each pixel. However, it is impossible to determine parameters because a constraint plane contains three parameters. Therefore, we use an assumption "a notice pixel and the neighboring pixels have the similar values of parameters in the constraint equation". It is possible to determine the value of the parameters uniquely unless constraint planes are not parallel to each other in at least three constraint planes (Figure 4.1). By using this assumption, We can determine parameters in the constraint equation, since the coefficients I_x, I_y and I_t in the constraint equation (4.4) are able to be determined from 2 image frames in an image sequence. Thus, it is possible to obtain property 1.

4.4.2 A velocity vector estimation by using voting process

In the actual situations, intersections of constraint planes are scattered by following factors from **(A)** to **(C)**.

(A) Fluctuation of the value of parameter w

Intensity $I(x, y, t)$ is expressed by using a reflection model [67] such as

$$I(x, y, t) = R_a I_a + R_d I_q \cos \theta_1 + R_f I_q \cos^n \theta_2, \tag{4.7}$$

where

I_a : Intensity of ambient

I_q : Intensity of a light source

R_a : Ambient reflection rate

R_d : Diffuse reflection rate

θ_1 : Angle between the normal vector on a object surface and the direction of incidence light

θ_2 : Angle between the direction of reflection light and eyes

R_f : Specular reflection rate

n : Parameter of high light.

By using the reflection model, an intensity of a corresponding point $I(x+\Delta x, y+\Delta y, t+\Delta t)$ is expressed as

$$I(x + \Delta x, y + \Delta y, t + \Delta t) = R_a I_a' + R_d I_q' \cos \theta_1' + R_f I_q' \cos^n \theta_2', \tag{4.8}$$

where

I_a' : Intensity of ambient in a corresponding point

I_q' : Intensity of a light source in a corresponding point

θ_1' : Angle between normal vector on an object surface and incidence light in a corresponding point

θ_2' : Angle between reflection light and eye in a corresponding point.

By using equation (4.1) and (4.3)w in (4.4) is expressed as

$$w = \frac{1}{dt}\{I(x + \Delta x, y + \Delta y, t + \Delta t) - I(x, y, t)\}. \tag{4.9}$$

I substitute equation (4.7) and (4.8) for (4.9) and obtain

$$w = \frac{1}{dt}\{R_a(I_a' - I_a) + R_d(I_q' \cos \theta_1' - I_q \cos \theta_1) + R_f(I_q' \cos^n \theta_2' - I_q \cos^n \theta_2)\}. \tag{4.10}$$

In equation (4.10), the parameters which change spatially are θ_1, θ_2, R_a, R_d and R_f. The quantity of spatial change Δw of the parameter w is expressed by

$$
\begin{aligned}
\Delta w \;=\; & \frac{1}{dt}\Bigg[\{(R_a + \Delta R_a)(I_a' - I_a) - R_a(I_a' - I_a)\} \\
& + \; (R_d + \Delta R_d)\left\{I_q' \cos(\theta_1 + \Delta\theta_1)' - I_q \cos(\theta_1 + \Delta\theta_1)\right\} \\
& - \; R_d\left(I_q' \cos\theta_1' - I_q \cos\theta_1\right) \\
& + \; (R_f + \Delta R_f)\left\{I_q' \cos^n(\theta_2 + \Delta\theta_2)' - I_q \cos^n(\theta_2 + \Delta\theta_2)\right\} \\
& - \; R_f\left(I_q' \cos^n \theta_2' - I_q' \cos^n \theta_2\right)\Bigg].
\end{aligned}
$$

$$\tag{4.11}$$

If $\Delta\theta_1 \to 0$, $\Delta\theta_2 \to 0$, $\Delta R_a \to 0$, $\Delta R_d \to 0$, $\Delta R_f \to 0$, then Δw converges to zero. However, in an actual image space which is discrete, there is quantity of spatial change because the each delta parameter has enough large values in an actual image space.

(B) Fluctuation of the value of parameters u,v

A point (x, y, z) in three-dimensional space is projected to a point (X, Y) in two-dimensional projection plane such as

$$\begin{pmatrix} X \\ Y \end{pmatrix} = f \begin{pmatrix} \frac{x}{z} \\ \frac{y}{z} \end{pmatrix}, \tag{4.12}$$

where f is a focal length. Similarly, a point of (x', y', z') which is moved from (x, y, z) in a three-dimensional space is projected to a point (X', Y') in two-dimensional projection plane such as

$$\begin{pmatrix} X' \\ Y' \end{pmatrix} = f \begin{pmatrix} \frac{x'}{z'} \\ \frac{y'}{z'} \end{pmatrix}. \tag{4.13}$$

A velocity vector $(u, v)^\top$ is expressed as

$$\begin{pmatrix} u \\ v \end{pmatrix} = \begin{pmatrix} X' \\ Y' \end{pmatrix} - \begin{pmatrix} X \\ Y \end{pmatrix}. \tag{4.14}$$

We substitute (4.12) and (4.13) for (4.14) and then obtain

$$\begin{pmatrix} u \\ v \end{pmatrix} = f \begin{pmatrix} \frac{x'}{z'} - \frac{x}{z} \\ \frac{y'}{z'} - \frac{y}{z} \end{pmatrix}. \tag{4.15}$$

Similarly, a velocity vector $(u^*, v^*)^\top$ in a coordinate $(x + \Delta x, y + \Delta y, t + \Delta t)$ is expressed as the following equation in a two-dimensional projection plane

$$\begin{pmatrix} u^* \\ v^* \end{pmatrix} = f \begin{pmatrix} \frac{(x+\Delta x)'}{(z+\Delta z)'} - \frac{(x+\Delta x)}{(z+\Delta z)} \\ \frac{(y+\Delta y)'}{(z+\Delta z)'} - \frac{(y+\Delta y)}{(z+\Delta z)} \end{pmatrix}. \tag{4.16}$$

We define a spatial changes of velocity vectors $(\Delta u, \Delta v)^\top$ by

$$\begin{pmatrix} \Delta u \\ \Delta v \end{pmatrix} = \begin{pmatrix} u^* \\ v^* \end{pmatrix} - \begin{pmatrix} u \\ v \end{pmatrix} \tag{4.17}$$

$$= f \begin{pmatrix} \frac{(x+\Delta x)'}{(z+\Delta z)'} - \frac{x+\Delta x}{z+\Delta z} \\ \frac{(y+\Delta y)'}{(z+\Delta z)'} - \frac{y+\Delta y}{z+\Delta z} \end{pmatrix} - f \begin{pmatrix} \frac{x'}{z'} - \frac{x}{z} \\ \frac{y'}{z'} - \frac{y}{z} \end{pmatrix}. \tag{4.18}$$

We consider in isotropic motion. Any isotropic motion for a point (x, y, z) is expressed as

$$\begin{pmatrix} x' \\ y' \\ z' \end{pmatrix} = \boldsymbol{ER} \begin{pmatrix} x \\ y \\ z \end{pmatrix} + \boldsymbol{T} \tag{4.19}$$

where

$$\boldsymbol{E} = \begin{pmatrix} a & 0 & 0 \\ 0 & b & 0 \\ 0 & 0 & c \end{pmatrix}, \boldsymbol{R} = \begin{pmatrix} \cos\gamma & -\sin\gamma & 0 \\ \sin\gamma & \cos\gamma & 0 \\ 0 & 0 & 1 \end{pmatrix} \begin{pmatrix} \cos\beta & 0 & \sin\beta \\ 0 & 1 & 0 \\ -\sin\beta & 0 & \cos\beta \end{pmatrix} \begin{pmatrix} 1 & 0 & 0 \\ 0 & \cos\alpha & -\sin\alpha \\ 0 & \sin\alpha & \cos\alpha \end{pmatrix},$$

$$\boldsymbol{T} = \begin{pmatrix} t_x \\ t_y \\ t_z \end{pmatrix},$$

a,b,c are expansion/contraction rate for x,y,z axis respectively, α,β,γ are rotation angle for x,y,z axis respectively, t_x,t_y,t_z are quantity of translation for x,y,z axis respectively. Similarly, isotropic motions in a point on the coordinate $(x + \Delta x, y + \Delta y, z + \Delta z)$ is expressed as

$$\begin{pmatrix} (x + \Delta x)' \\ (y + \Delta y)' \\ (z + \Delta z)' \end{pmatrix} = \boldsymbol{ER} \begin{pmatrix} x + \Delta x \\ y + \Delta y \\ z + \Delta z \end{pmatrix} + \boldsymbol{T}. \tag{4.20}$$

We substitute (4.19) and (4.20) for (4.18) and obtain

$$\begin{pmatrix} \Delta u \\ \Delta v \end{pmatrix} = f \begin{pmatrix} \frac{a\{\cos\beta\cos\alpha(x+\Delta x)+(-\cos\alpha\sin\gamma+\sin\alpha\sin\beta\sin\gamma)(y+\Delta y)+(\sin\alpha\sin\gamma+\cos\alpha\sin\beta\cos\gamma)(z+\Delta z)\}+t_x}{c\{-\sin\beta(x+\Delta x)+\sin\alpha\cos\beta(y+\Delta y)+\cos\alpha\cos\beta(z+\Delta z)\}+t_z} \\ \frac{b\{\cos\beta\sin\gamma(x+\Delta x)+(\cos\alpha\cos\gamma+\sin\alpha\sin\beta\sin\gamma)(y+\Delta y)+(-\sin\alpha\cos\gamma+\cos\alpha\sin\beta\sin\gamma(z+\Delta z)\}+t_y}{c\{-\sin\beta(x+\Delta x)+\sin\alpha\cos\beta(y+\Delta y)+\cos\alpha\cos\beta(z+\Delta z)\}+t_z} \end{pmatrix}$$
$$- f \begin{pmatrix} \frac{a\{\cos\beta\cos\alpha x+(-\cos\alpha\sin\gamma+\sin\alpha\sin\beta\sin\gamma)y+(\sin\alpha\sin\gamma+\cos\alpha\sin\beta\cos\gamma)z\}+t_x}{c\{-\sin\beta x+\sin\alpha\cos\beta y+\cos\alpha\cos\beta z\}+t_z} \\ \frac{b\{\cos\beta\sin\gamma x+(\cos\alpha\cos\gamma+\sin\alpha\sin\beta\sin\gamma)y+(-\sin\alpha\cos\gamma+\cos\alpha\sin\beta\sin\gamma z)\}+t_y}{c\{-\sin\beta x+\sin\alpha\cos\beta y+\cos\alpha\cos\beta z\}+t_z} \end{pmatrix}. \tag{4.21}$$

If $\Delta x \to 0$, $\Delta y \to 0$, $\Delta z \to 0$, then each element of $(\Delta u, \Delta v)^\top$ converges to zero. However, in an actual image space which is discrete, there is quantity of spatial change because the each delta parameter has enough large values in an actual image space.

(C) Fluctuation of intersections of constraint equation by influence of intersections of constraint equations in regions where pattern changes intensely or constraint equations effected by noise

I consider three constraint equations (4.4) that satisfy realizable conditions of the constraint equations in a support region. The equations are expressed by

$$I_x^{(1)}u + I_y^{(1)}v + I_t^{(1)} = w, \tag{4.22}$$

$$I_x^{(2)}u + I_y^{(2)}v + I_t^{(2)} = w, \tag{4.23}$$

$$I_x^{(3)}u + I_y^{(3)}v + I_t^{(3)} = w, \tag{4.24}$$

where $I_x^{(1)}$, $I_y^{(1)}$ or $I_t^{(1)}$ denote partial differential coefficients of $I(x, y, t)$ with respect to x, y and t on a first pixel in a support region respectively, $I_x^{(2)}$, $I_y^{(2)}$ or $I_t^{(2)}$ denote partial differential coefficients of $I(x, y, t)$ with respect to x, y and t on a second pixel in a support region respectively, $I_x^{(3)}$, $I_y^{(3)}$ or $I_t^{(3)}$ denote partial differential coefficients of $I(x, y, t)$ with respect to x, y and t on a third pixel in a support region respectively, An intersection $(u, v, w)^\top$ of these constraint equations is expressed as

$$\begin{pmatrix} u \\ v \\ w \end{pmatrix} = \begin{pmatrix} \frac{(I_t^{(1)}I_y^{(2)}-I_t^{(2)}I_y^{(1)})(I_y^{(3)}-I_y^{(1)})-(I_y^{(2)}-I_y^{(1)})(I_t^{(1)}I_y^{(3)}-I_t^{(3)}I_y^{(1)})}{(I_x^{(1)}I_y^{(2)}-I_x^{(2)}I_y^{(1)})(I_y^{(3)}-I_y^{(1)})-(I_x^{(1)}I_y^{(3)}-I_x^{(3)}I_y^{(1)})(I_y^{(2)}-I_y^{(1)})} \\ \frac{(I_t^{(1)}I_x^{(2)}-I_t^{(2)}I_x^{(1)})(I_x^{(3)}-I_x^{(1)})-(I_x^{(2)}-I_x^{(1)})(I_t^{(1)}I_x^{(3)}-I_t^{(3)}I_x^{(1)})}{(I_y^{(1)}I_x^{(2)}-I_y^{(2)}I_x^{(1)})(I_x^{(3)}-I_x^{(1)})-(I_y^{(1)}I_x^{(3)}-I_y^{(3)}I_x^{(1)})(I_x^{(2)}-I_x^{(1)})} \\ \frac{(I_t^{(1)}I_x^{(2)}-I_t^{(2)}I_x^{(1)})(I_y^{(1)}I_x^{(3)}-I_y^{(3)}I_x^{(1)})-(I_y^{(1)}-I_x^{(2)}-I_y^{(2)}-I_x^{(1)})(I_t^{(1)}-I_x^{(3)}-I_t^{(3)}-I_x^{(1)})}{(I_x^{(2)}I_x^{(1)})((I_y^{(1)}I_x^{(3)}-I_y^{(3)}I_x^{(1)})-(I_y^{(1)}-I_x^{(2)}-I_y^{(2)}-I_x^{(1)})(I_x^{(3)}-I_x^{(1)}))} \end{pmatrix}. \tag{4.25}$$

If the equation (4.22) is a constraint equation in regions where pattern changes intensely such as regions in boundaries of objects or a constraint equation effected by noise, the

spatial/temporal gradients in the image are changed intensely. Thus, (4.22) is replaced by

$$I_x^{(1)'} u + I_y^{(1)'} v + I_t^{(1)'} = w, \tag{4.26}$$

where $I_x^{(1)'}$, $I_y^{(1)'}$ or $I_t^{(1)'}$ are changed coefficients of equation (4.22). Therefore the intersection $(u, v, w)^\top$ of the constraint equations is changed to

$$\begin{pmatrix} u' \\ v' \\ w' \end{pmatrix} = \begin{pmatrix} \frac{(I_t^{(1)'} I_y^{(2)} - I_t^{(2)} I_y^{(1)'})(I_y^{(3)} - I_y^{(1)'}) - (I_y^{(2)} - I_y^{(1)'})(I_t^{(1)'} I_y^{(3)} - I_t^{(3)} I_y^{(1)'})}{(I_x^{(1)'} I_y^{(2)} - I_x^{(2)} I_y^{(1)'})(I_y^{(3)} - I_y^{(1)'}) - (I_x^{(1)'} I_y^{(3)} - I_x^{(3)} I_y^{(1)'})(I_y^{(2)} - I_y^{(1)'})} \\ \frac{(I_t^{(1)'} I_x^{(2)} - I_t^{(2)} I_x^{(1)'})(I_x^{(3)} - I_x^{(1)'}) - (I_x^{(2)} - I_x^{(1)'})(I_t^{(1)'} I_x^{(3)} - I_t^{(3)} I_x^{(1)'})}{(I_y^{(1)'} I_x^{(2)} - I_y^{(2)} I_x^{(1)'})(I_x^{(3)} - I_x^{(1)'}) - (I_y^{(1)'} I_x^{(3)} - I_y^{(3)} I_x^{(1)'})(I_x^{(2)} - I_x^{(1)'})} \\ \frac{(I_t^{(1)'} I_x^{(2)} - I_t^{(2)} I_x^{(1)'})(I_y^{(1)'} I_x^{(3)} - I_y^{(3)} I_x^{(1)'}) - (I_y^{(1)'} - I_x^{(2)} - I_y^{(2)} - I_x^{(1)'})(I_t^{(1)'} - I_x^{(3)} - I_t^{(3)} - I_x^{(1)'})}{(I_x^{(2)} I_x^{(1)'})((I_y^{(1)'} I_x^{(3)} - I_y^{(3)} I_x^{(1)'}) - (I_y^{(1)'} - I_x^{(2)} - I_y^{(2)} - I_x^{(1)'})(I_x^{(3)} - I_x^{(1)'})} \end{pmatrix}. \tag{4.27}$$

Then, I define a difference vector $(\Delta u, \Delta v, \Delta w)^\top$ as

$$\begin{pmatrix} \Delta u \\ \Delta v \\ \Delta w \end{pmatrix} = \begin{pmatrix} u - u' \\ v - v' \\ w - w' \end{pmatrix}. \tag{4.28}$$

Since $I_x^{(1)} \neq I_x^{(1)'}$, $I_y^{(1)} \neq I_y^{(1)'}$, $I_t^{(1)} \neq I_t^{(1)'}$, the difference vector $(\Delta u, \Delta v, \Delta w)^\top$ is not zero vector. This means, if there is a constraint equation in regions where pattern changes intensely or a constraint equation effected by noise in a support region, intersections of constraint equation are scattered.
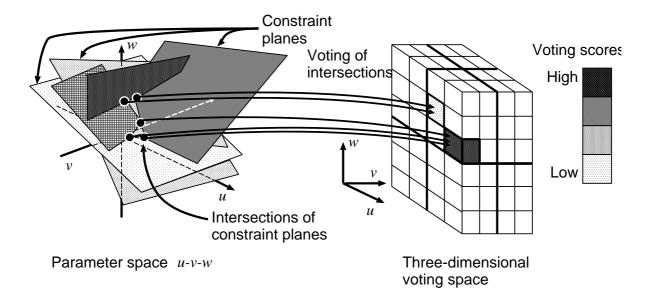

Figure 4.2: Voting of intersection to three-dimensional voting space

I use voting process to estimate values of estimation parameters from scattered intersections of constraint planes by the factors of (**A**) and (**B**), excluding intersections of constraint planes by the factors of (**C**). By voting of intersections in the parameter space

u-v-w to the voting space, if scattered intersections of constraint planes by the factors of (**A**) and (**B**) converge into a cell in voting space, the voting score in the cell will be the maximum voting score. Then we decide the coordinate of the maximum voting score as estimated parameters u, v and w. By this process, we can expect to precisely estimate estimated parameters u and v excluding the intersections of constraint planes by the factors of (**C**) (Figure 4.2).

In order to separate different motions from an interest pixel, we use constraint planes that satisfy the following constraint planes such as

· Constraint planes on pixels of the same object as on an interest pixel.

We assume that intensity of an interest pixel and the neighboring pixels are almost equivalent, if they are in a same object. If the assumption holds, the condition is formularize as

$$|I(x, y, t) - I(a, b, t)| \leq Th_b, \tag{4.29}$$

where $I(a, b, t)$ is intensity of an interest pixel (a, b) at time t, $I(x, y, t)$ is intensity of neighboring pixels of the interest pixel at time t, Th_b is a threshold in the condition. We adopt constraint equations that satisfy the above condition to voting process.

It is possible to obtain the properties from 2 through 6 because fluctuation of intersections is restrained by using voting procedure and a condition of constraint equation for voting.

4.4.3 Weighting of voting score by weight function

In case that intersections of constraint planes do not converge into a cell in voting space, There is a case that we cannot obtain the maximum voting score by fluctuation of voting scores. To obtain the reasonable maximum voting score in case of fluctuation of voting scores, a method of voting process with a weighting function has been proposed. This method detects the reasonable maximum voting score $(u_{med}, v_{med}, w_{med})$ in $f'(u_\alpha, v_\alpha, w_\alpha)$ convoluting voting score $f(u, v, w)$ by a weighting function $w(u - u_\alpha, v - v_\alpha, w - w_\alpha; \sigma_{uv}, \sigma_w)$. The $f'(u_\alpha, v_\alpha, w_\alpha)$ is expressed as

$$f'(u_\alpha, v_\alpha, w_\alpha) = \sum_{u=-V/2}^{V/2} \sum_{v=-V/2}^{V/2} \sum_{w=-V_w/2}^{V_w/2} w(u - u_\alpha, v - v_\alpha, w_\alpha; \sigma_{uv}, \sigma_w) f(u, v, w), \tag{4.30}$$

where V denotes axis size of each u and v in the voting space, V_w denotes axis size of w in the voting space, u_α, v_α and w_α denote interest coordinates in voting space. We use Gaussian function as a weighting function

$$w(u - u_\alpha, v - v_\alpha, w - w_\alpha; \sigma_{uv}, \sigma_w) = \frac{1}{(2\pi)^{3/2} \sqrt{\sigma_{uv}} \sqrt{\sigma_w}} \exp(A) \tag{4.31}$$

experimentally, where

$$A = \left\{ -\frac{(u - u_\alpha)^2 + (v - v_\alpha)^2}{2\sigma_{uv}^2} - \frac{(w - w_\alpha)^2}{2\sigma_w^2} \right\} \tag{4.32}$$

σ_{uv} and σ_w are a variance parameter on u and v axis in the voting space and a variance parameter on w axis in the voting space respectively.
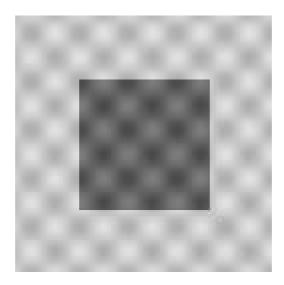
Figure 4.3: An image used for this experiment on evaluating property 1 and property 2.

4.5 Experiments for evaluating properties in a estimation method of velocity vectors for brightness change using a 3-dimensional voting space

In order to evaluate that the proposed method has all properties of conventional methods, I first experiment on comparison of velocity vector estimation precision of conventional methods and the proposed method in synthesis image sequences generated by computer graphics. I then apply the conventional methods and the proposed method to actual image sequence. In velocity vector estimation using actual image sequences, we can not obtain actual velocity vectors, we can not quantitatively evaluate precision of velocity vevtor estimation. Thus, we qualitatively evaluate results of velocity vector estimation.

4.5.1 Experiments in synthesis image sequences

In order to quantitatively evaluate that the proposed method has all properties, I experiment on comparison of velocity vector estimation precision of the conventional methods and the proposed method in synthesis image sequences generated by computer graphics.

Experiments on evaluating property 1 and property 2

In order to evaluate that the proposed method has property 1 and property 2, I experiment on comparison of velocity vector estimation precision of conventional methods and the proposed method by applying these methods to image sequence whose temporal intensity change on inside of an object is different from its on outside of an object by difference of reflection rate. The first image frame used in this experiment is shown in Figure 4.3. the second and third image frames used in this experiment are transformed by affine transformation shown in Table 4.8, Table 4.9, Table 4.10 and Table 4.11, on condition that parameters in Table 4.8 are defined right direction as positive direction, parameters in Table 4.11 are defined counterclockwise as positive direction. Parameters

of image frames used in this experiment are shown in Table 4.2.

Table 4.2: Parameters in generated images used in this experiment

Frequency of a sine wave (Texture)	0.12[Hz]
Amplitude of a sine wave (Texture)	25[intensity]
Bias of intensity (Inside of the object)	100[intensity]
Bias of intensity (Outside of the object)	200[intensity]
Quantity of temporal intensity change (Inside of the object)	-20[intensity/frame]
Quantity of temporal intensity change (Outside of the object)	-10[intensity/frame]
Resolution	128×128[pixels]

Parameters of the conventional methods and the proposed method are shown in from Table 4.3 through Table 4.7.

Table 4.3: Parameters in the proposed method

The threshold in the voting possible condition	30[intensity]
The size of the support region	30×30[pixels]
The size of a cell in the voting space	1.0×10^{-2}
The variance parameter in the weighting function σ_{uv}	4
The variance parameter in the weighting function σ_w	4

Table 4.4: Parameters in Cornelius's method

Weighting of spatial smoothness of velocity vectors α	3.2
Weighting of spatial smoothness of temporal intensity change β	1.8
The number of times of iterative calculation	50000[Times]

As evaluation scale for evaluating precision of velocity vector estimation, I use the mean of normalized error

$$\bar{e_n} = \frac{1}{MN} \sum_{x=0}^{M-1} \sum_{y=0}^{N-1} \frac{||\tilde{\boldsymbol{f}}_{xy} - \hat{\boldsymbol{f}}_{xy}||}{||\tilde{\boldsymbol{f}}_{xy}||}, \tag{4.33}$$

where M, N are the vertical/horizontal size of image frame respectively, $\tilde{\boldsymbol{f}}_{xy}$ is a correct velocity vector in (x, y), $\hat{\boldsymbol{f}}_{xy}$ is an estimated velocity vector in (x, y).

As examples, a correct velocity vector field and estimated velocity vector fields in P12_Trans1 are shown in from Figure 4.4 though Figure 4.9. In regions where reflection rate changes intensely, we see that the proposed method could estimate velocity vectors precisely in comparison with the other methods.

The results of mean of normalized error in each image sequence are shown in from Figure 4.10 though Figure 4.13.

Table 4.5: Parameters in Nomura's method

The number of frame for velocity vector estimation K	3
Order of constraint equation with respect to temporal change of velocity vectors N	1

Table 4.6: Parameters in Mukawa's method

Weighting of the velocity vector constraint equation considering temporal change of intensity λ	5.4
Weighting of spatial constraint equation with respect to temporal change of intensity μ	2.5
Weighting of spatial constraint of c ν	1.3
The number of times of iterative calculation	50000[Times]

From the result, we see that the result of velocity vector estimation by using the proposed method is well in comparison with the other methods. The factor is supposed that the proposed method has property 1 and property 2.

93

Table 4.7: A parameter in Negahdaripour's method

The size of support region	4×4

Table 4.8: Parameters of generated image in translation motions

Names of each image sequence	Parameters in translation motions [pixel/frame]
P12_Trans1	1.0
P12_Trans2	2.0
P12_Trans3	3.0
P12_Trans4	4.0
P12_Trans5	5.0

Table 4.9: Parameters of generated image in expansion motions

Names of each image sequence	Parameters in expansion motions [times/frame]
P12_Exp1	1.01
P12_Exp2	1.02
P12_Exp3	1.03
P12_Exp4	1.04
P12_Exp5	1.05

Table 4.10: Parameters of generated image in contraction motions

Names of each image sequence	Parameters in contraction motions [times/frame]
P12_Cont1	0.99
P12_Cont2	0.98
P12_Cont3	0.97
P12_Cont4	0.96
P12_Cont5	0.95

Table 4.11: Parameters of generated image in rotation motions

Names of each image sequence	Parameters in rotation motions [degree/frame]
P12_Rot1	1.0
P12_Rot2	2.0
P12_Rot3	3.0
P12_Rot4	4.0
P12_Rot5	5.0
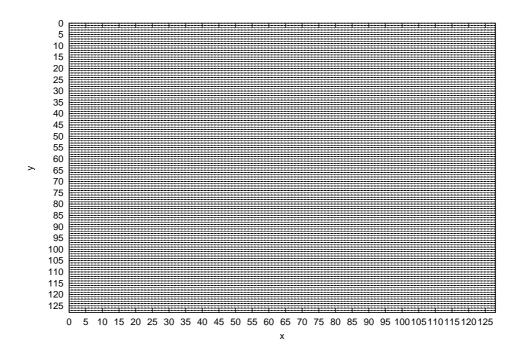
Figure 4.4: A correct velocity vector field in P12_Trans1
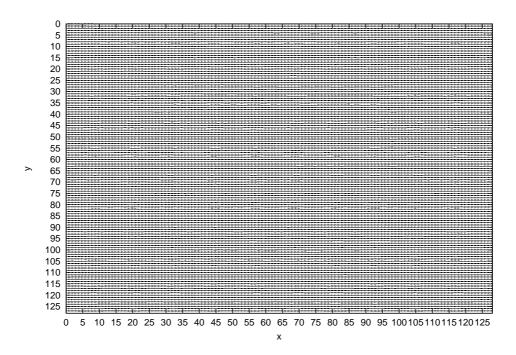
Figure 4.5: An estimated velocity vector field by the proposed method in P12_Trans1
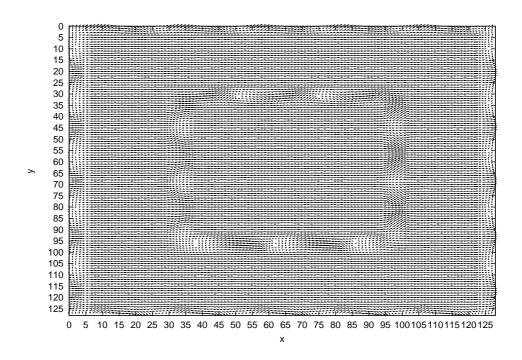
Figure 4.6: An estimated velocity vector field by Nomura's method in P12_Trans1
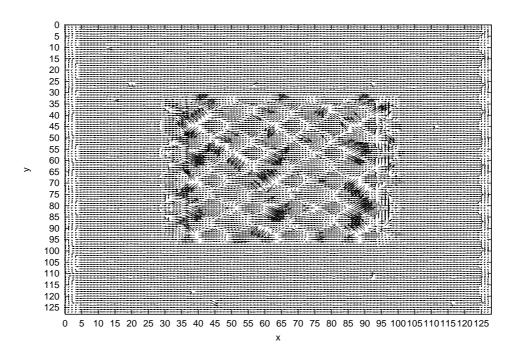
Figure 4.7: An estimated velocity vector field by Cornelius's method in P12_Trans1

96
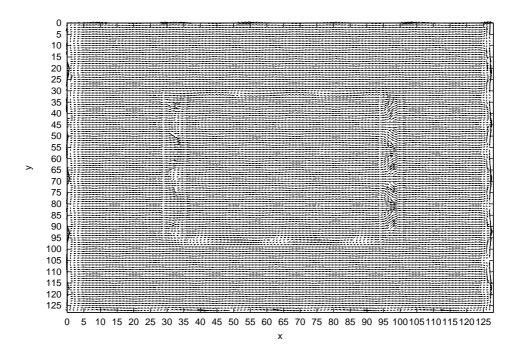
Figure 4.8: An estimated velocity vector field by Mukawa's method in P12_Trans1

Figure 4.9: An estimated velocity vector field by Negahdaripour's method in P12_Trans1

97

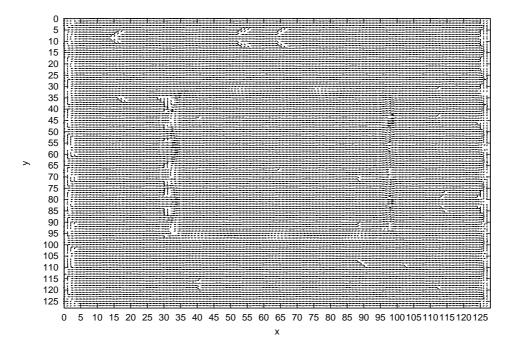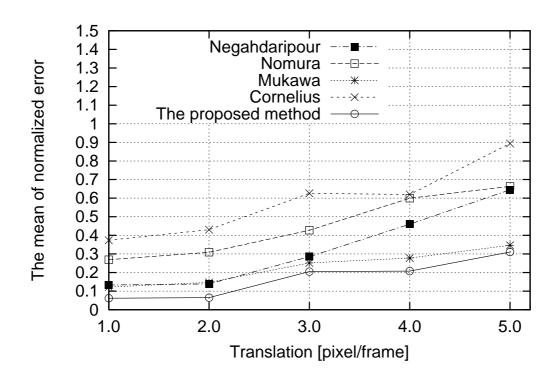Figure 4.10: The mean of normalized error in translation motions
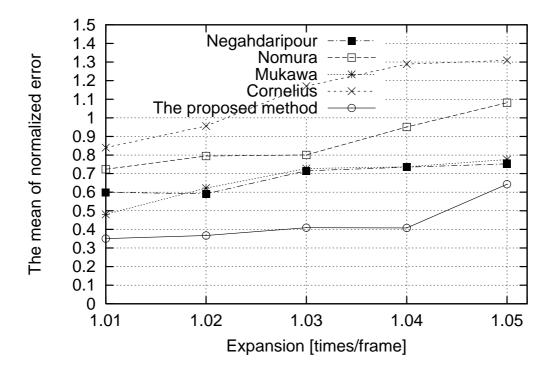
Figure 4.11: The mean of normalized error in expansion motions

98
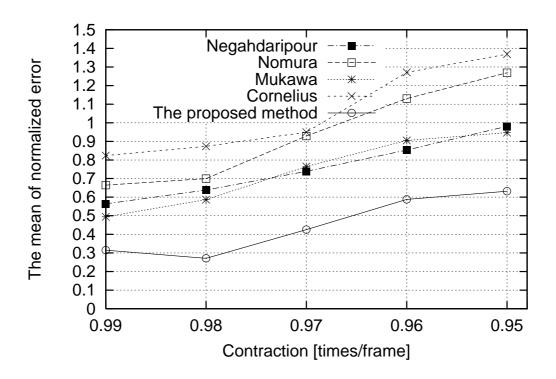
Figure 4.12: The mean of normalized error in contraction motions
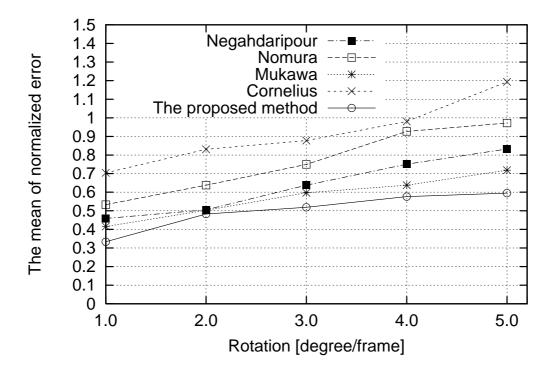
Figure 4.13: The mean of normalized error in rotation motions

Experiments on evaluating property 3

In order to evaluate that the proposed method has property 3, I experiment on comparison of velocity vector estimation precision of conventional methods and the proposed method by applying these methods to image sequence whose intensity changes temporally by effectiveness of shading in case that objects move. An image frame used in this experiment is shown in Figure 4.14. In a situation that light source irradiates light from right upper front position to an object, the first image frame used in this experiment is cut off not to include boundaries of an object, the second and third image frames used in this experiment are cut off not to include boundaries of an object from an image whose an object is 3-dimensionally transformed by affine transformation shown in Table 4.12, Table 4.13, Table 4.14 and Table 4.15, on condition that parameters in Table 4.12 are defined right direction as positive direction, parameters in Table 4.15 are defined counterclockwise as positive direction. Parameters of image frames used in this experiment are shown in Table 4.16.

Table 4.12: Parameters of generated image in translation motions

Names of each image sequence	Parameters in translation motions [coordinate/frame]
P3_Trans1	2.0
P3_Trans2	4.0
P3_Trans3	6.0
P3_Trans4	8.0
P3_Trans5	10.0
P3_Trans6	12.0
P3_Trans7	14.0
P3_Trans8	16.0
P3_Trans9	18.0
P3_Trans10	20.0

Table 4.13: Parameters of generated image in expansion motions

Names of each image sequence	Parameters in expansion motions [times/frame]
P3_Exp1	1.02
P3_Exp2	1.04
P3_Exp3	1.06
P3_Exp4	1.08
P3_Exp5	1.10
P3_Exp6	1.12
P3_Exp7	1.14
P3_Exp8	1.16
P3_Exp9	1.18
P3_Exp10	1.20

Parameters of the conventional methods and the proposed method are used the same parameters as shown in from Table 4.3 through Table 4.7.
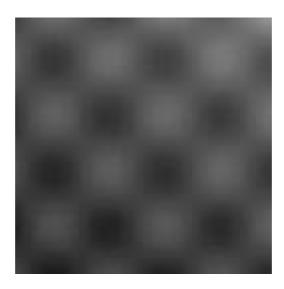
Figure 4.14: An image used for this experiment on evaluating property 3.

As evaluation scale for evaluating precision of velocity vector estimation, I use the mean of normalized error (Equation (4.33)).

As examples, a correct velocity vector field and estimated velocity vector fields in P3_Trans2 are shown in from Figure 4.15 though Figure 4.20. In regions where shading changes intensely, we see that the proposed method could estimate velocity vectors precisely in comparison with the other methods.

The results of the mean of normalized error in each image sequence are shown in from Figure 4.21 though Figure 4.24. In these figures of the results, the mean of normalized error intensely increased after P3_Trans6, P3_Exp6, P3_Cont6, P3_Rot6 respectively. The factor is supposed that spatial gradients of intensity reverse by shifting of a half-period of the sin-wave texture on the object in the image sequences.

From the result, we see that the result of velocity vector estimation by using the proposed method is well in comparison with the other methods. The factor is supposed that the proposed method has property 3.

Table 4.14: Parameters of generated image in contraction motions

Names of each image sequence	Parameters in contraction motions [times/frame]
P3_Cont1	0.98
P3_Cont2	0.96
P3_Cont3	0.94
P3_Cont4	0.92
P3_Cont5	0.90
P3_Cont6	0.88
P3_Cont7	0.86
P3_Cont8	0.84
P3_Cont9	0.82
P3_Cont10	0.80

Table 4.15: Parameters of generated image in rotation motions

Names of each image sequence	Parameters in rotation motions [degree/frame]
P3_Rot1	2.0
P3_Rot2	4.0
P3_Rot3	6.0
P3_Rot4	8.0
P3_Rot5	10.0
P3_Rot6	12.0
P3_Rot7	14.0
P3_Rot8	16.0
P3_Rot9	18.0
P3_Rot10	20.0

Table 4.16: Parameters in generated images used in this experiment

Frequency of a sine wave (Texture)	0.12[Hz]
Amplitude of a sine wave (Texture)	25[intensity]
Bias of intensity (Texture)	100[intensity]
Resolution	128×128[pixels]
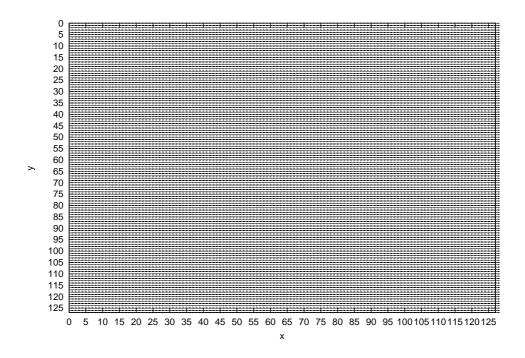
Figure 4.15: A correct velocity vector field in P3_Trans2
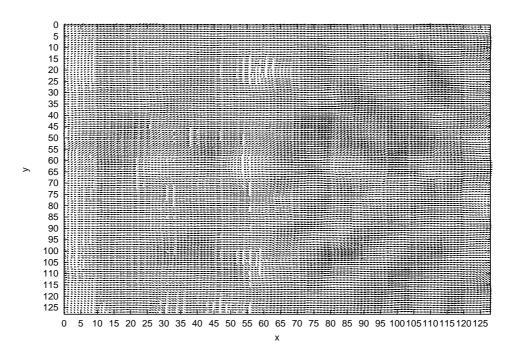
Figure 4.16: An estimated velocity vector field by the proposed method in P3_Trans2

103

Figure 4.17: An estimated velocity vector field by Nomura's method in P3_Trans2

Figure 4.18: An estimated velocity vector field by Cornelius's method in P3_Trans2

104

Figure 4.19: An estimated velocity vector field by Mukawa's method in P3_Trans2

Figure 4.20: An estimated velocity vector field by Negahdaripour's method in P3_Trans2
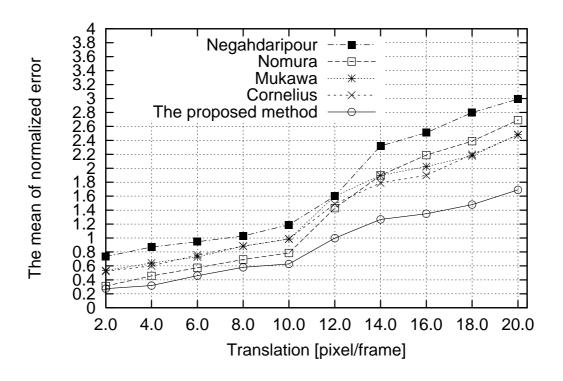
Figure 4.21: The mean of normalized error in translation motions

Figure 4.22: The mean of normalized error in expansion motions

106
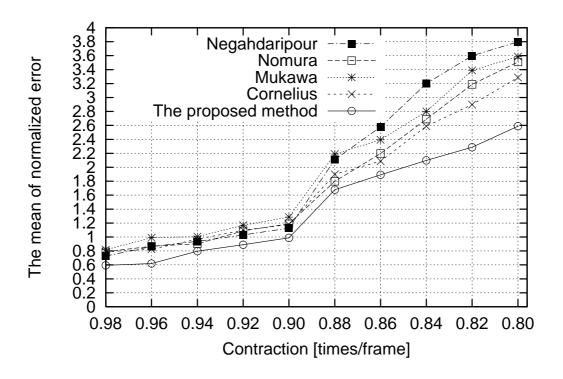
Figure 4.23: The mean of normalized error in contraction motions
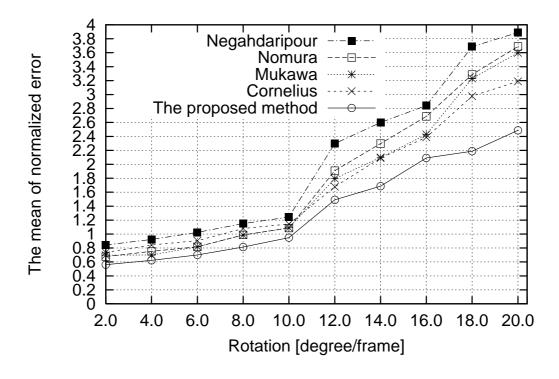
Figure 4.24: The mean of normalized error in rotation motions

Experiments on evaluating property 4

In order to evaluate that the proposed method has property 4, I experiment on comparison of velocity vector estimation precision of conventional methods and the proposed method applying to image sequence whose intensity changes temporally by temporal changing of light source intensity. An image frame used in this experiment is shown in Figure 4.25. In a situation that light source irradiates light from right upper front position to the object, the first image frame used in this experiment is cut off not to include boundaries of an object, the second and third image frames used in this experiment are cut off not to include boundaries of an object from an image whose light source intensity changes temporally as shown in Table 4.17. Parameters of image frames used in this experiment are shown in Table 4.18.

Table 4.17: Parameters of generated image in temporal intensity change

Names of each image sequence	Parameters in temporal intensity change [quantity/frame]
P4_Intense1	-10.0
P4_Intense2	-20.0
P4_Intense3	-30.0
P4_Intense4	-40.0
P4_Intense5	-50.0
P4_Intense6	-60.0
P4_Intense7	-70.0
P4_Intense8	-80.0
P4_Intense9	-90.0
P4_Intense10	-100.0

Table 4.18: Parameters in generated images used in this experiment

Frequency of a sine wave (Texture)	0.12[Hz]
Amplitude of a sine wave (Texture)	25[intensity]
Bias of intensity (Texture)	100[intensity]
Resolution	128×128[pixels]

Parameters of the conventional methods and the proposed method are used the same parameters as shown in from Table 4.3 through Table 4.7.

As examples, a correct velocity vector field and estimated velocity vector fields in P4_Intense5 are shown in from Figure 4.26 though Figure 4.31. In regions where intensity changes intensely, we see that the proposed method could estimate velocity vectors precisely in comparison with the other methods.

As evaluation scale for evaluating precision of velocity vector estimation, I use the mean of normalized error (Equation (4.33)). The results of the mean of normalized error are shown in Figure 4.32. In the Figure 4.32, the mean of normalized error abruptly increased from P4_Intense8. The factor is supposed that intensity which was transformed
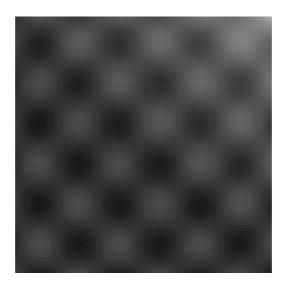
Figure 4.25: An image used for this experiment on evaluating property 4.

by change of intensity of light source got off the dynamic range of intensity of the image sequences used in this experiment.

From the result, we see that the result of velocity vector estimation by using the proposed method is well in comparison with the other methods. The factor is supposed that the proposed method has property 4.

Figure 4.26: A correct velocity vector field in P4_Intense5

Figure 4.27: An estimated velocity vector field by the proposed method in P4_Intense5
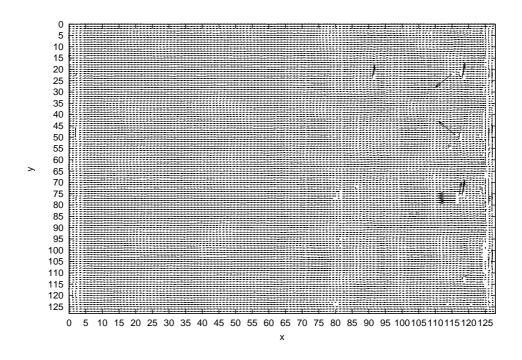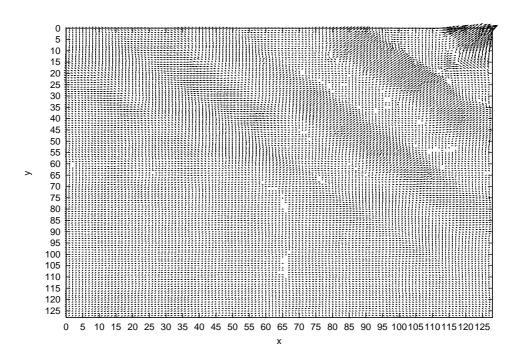
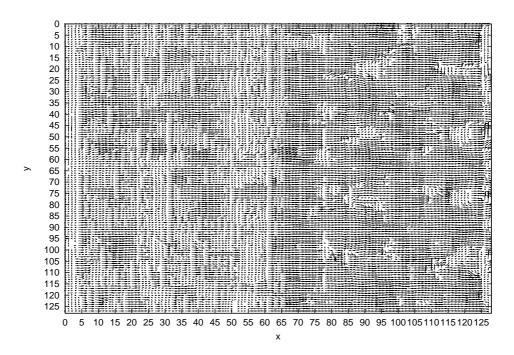Figure 4.28: An estimated velocity vector field by Nomura's method in P4_Intense5
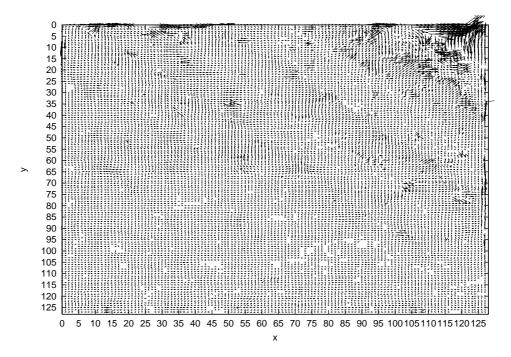
Figure 4.29: An estimated velocity vector field by Cornelius's method in P4_Intense5
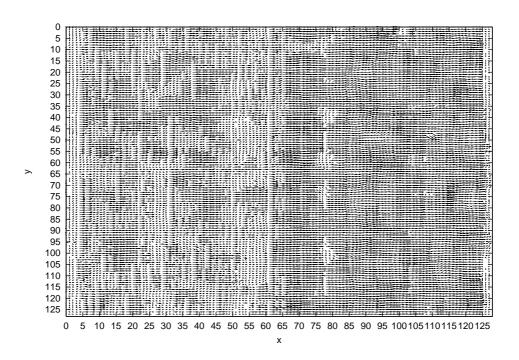
111
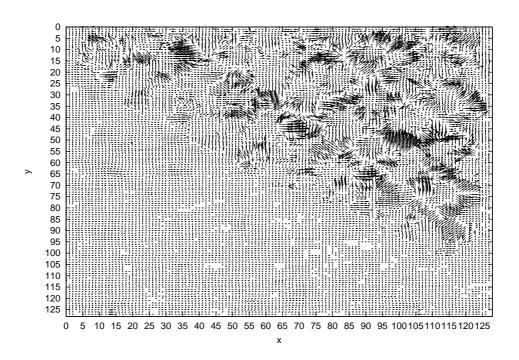
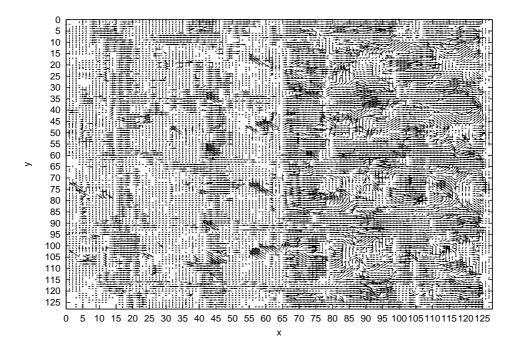Figure 4.30: An estimated velocity vector field by Mukawa's method in P4_Intense5
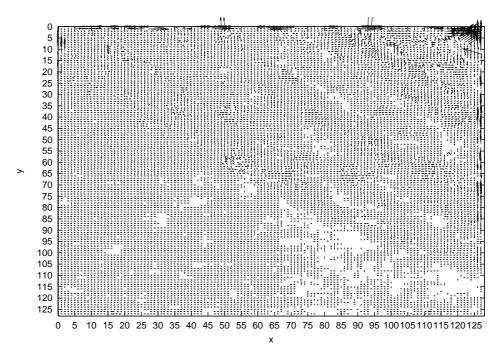
Figure 4.31: An estimated velocity vector field by Negahdaripour's method in P4_Intense5
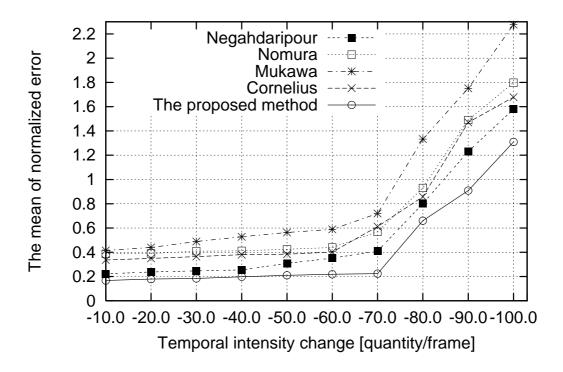
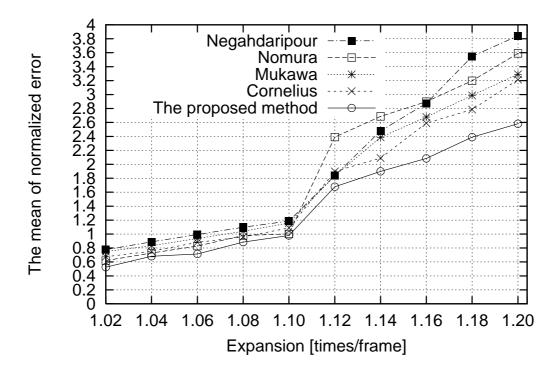Figure 4.32: The mean of normalized error in temporal intensity change
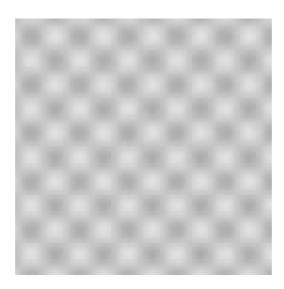
Figure 4.33: An image used for this experiment on evaluating property 5.

Experiments on evaluating property 5

In order to evaluate that the proposed method has property 5, I experiment on comparison of velocity vector estimation precision of conventional methods and the proposed method in case of applying to image sequences added Gaussian noise. The first image frame used in this experiment is shown in Figure 4.33, the second and third image frames used in this experiment are transformed by affine transformation shown in Table 4.19, Table 4.20, Table 4.21 and Table 4.22, on condition that parameters in Table 4.19 are defined right direction as positive direction, parameters in Table 4.22 are defined counterclockwise as positive direction. Parameters of image frames used in this experiment are shown in Table 4.23. Each image sequence is added Gaussian noise n whose probability is expressed as

$$P(n) = \frac{1}{\sqrt{2\pi}\sigma} \exp^{-\frac{n^2}{2\sigma^2}}, \tag{4.34}$$

I use

$$PSNR[dB] = 20\log\frac{255}{\sigma} \tag{4.35}$$

as a evaluation scale of quantity of noise.

Table 4.19: Parameters of generated image in translation motions

Names of each image sequence	Parameters in translation motions [pixels/frame]
P5_Trans1	1.0

Table 4.20: Parameters of generated image in expansion motions

Names of each image sequence	Parameters in expansion motions [times/frame]
P5_Exp1	1.01

Table 4.21: Parameters of generated image in contraction motions

Names of each image sequence	Parameters in contraction motions [times/frame]
P5_Cont1	0.99

Table 4.22: Parameters of generated image in rotation motions

Names of each image sequence	Parameters in rotation motions [degree/frame]
P5_Rot1	1.0

Table 4.23: Parameters in generated images used in this experiment

Frequency of a sine wave (Texture)	0.12[Hz]
Amplitude of a sine wave (Texture)	25[intensity]
Bias of intensity (Texture)	200[intensity]
Resolution	128×128[pixels]

Parameters of the conventional methods and the proposed method are used the same parameters as shown in from Table 4.3 through Table 4.7.

As evaluation scale for evaluating precision of velocity vector estimation, I use the mean of normalized error (Equation (4.33)).

As examples, a correct velocity vector field and estimated velocity vector fields in P5_Trans1 of $PSNR$=31.4[dB] are shown in from Figure 4.34 though Figure 4.39. In whole regions of image sequences, we see that the proposed method could estimate velocity vectors precisely in comparison with the other methods.

The results of mean of normalized error in each image sequence are shown in from Figure 4.40 though Figure 4.43.

From the result, we see that the result of velocity vector estimation by using the proposed method is well in comparison with the other methods. The factor is supposed that the proposed method has property 5.
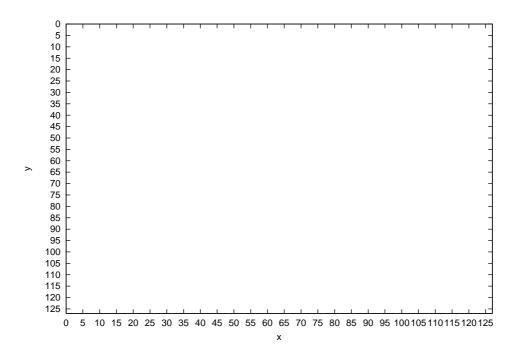
Figure 4.34: A correct velocity vector field in P5_Trans1 of $PSNR$=31.4[dB]
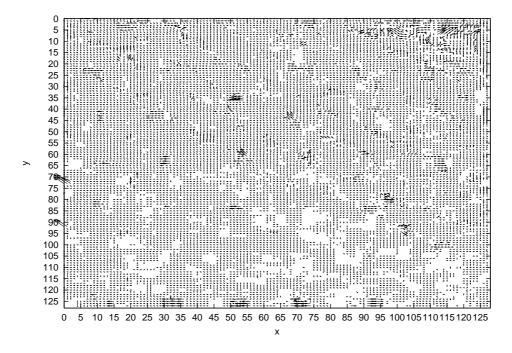

Figure 4.35: An estimated velocity vector field by the proposed method in P5_Trans1 of $PSNR$=31.4[dB]

116
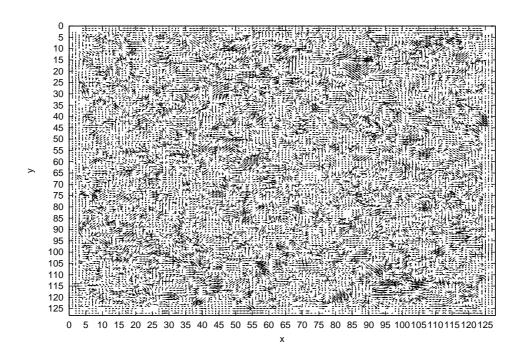
Figure 4.36: An estimated velocity vector field by Nomura's method in P5_Trans1 of $PSNR$=31.4[dB]

Figure 4.37: An estimated velocity vector field by Cornelius's method in P5_Trans1 of $PSNR$=31.4[dB]

Figure 4.38: An estimated velocity vector field by Mukawa's method in P5_Trans1 of $PSNR$=31.4[dB]

Figure 4.39: An estimated velocity vector field by Negahdaripour's method in P5_Trans1 of $PSNR$=31.4[dB]

Figure 4.40: The mean of normalized error in translation motions

Figure 4.41: The mean of normalized error in expansion motions

119

Figure 4.42: The mean of normalized error in contraction motions
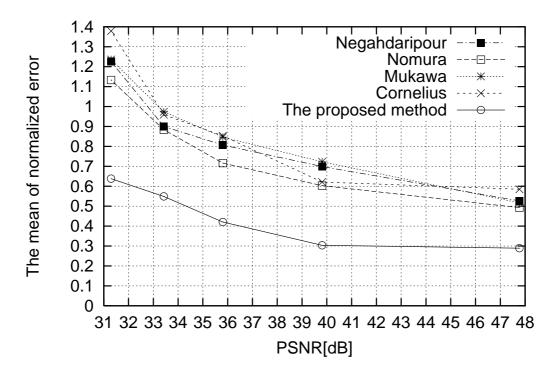
Figure 4.43: The mean of normalized error in rotation motions

Figure 4.44: An image used for this experiment on evaluating property 6.

Experiments on evaluating property 6

In order to evaluate that the proposed method has property 6, I experiment on comparison of velocity vector estimation precision of conventional methods and the proposed method in case of applying to image sequences including regions where pattern change is intense. The first image frame used in this experiment is shown in Figure 4.44. The second and third image frames used in this experiment are transformed by affine transformation shown in Table 4.24, Table 4.25, Table 4.26 and Table 4.27, on condition that parameters in Table 4.24 are defined right direction as positive direction, parameters in Table 4.27 are defined counterclockwise as positive direction. Parameters of image frames used in this experiment are shown in Table 4.28.

Table 4.24: Parameters of generated image in translation motions

Names of each image sequence	Parameters in translation motions [coordinate/frame]
P6_Trans1	1.0
P6_Trans2	2.0
P6_Trans3	3.0
P6_Trans4	4.0
P6_Trans5	5.0

Table 4.25: Parameters of generated image in expansion motions

Names of each image sequence	Parameters in expansion motions [times/frame]
P6_Exp1	1.01
P6_Exp2	1.02
P6_Exp3	1.03
P6_Exp4	1.04
P6_Exp5	1.05

121

Table 4.26: Parameters of generated image in contraction motions

Names of each image sequence	Parameters in contraction motions [times/frame]
P6_Cont1	0.99
P6_Cont2	0.98
P6_Cont3	0.97
P6_Cont4	0.96
P6_Cont5	0.95

Table 4.27: Parameters of generated image in rotation motions

Names of each image sequence	Parameters in rotation motions [degree/frame]
P6_Rot1	1.0
P6_Rot2	2.0
P6_Rot3	3.0
P6_Rot4	4.0
P6_Rot5	5.0

Table 4.28: Parameters in generated images used in this experiment

Frequency of a sine wave (Object)	0.12[Hz]
Amplitude of a sine wave (Object)	25[intensity]
Bias of intensity (Texture)	200[intensity]
Frequency of a sine wave (Background)	0.12[Hz]
Amplitude of a sine wave (Background)	15[intensity]
Bias of intensity (Texture)	30[intensity]
Resolution	128×128[pixels]

Parameters of the conventional methods and the proposed method are used the same parameters as shown in from Table 4.3 through Table 4.7.

As evaluation scale for evaluating precision of velocity vector estimation, since image sequences used in this experiment include non motion regions, I use the mean of error,

$$\bar{e} = \frac{1}{M} \sum_{x,y \in R_o} ||\boldsymbol{f}_c(x,y) - \boldsymbol{f}_e(x,y)||, \tag{4.36}$$

where M is number of pixels in occluded/appearance regions extracted by the proposed method, R_o is a occluded/appearance region, $\boldsymbol{f}_c(x,y)$ is a correct velocity vector in (x,y), $\boldsymbol{f}_e(x,y)$ is an estimated velocity vector by extrapolation in (x,y).

As examples, a correct velocity vector field and estimated velocity vector fields in P6_Trans1 are shown in from Figure 4.45 though Figure 4.50. In regions where pattern changes intensely, we see that the proposed method could estimate velocity vectors precisely in comparison with the other methods.

The results of mean of error in each image sequence are shown in from Figure 4.51 though Figure 4.54.

From the result, we see that the result of velocity vector estimation by using the proposed method is well in comparison with the other methods. The factor is supposed that the proposed method has property 6.
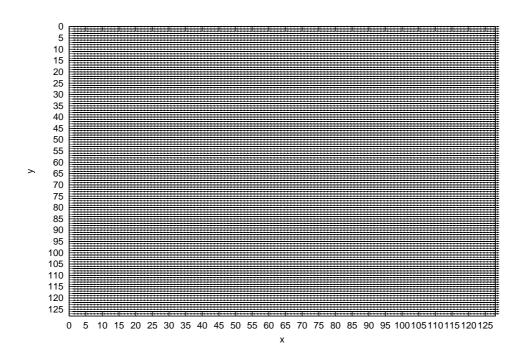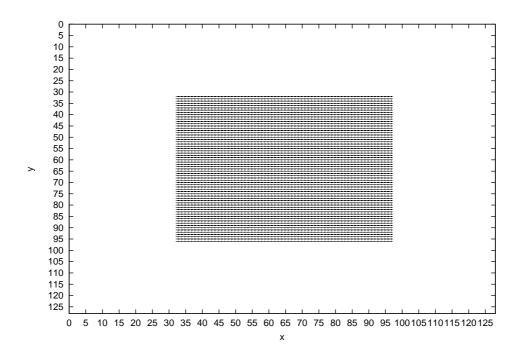
Figure 4.45: An correct velocity vector field in P6_Trans1
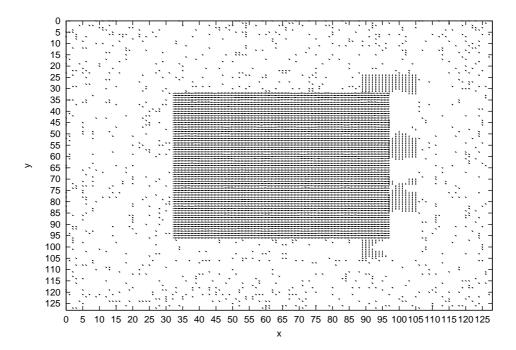
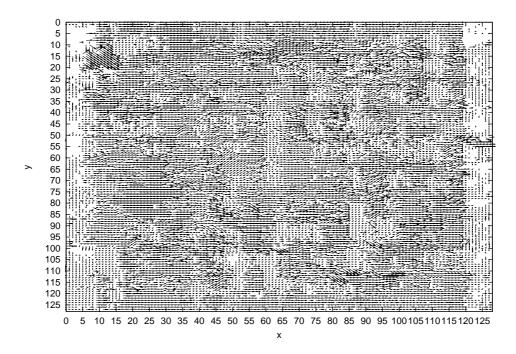Figure 4.46: An estimated velocity vector field by the proposed method in P6_Trans1

124
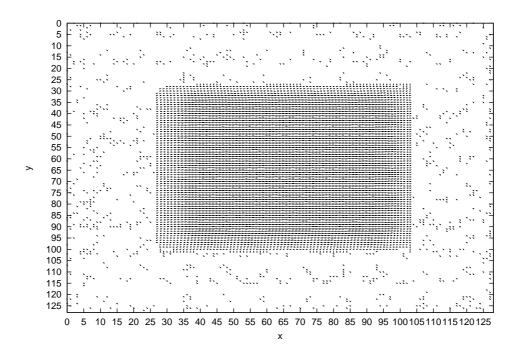
Figure 4.47: An estimated velocity vector field by Nomura's method in P6_Trans1
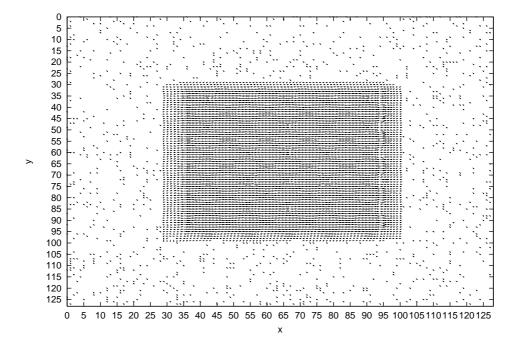
Figure 4.48: An estimated velocity vector field by Cornelius's method in P6_Trans1

125
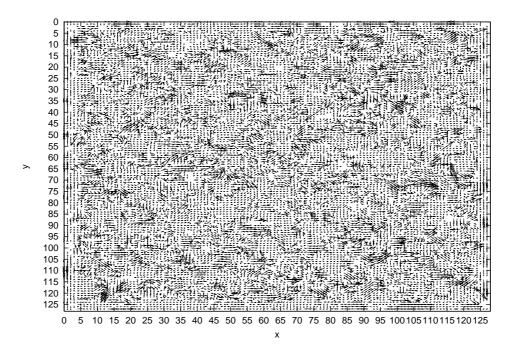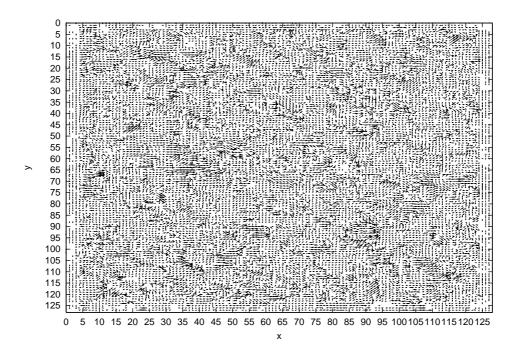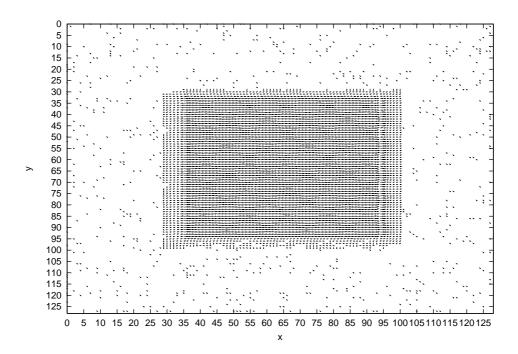
Figure 4.49: An estimated velocity vector field by Mukawa's method in P6_Trans1
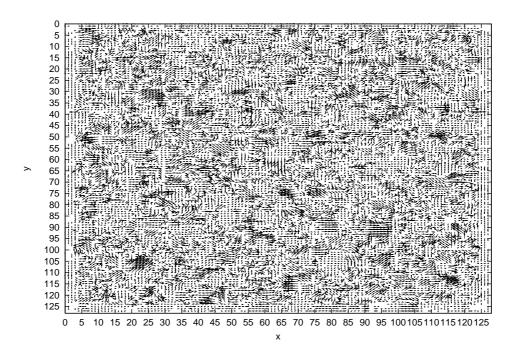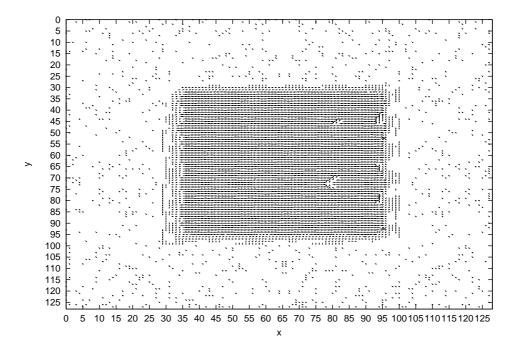

Figure 4.50: An estimated velocity vector field by Negahdaripour's method in P6_Trans1

126
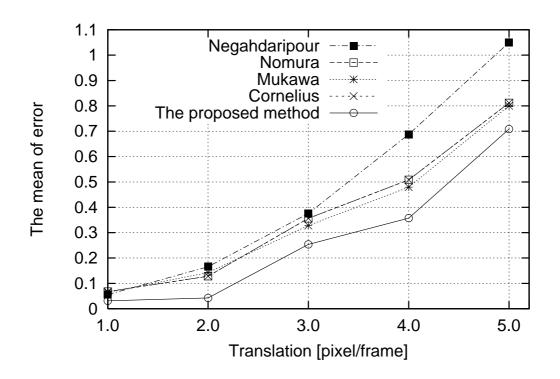
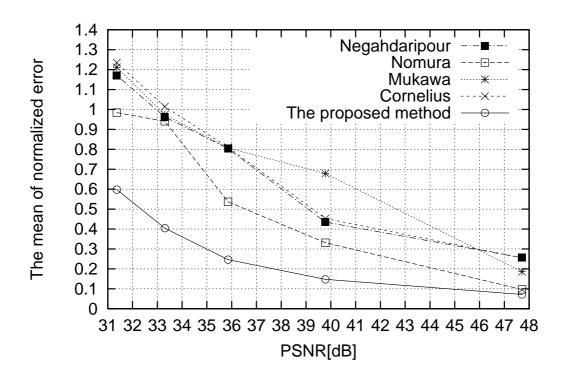Figure 4.51: The mean of error in translation motions
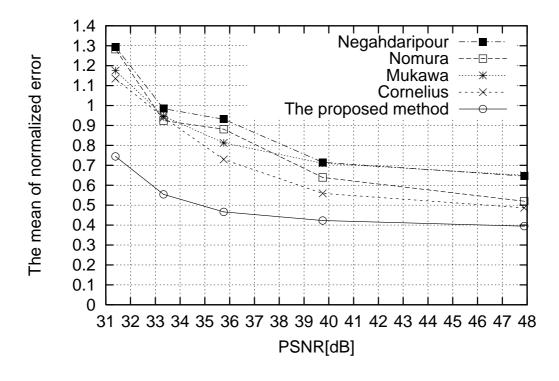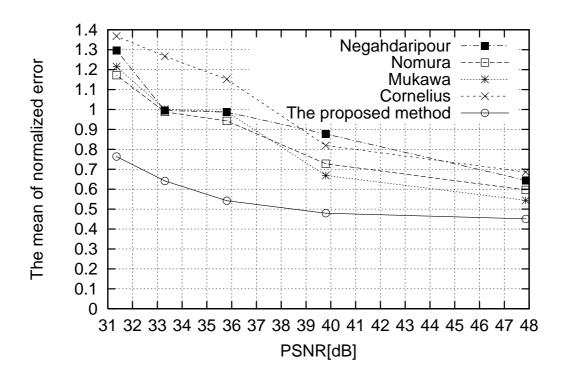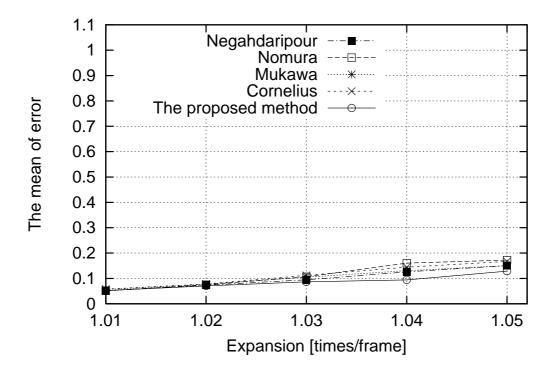

Figure 4.52: The mean of error in expansion motions
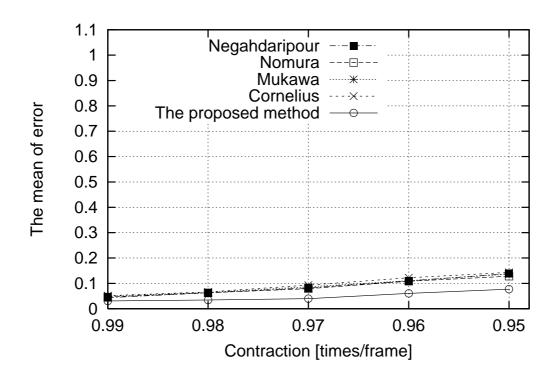
Figure 4.53: The mean of error in contraction motions
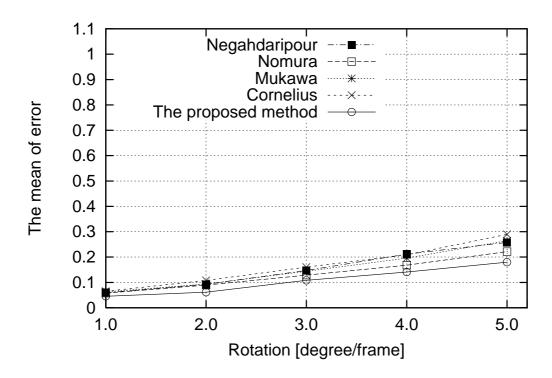
Figure 4.54: The mean of error in rotation motions

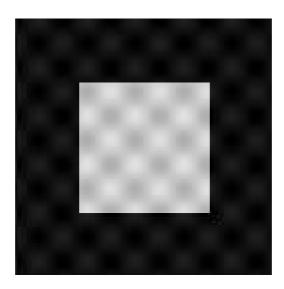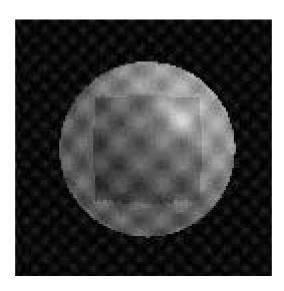Figure 4.55: An image used for this experiment on evaluating all properties.

Experiments on evaluating in case of including factors of all properties

In order to evaluate that the proposed method has all properties from 1 through 6, I experiment on comparison of velocity vector estimation precision of conventional methods and the proposed method in case of applying to image sequences including factors of the all properties from 1 though 6. The first image frame used in this experiment is shown in Figure 4.55 that includes factors of the all properties from 1 through 6. Objects in the second and third image frames used in this experiment are transformed by affine transformation shown in Table 4.29, Table 4.30, Table 4.31 and Table 4.32, on condition that parameters in Table 4.29 are defined right direction as positive direction, parameters in Table 4.32 are defined counterclockwise as positive direction. Parameters of image frames used in this experiment are shown in Table 4.33.

Table 4.29: Parameters of generated image in translation motions

Names of image sequence	Motion parameters of translation[coordinate/frame]	Quantity of temporal change of light source intensity	Quantity of noise[dB]
Pa_Trans	1.0	-20	36.1

Table 4.30: Parameters of generated image in expansion motions

Names of image sequence	Motion parameters of expansion[times/frame]	Quantity of temporal change of light source intensity	Quantity of noise[dB]
Pa_Exp	1.01	-20	36.1

Parameters of the conventional methods and the proposed method are used the same parameters as shown in from Table 4.3 through Table 4.7.

As evaluation scale for evaluating precision of velocity vector estimation, since image sequences used in this experiment include non motion regions, I use the mean of error $\bar{e}$.

Table 4.31: Parameters of generated image in contraction motions

Names of image sequence	Motion parameters of contraction[times/frame]	Quantity of temporal change of light source intensity	Quantity of noise[dB]
Pa_Cont	0.99	-20	36.1

Table 4.32: Parameters of generated image in rotation motions

Names of image sequence	Motion parameters of rotation[degree/frame]	Quantity of temporal change of light source intensity	Quantity of noise[dB]
Pa_Rot	1.0	-20	36.1

Table 4.33: Parameters in generated images used in this experiment

Frequency of a sine wave (Object)	0.12[Hz]
Amplitude of a sine wave (Object)	25[intensity]
Bias of intensity (Outside of the object)	200[intensity]
Bias of intensity (Inside of the object)	100[intensity]
Frequency of a sine wave (Background)	0.12[Hz]
Amplitude of a sine wave (Background)	15[intensity]
Bias of intensity (Background)	30[intensity]
Resolution	128×128[pixels]

As examples, a correct velocity vector field and estimated velocity vector fields in Pa_trans are shown in from Figure 4.56 though Figure 4.61. In these figures, we see that the proposed method could estimate velocity vectors precisely in comparison with the other methods.

The results of mean of error of each method in each image sequence are shown in from Table 4.62.

From the result, we see that the result of velocity vector estimation by using the proposed method is well in comparison with the other methods. The factor is supposed that the proposed method has all properties from 1 through 6.
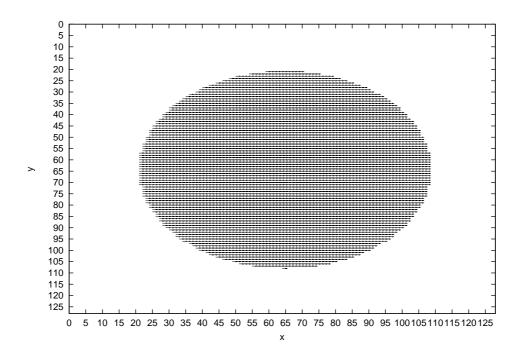
Figure 4.56: A correct velocity vector field in Pa_Trans
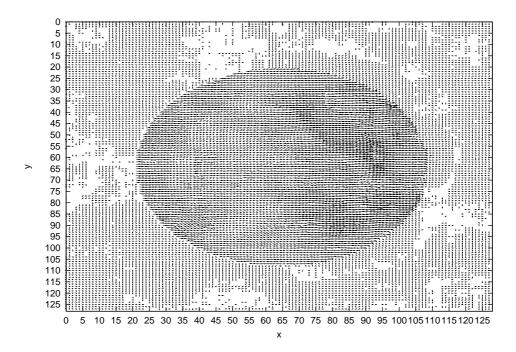
Figure 4.57: An estimated velocity vector field by the proposed method in Pa_Trans

131
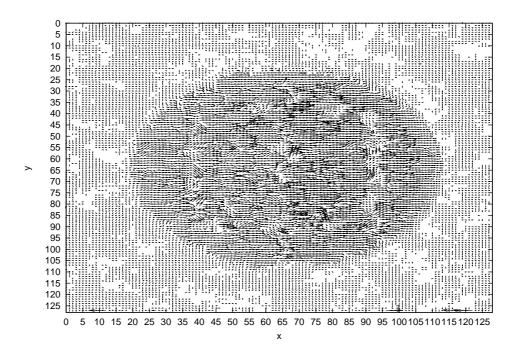
Figure 4.58: An estimated velocity vector field by Nomura's method in Pa_Trans
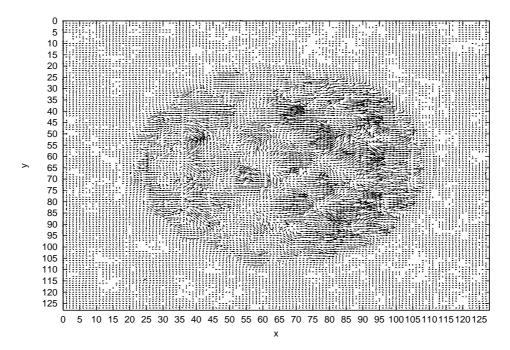
Figure 4.59: An estimated velocity vector field by Cornelius's method in Pa_Trans
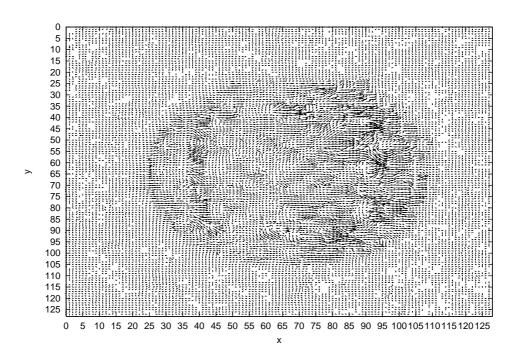
Figure 4.60: An estimated velocity vector field by Mukawa's method in Pa_Trans
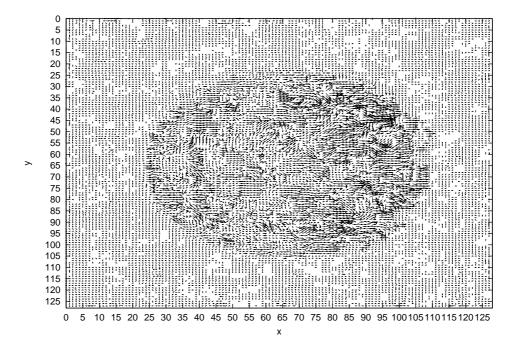
Figure 4.61: An estimated velocity vector field by Negahdaripour's method in Pa_Trans

Figure 4.62: The mean of error of each method in each image sequence, A:The proposed method, B: Conelius's method, C:Nomura's method, D:Mukawa's method, E:Negahdaripour's method.

| Names of | The mean of error in each method | | | | |
each image sequence	A	B	C	D	E
Pa_Trans	2.73×10^{-1}	4.38×10^{-1}	4.14×10^{-1}	4.70×10^{-1}	4.89×10^{-1}
Pa_Exp	2.82×10^{-1}	3.70×10^{-1}	3.08×10^{-1}	3.31×10^{-1}	3.42×10^{-1}
Pa_Cont	2.86×10^{-1}	3.96×10^{-1}	3.11×10^{-1}	3.97×10^{-1}	4.14×10^{-1}
Pa_Rot	3.78×10^{-1}	5.12×10^{-1}	4.30×10^{-1}	5.08×10^{-1}	5.30×10^{-1}

4.5.2 Application to actual image sequences

In order to evaluate effectiveness of the proposed method in actual image sequences, I experiment on comparison of velocity vector estimation precision of conventional methods and the proposed method in case of applying to actual image sequences. I apply each method to the actual image sequences including translation, expansion, contraction or rotation motions as shown in Figure 4.63, Figure 4.69, Figure 4.75 or Figure 4.81 respectively. The resolution of each image sequence are 111×56[pixels], 56×46[pixels], 56×46[pixels] or 76×41[pixels] respectively.

I use the same parameters of the conventional methods and the proposed method as shown in from Table 4.3 through Table 4.7.

Estimated velocity vector fields in the actual image sequences are shown in from Figure 4.64 though Figure 4.86 respectively.

From the result, we see that the result of velocity vector estimation by using the proposed method is the best. The main factor is supposed that the proposed method has all properties from 1 through 6. .

Frame1

Frame2

Frame3

Figure 4.63: An actual image sequence including a translation motion
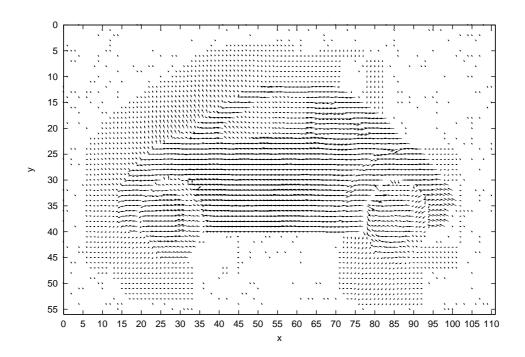
Figure 4.64: An estimated velocity vector field of the proposed method in the actual image sequence including a translation motion
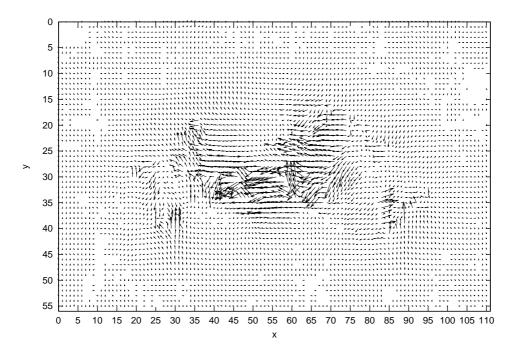
Figure 4.65: An estimated velocity vector fields of Cornelius's method in the actual image sequence including a translation motion

137
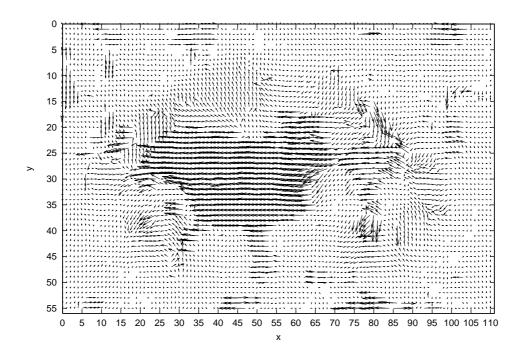
Figure 4.66: An estimated velocity vector field of Nomura's method in the actual image sequence including a translation motion
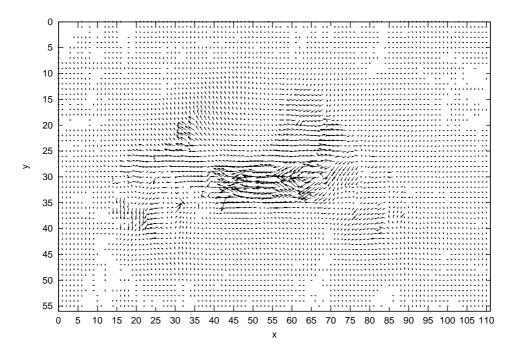
Figure 4.67: An estimated velocity vector field of Mukawa's method in the actual image sequence including a translation motion

138
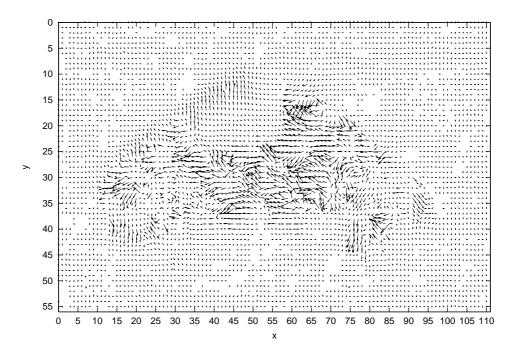
Figure 4.68: An estimated velocity vector field of Negahdaripour's method in the actual image sequence including a translation motion

Frame1

Frame2

Frame3

Figure 4.69: An actual image sequence including an expansion motion
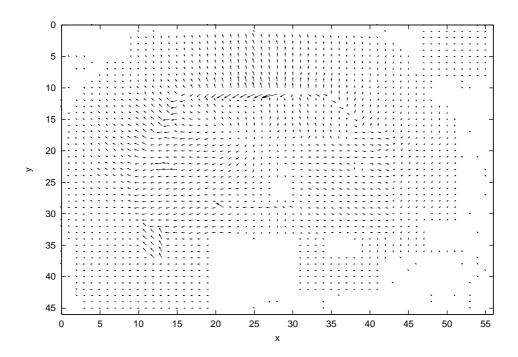
Figure 4.70: An estimated velocity vector field of the proposed method in the actual image sequence including a expansion motion
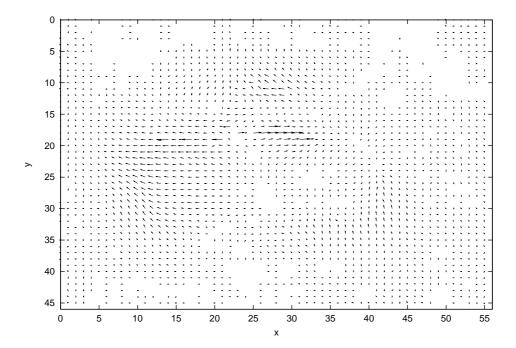
Figure 4.71: An estimated velocity vector field of Cornelius's method in the actual image sequence including a expansion motion

141
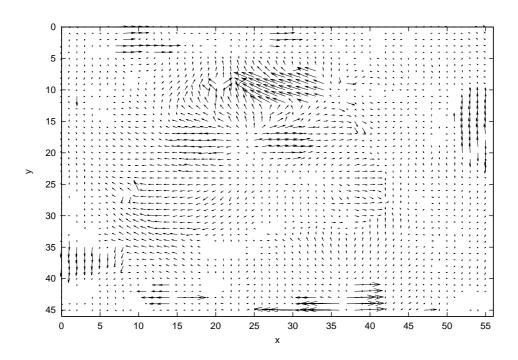
Figure 4.72: An estimated velocity vector field of Nomura's method in the actual image sequence including a expansion motion
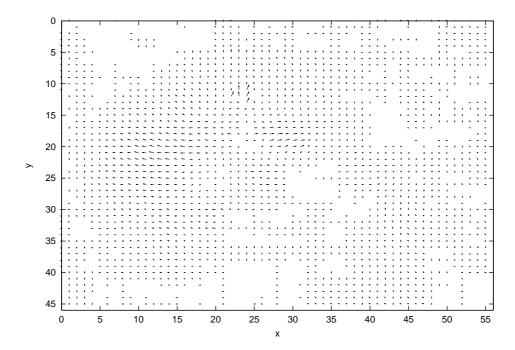
Figure 4.73: An estimated velocity vector field of Mukawa's method in the actual image sequence including a expansion motion

142
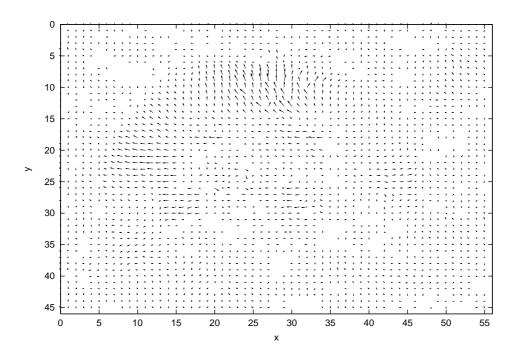
Figure 4.74: An estimated velocity vector field of Negahdaripour's method in the actual image sequence including a expansion motion

Frame1

Frame2

Frame3

Figure 4.75: An actual image sequence including an contraction motion
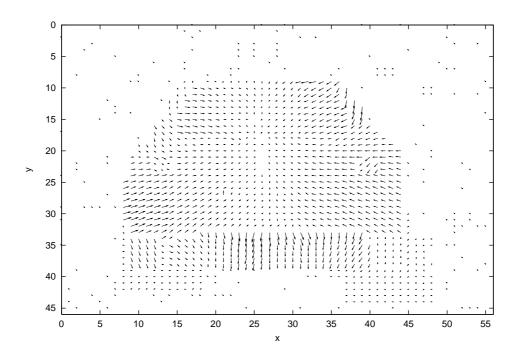
Figure 4.76: An estimated velocity vector field of the proposed method in the actual image sequence including a contraction motion
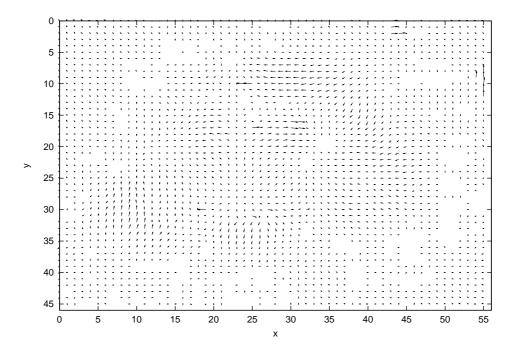
Figure 4.77: An estimated velocity vector field of Cornelius's method in the actual image sequence including a contraction motion
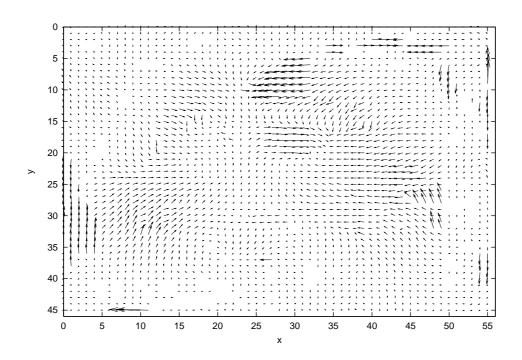
Figure 4.78: An estimated velocity vector field of Nomura's method in the actual image sequence including a contraction motion
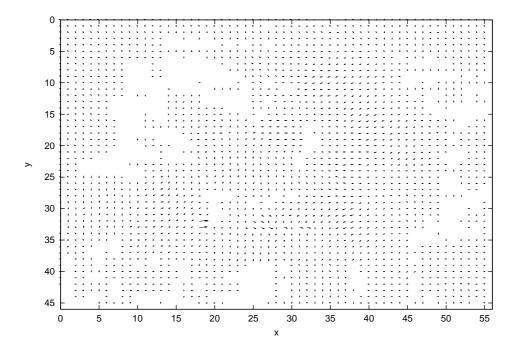
Figure 4.79: An estimated velocity vector field of Mukawa's method in the actual image sequence including a contraction motion
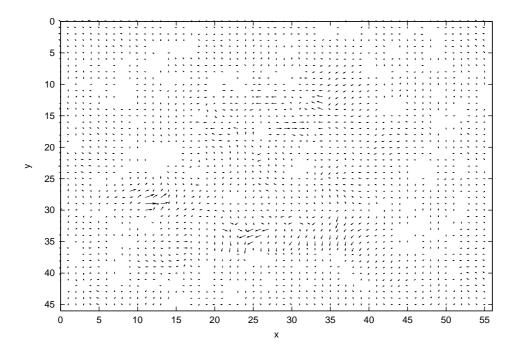
Figure 4.80: An estimated velocity vector field of Negahdaripour's method in the actual image sequence including a contraction motion

Frame1

Frame2

Frame3

Figure 4.81: An actual image sequence including an rotation motion
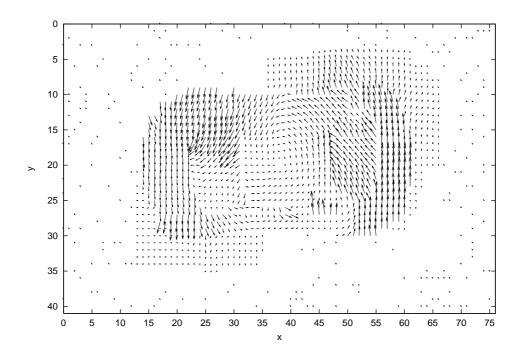
Figure 4.82: An estimated velocity vector field of the proposed method in the actual image sequence including a rotation motion
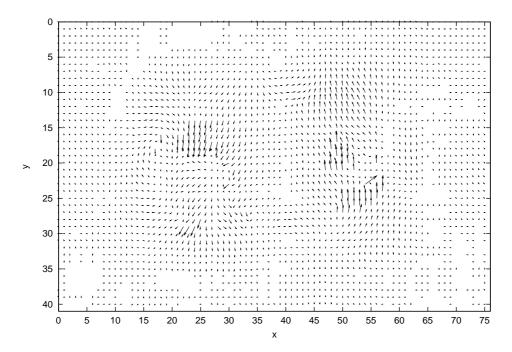
Figure 4.83: An estimated velocity vector field of Cornelius's method in the actual image sequence including a rotation motion
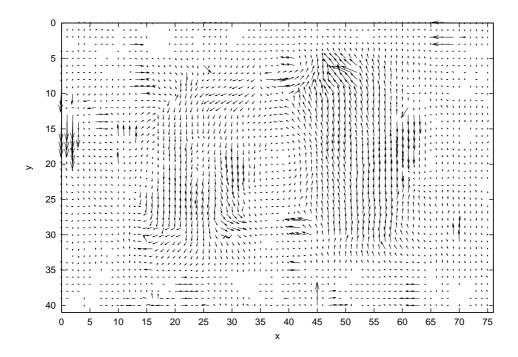
Figure 4.84: An estimated velocity vector field of Nomura's method in the actual image sequence including a rotation motion
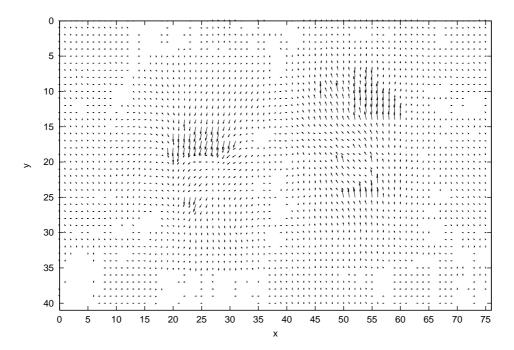
Figure 4.85: An estimated velocity vector field of Mukawa's method in the actual image sequence including a rotation motion
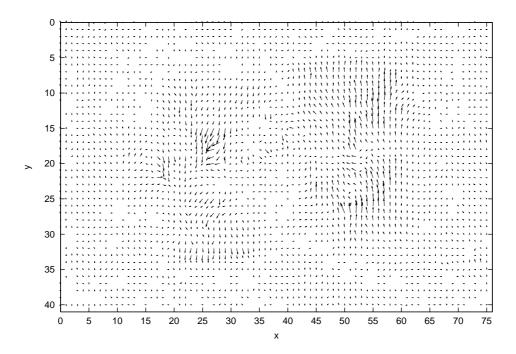
Figure 4.86: An estimated velocity vector field of Negahdaripour's method in the actual image sequence including a rotation motion

4.6 Summary

In order to precisely estimate velocity vectors in the situation of brightness change, I attempted to proposed a method that has all properties in conventional methods such as

Property 1: The parameters in a constraint equation can be estimated in 2 frames,

Property 2: The reflection rate on the surface of an object is not necessary to be constant

Property 3: Change of intensity by effectiveness of shading is considered

Property 4: Change of intensity by changing of a light source intensity is considered

Property 5: The method has robustness against noise

Property 6: The method has robustness in the region where pattern changes intensely.

To obtain property 1, I adopted an assumption for velocity vector estimation in the situation of brightness change. To obtain from property 2 through property 6, I analyzed fluctuation of intersections of constraint equation considering brightness change in parameter space u-v-w. From the result of the analysis, I decided to use a method using 3-dimensional voting process and a condition of constraint equations for voting.

In order to evaluate that the proposed method has the all properties from property 1 through property 6, I first experimented on comparison of precision of velocity vectors in following image sequence.

For evaluating property 1 and property 2 : Image sequences including effectiveness of different reflection rate on an object

For evaluating property 3 : Image sequences including effectiveness of shading on an object

For evaluating property 4 : Image sequences including effectiveness of intensity change of a light source

For evaluating property 5 : Image sequences including effectiveness of noise

For evaluating property 6 : Image sequences including effectiveness of regions where pattern changes intensely

From the results of the experiments, precision of velocity vector estimation by using the proposed method was well in comparison with the other method. The factor is supposed that the proposed method has each property.

I next experimented on comparison of precision of velocity vectors in image sequences that have factors of all properties. From the result of the experiment, by using the proposed method I obtained approximately 34% higher precision of velocity vector estimation in the maximum than precision of velocity vector estimation in conventional methods. The factor is supposed that the proposed method has all properties. In order to moreover obtain precise estimation results, primarily, we have to investigate the optimum weighting function for each application in velocity vector estimation considering brightness change.

I finally applied the proposed method and the conventional methods to actual image sequences that include translation, expansion, contraction or rotation. From the result of the experiment, precision of velocity vector estimation by using the proposed method was qualitatively well in comparison with the other methods.

Chapter 5

A new method of velocity vector estimation for incompressible viscous fluid analysis

5.1 Introduction

Methods of fluid analysis using image sequences are classified into two category such as particle base methods[55]$\sim$[60] called PIV (Particle Image Velocitmetry) that analyze fluid motions using particles and texture base methods[61][62][63] that analyze fluid motions using dyestuffs. The particle base methods can estimate velocity vectors of fluid in the less cost of calculation. However, the methods can not basically estimate velocity vectors in high density. The texture base methods can estimate velocity vectors in spatial high density, However, the methods can not estimate velocity vectors in less calculation in comparison with the particle base methods. I focus on texture base methods which can estimate velocity vectors in spatial high density.

The texture base methods are classified into two categories. One is a method considering constraints of perfect fluid[61][62], the other is a method considering constraint of incompressible viscous fluid[63]. These methods estimate velocity vectors using evaluation function of constraint equations with respect to estimation parameters on whole pixels in an image. Therefore, if the constraint equations are influenced by noise, precision of velocity vector estimation declines. In order to precisely estimate velocity vectors in actual image sequences including fluid object, we have to exclude effectiveness of noise.

As a method that can precisely estimate parameters excluding effectiveness of noise, A voting process with a weighting function has been proposed[66]. The method estimates the most likelihood parameters from intersections of a constraint equation. However, constraint equations used in conventional methods include partial differential coefficients of velocity vector components u and v, we cannot determine the partial differential coefficients of velocity vector components u and v. Thus, we cannot apply the constraint equations used in conventional methods to the method via voting process with a weighting function.

I assume that a premise condition of a theorem such that "partial differential coefficients including u and v can be determined by using intersections of intensity constraint equations of a velocity vector" holds. If the theorem holds, we can determine the partial differential coefficients. By determining the partial differential coefficients based on

154

the theorem, we can apply the constraint equations used in conventional methods to the method via voting process with a weighting function. In the field of fluid analysis, the incompressible viscous fluid is mainly used as an application object. Thus, I aim to apply to the incompressible viscous fluid. In order to apply to the incompressible viscous fluid, I derive an incompressible viscous fluid velocity vector constraint equation determined coefficients by intensity constraint, based on constraint equations considering physical constraints of incompressible viscous fluid used in Nakajima's method[63]. The constraint equation includes three parameters such as velocity vector parameters and spatial change of pressure. Thus, I expand the parameter space to a 3-dimensional parameter space. I then estimate the parameters in the constraint equation by using a voting process with a weighting function in a 3-dimensional voting space.

In weather anticipations using image sequences of clouds taken by weather satellites, we have to estimate velocity vectors of the clouds in the image sequences to precisely anticipate weather. Thus, we can apply the proposed method to the weather anticipations.

5.2 Effective of noise in estimation values in the conventional methods considering physical constraint of fluid

In a situation of non-noise, constraint equations with respect to estimation parameters used in conventional methods considering physical constraint of fluid can be regularized as

$$\sum_{i=1}^{\Omega}\sum_{j=1}^{T} \boldsymbol{a'}_{hij}^{\top}\boldsymbol{v}_{ij} + b'_{hi} = 0, \tag{5.1}$$

where $\top$ is transposition, Ω is the number of pixels in an image region, T is the number of estimation parameters in a constraint equation, $\boldsymbol{v}_{ij}$ is a vector of an estimation parameter j on i pixel in an image region, $\boldsymbol{a'}_{hij}$ is a coefficient vector of $\boldsymbol{v}_{ij}$ in h order of the constraint equations. b'_{hi} is a constant term in h and i. Evaluation functions used in conventional methods[63][61][62] to estimate estimation parameters $v_{11}, v_{12}, \cdots, v_{\Omega T}$ can be regularized as

$$E(\boldsymbol{v}_{11}, \boldsymbol{v}_{12}, \cdots, \boldsymbol{v}_{\Omega T}) = \sum_{h=1}^{C}\left\{\sum_{i=1}^{\Omega}\sum_{j=1}^{T}\left(\boldsymbol{a}_{hij}^{\top}\boldsymbol{v}_{ij} + b_{hi}\right)\right\}^{2}, \tag{5.2}$$

where $\boldsymbol{a}_{hij}$ is a coefficient vector of $\boldsymbol{v}_{ij}$ in the h order of the constraint equations in the evaluation function, b_{hi} is a constant term in h and i in the evaluation function. If noise is added to m pixels ($0 \leq m \leq \Omega$), the evaluation function $E_e(v_{11}, v_{12}, \cdots, v_{\Omega T})$ can be represented as

$$
\begin{aligned}
&E_e(\boldsymbol{v}_{11}, \boldsymbol{v}_{12}, \cdots, \boldsymbol{v}_{\Omega T}) \\
&= \sum_{h=1}^{C}\left[\sum_{i=1}^{m}\sum_{j=1}^{T}\left\{(\boldsymbol{a}_{hij} + \boldsymbol{e_a}_{hij})^{\top}\boldsymbol{v}_{ij} + (b_{hi} + e_{bhi})\right\} + \sum_{k=m+1}^{\Omega}\sum_{j=1}^{T}\left(\boldsymbol{a}_{hkj}^{\top}\boldsymbol{v}_{kj} + b_{hk}\right)\right]^{2},
\end{aligned}
$$

where $\boldsymbol{e_a}_{hij}$ is noise added to $\boldsymbol{a}_{hij}$, e_{bhi} is noise added to b_{hi}. Since the evaluation function $E(v_{11}, v_{12}, \cdots, v_{\Omega T})$ is a second order function, the optimum value of a component $v_{\alpha\beta o}$ in a order o of an estimation parameter $v_{\alpha\beta}$ ($0 \leq \alpha \leq \Omega$, $0 \leq \beta \leq T$) is the extremal value. To

estimate the extremal value, I execute partial differentiation for the evaluation function $E(v_{11}, v_{12}, \cdots, v_{\Omega T})$ with respect to $v_{\alpha\beta o}$. Then I set the partial differentiation is 0. By solving the partial differentiation with respect to $v_{\alpha\beta o}$, we obtain

$$v_{\alpha\beta o} = \frac{-\sum_{h=1}^{C}\sum_{i=1}^{\Omega}\sum_{j=1}^{T}(\boldsymbol{a}_{hij}^{\top}\boldsymbol{v}_{ij} + b_{hi})}{\sum_{h=1}^{C} a_{h\alpha\beta o}}, \tag{5.3}$$

where $a_{h\alpha\beta o}$ is a coefficient of $v_{\alpha\beta o}$ in a h order of the constraint equation. I do not deal with a term of $a_{h\alpha\beta o}^{\top} v_{\alpha\beta o}$ in the term $\boldsymbol{a}_{hij}^{\top}\boldsymbol{v}_{ij}$ in the left side of the equation 5.3. Similarly, the optimum value with respect to $v_{\alpha\beta o}$ in the evaluation function $E_e(v_{11}, v_{12}, \cdots, v_{\Omega T})$ is

$$\begin{aligned}
v_{\alpha\beta o} &= \frac{-\sum_{h=1}^{C}\sum_{i=1}^{m}\sum_{j=1}^{T}(\boldsymbol{a}_{hij} + \boldsymbol{e}\boldsymbol{a}_{hij})^{\top}\boldsymbol{v}_{ij}}{\sum_{h=1}^{C}(a_{h\alpha\beta o} + e_{h\alpha\beta o})} \\
&+ \frac{-\sum_{h=1}^{C}\sum_{i=1}^{m}\sum_{j=1}^{T}(b_{hi} + e_{bhi})}{\sum_{h=1}^{C}(a_{h\alpha\beta o} + e_{h\alpha\beta o})} + \frac{-\sum_{h=1}^{C}\sum_{k=m+1}^{\Omega}\sum_{j=1}^{T}(\boldsymbol{a}_{hkj}^{\top}\boldsymbol{v}_{kj} + b_{hk})}{\sum_{h=1}^{C}(a_{h\alpha\beta o} + e_{h\alpha\beta o})}
\end{aligned}$$

$$\tag{5.4}$$

where $e_{h\alpha\beta o}$ is noise added to $a_{h\alpha\beta o}$. I do not deal with the term $(a_{h\alpha\beta o} + e_{h\alpha\beta o})v_{\alpha\beta o}$ in the $(\boldsymbol{a}_{hij} + \boldsymbol{e}\boldsymbol{a}_{hij})^{\top}\boldsymbol{v}_{ij}$ in the left side of the equation 5.4. Comparing the equation 5.3 with the equation 5.4, we can see that the optimum value is an estimation value including effectiveness of noise in the image.

5.3 An estimation method of velocity vector via voting process with a weighting function using an incompressible viscous fluid velocity vector constraint equation determined coefficients by intensity constraint

The conventional methods considering physical constraint of fluid estimate v_{11}, v_{12}, $\cdots$, $v_{\Omega T}$ using an evaluation function of constraint equations defined in each method on whole pixels in an image. In case of adding noise to the image, as shown in equation (5.4), precision of estimation parameters of velocity vector declines. We expect that we can precisely estimate velocity vectors, if we exclude effective of noise against estimation parameters.

As a method that can precisely estimate parameters excluding effectiveness of noise, A voting process with a weighting function has been proposed[66]. The method calculates each estimation value $v_{med11}, v_{med12}, \cdots, v_{med\Omega T}$ by using intersections of constraint equations with respect to estimation parameters in a parameter space of $v_{11}, v_{12}, \cdots, v_{\Omega T}$. The voting process with a weighting function, in the process of calculation of estimation values, excludes intersections of constraint equations influenced by noise. Therefore, the method has robustness against noise for estimating estimation parameters.

Since partial differential coefficients of velocity vector components u and v in constraint equations used in the conventional methods considering physical constraint of fluid include velocity vector parameters u and v, we cannot determine the partial differential coefficients of velocity vector components u and v. Thus, we cannot apply the constraint equations

used in the conventional methods to the voting process with a weighting function. I assume that a premise condition of a theorem such that "partial differential coefficients including u and v can be determined by using intersections of intensity constraint equation of a velocity vector" is satisfied. If the theorem holds, we can determine the partial differential coefficients. By determining the partial differential coefficients based on the theorem, we can apply the constraint equations used in conventional methods to the method via voting process with a weighting function. In the field of fluid analysis, the incompressible viscous fluid is mainly used as an application object. Thus, I aim to apply to the incompressible viscous fluid.

In order to apply to the incompressible viscous fluid, I derive an incompressible viscous fluid velocity vector constraint equation determined coefficients by intensity constraint based on constraint equations considering physical constraints of incompressible viscous fluid used in Nakajima's method[63]. The constraint equation includes three parameters such as velocity vector parameters and spatial change of pressure. Thus, I expand the parameter space to a 3-dimensional parameter space. I then estimate the parameters in the constraint equation by using a voting process with a weighting function in a 3-dimensional voting space.

In this section, first, I derive an incompressible viscous fluid velocity vector constraint equation determined coefficients by intensity constraint. Second, I mention about an estimation method of velocity vector via voting process with a weighting function using the incompressible viscous fluid velocity vector constraint equation determined coefficients by intensity constraint.

5.3.1 Derivation of an incompressible viscous fluid velocity vector constraint equation determined coefficients by intensity constraint

Let (x, y, t) be a pixel (x, y) at time t. A velocity vector on (x, y, t) satisfies an intensity constraint equation of velocity vector[7]

$$\frac{\partial I}{\partial x}u + \frac{\partial I}{\partial y}v + \frac{\partial I}{\partial t} = 0, \tag{5.5}$$

where $\partial I/\partial x$, $\partial I/\partial y$, $\partial I/\partial t$ are partial differential coefficients of an intensity $I(x, y, t)$ on (x, y, t) with respect to x, y, t, respectively, u, v are components of velocity vector axis on (x, y, t) for x axis and y axis respectively. In case that objects in an image is incompressible viscous fluid, the objects satisfy continuity equation

$$\frac{\partial u}{\partial x} + \frac{\partial v}{\partial y} = 0 \tag{5.6}$$

and Navier-Stokes's equation

$$\frac{\partial u}{\partial t} + \frac{\partial u}{\partial x}u + \frac{\partial u}{\partial y}v = -\frac{1}{\rho}\frac{\partial p}{\partial x} + \nu\left(\frac{\partial^2 u}{\partial x^2} + \frac{\partial^2 u}{\partial y^2}\right) + X \tag{5.7}$$

$$\frac{\partial v}{\partial t} + \frac{\partial v}{\partial x}u + \frac{\partial v}{\partial y}v = -\frac{1}{\rho}\frac{\partial p}{\partial y} + \nu\left(\frac{\partial^2 v}{\partial x^2} + \frac{\partial^2 v}{\partial y^2}\right) + Y \tag{5.8}$$

where ρ, ν, and p are density, kinematic viscosity and pressure respectively, X and Y are components of external force on (x, y, t) for x axis and y axis respectively. In case that estimation parameters on (x, y, t) satisfy from equation (5.5) through equation (5.8), the estimation parameters satisfy

$$
\frac{\partial u}{\partial t} + \frac{\partial v}{\partial t} + \left(\frac{\partial u}{\partial x} + \frac{\partial v}{\partial x} - \frac{\partial I}{\partial x} \right) u + \left(\frac{\partial u}{\partial y} + \frac{\partial v}{\partial y} - \frac{\partial I}{\partial y} \right) v + \frac{1}{\rho} \left(\frac{\partial p}{\partial x} + \frac{\partial p}{\partial y} \right)
$$
$$
= \nu \left(\frac{\partial^2 u}{\partial x^2} + \frac{\partial^2 u}{\partial y^2} + \frac{\partial^2 v}{\partial x^2} + \frac{\partial^2 v}{\partial y^2} \right) + \frac{\partial I}{\partial t} + X + Y + \left(\frac{\partial u}{\partial x} + \frac{\partial v}{\partial y} \right). \tag{5.9}
$$

Equation (5.9) represents a velocity vector constraint equation considering physical constraint of incompressible viscous fluid. In equation (5.9), we can obtain the coefficients $\partial I/\partial x$, $\partial I/\partial y$, $\partial I/\partial t$ from an image, we can obtain values of the parameters ρ, ν, X, Y as known quantity from environment conditions. However, we cannot determine partial differential coefficients with respect to u and v directly since partial differential coefficients with respect to u and v include estimation parameters u and v. Thus, we cannot apply the equation (5.9) to the voting process with a weighting function. We regard Δx, Δy, Δt as $\Delta x \to 0$, $\Delta y \to 0$, $\Delta t \to 0$, by theorem 1 (See appendix), we regard u, v, p in equation (5.9) on a point (x, y, t) and its the temporal/spatial neighboring points as an equivalent value respectively. Then, we regard equation (5.9) as equation (5.5). In this case, if theorem 2 (See appendix) holds, we can obtain the partial differential coefficients with respect to u and v in equation (5.9) from equation (5.5). Finally, we can regard the equation (5.9) as liner equation with respect to u, v, $(\partial p/\partial x + \partial p/\partial y)$ (In following, we represent $(\partial p/\partial x + \partial p/\partial y)$ as p_{xy}). Since the equation (5.9) can be regarded as liner equation, we can apply the equation (5.9) to the voting process with a weighting function. We call the liner constraint equation as an incompressible viscous fluid velocity vector constraint equation determined coefficients by an intensity constraint.

5.3.2 Determination of estimation parameters u, v, p_{xy} in an incompressible viscous fluid velocity vector constraint equation determined coefficients by an intensity constraint via voting process with a weighting function

I set an interest pixel for estimating velocity vector in a support region (Figure 5.1), we can obtain n equations (5.9) on each pixel ($1 \sim n$) in the support region.

$$
\begin{aligned}
\alpha_1 u + \beta_1 v + \gamma_1 p_{xy} &= \phi_1 \\
\alpha_2 u + \beta_2 v + \gamma_2 p_{xy} &= \phi_2 \\
&\vdots \\
\alpha_n u + \beta_n v + \gamma_n p_{xy} &= \phi_n,
\end{aligned}
$$

where α, β and γ are coefficients of u, v, p_{xy} respectively, ϕ is a constant term. If the theorem 1 holds in the support region, u, v, p_{xy} are equivalent values U, V, P_{xy} respectively. Then, intersections of n equations (5.9) converge into U, V, P_{xy} in parameter space u, v, p_{xy}. In this case, we can determine the coordinate (U, V, P_{xy}) as estimated parameters of u, v and p_{xy} on the interest pixel (Figure 5.1). However, In case of following situations,
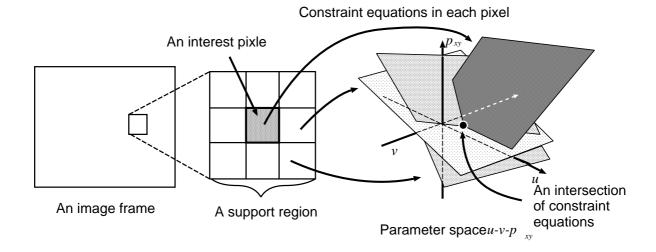
Figure 5.1: A support region and constraint planes in parameter space u-v-p_{xy}.

the constraint lines have different intersections from U, V and P_{xy}.

(A) Fluctuation of intersections of constraint equation by influence of spatial changes of motions and pressure In incompressible viscous fluid, there are spatial changes of velocity vector and pressure generally. In such a situation, each pixel in a support region has different parameter u, v and p_{xy} from other pixels in the support region. It means that there is fluctuation of intersections of constraint equation in parameter space u-v-p_{xy}.

(B) Fluctuation of intersections of constraint equation effected by noise

I consider three constraint equations (5.9) that satisfy premise conditions of the constraint equation (5.9) in a support region. The equations are expressed by

$$\alpha_1 u + \beta_1 v + \gamma_1 p_{xy} = \phi_1, \tag{5.10}$$

$$\alpha_2 u + \beta_2 v + \gamma_2 p_{xy} = \phi_2, \tag{5.11}$$

$$\alpha_3 u + \beta_3 v + \gamma_3 p_{xy} = \phi_3, \tag{5.12}$$

where α_1, β_1 or γ_1 denote coefficients with respect to u, v or p_{xy} in constraint equation (5.9) on a first pixel in a support region respectively, α_2, β_2 or γ_2 denote coefficients with respect to u, v or p_{xy} in constraint equation (5.9) on a second pixel in a support region respectively, α_3, β_3 or γ_3 denote coefficients with respect to u, v or p_{xy} in constraint equation (5.9) on a third pixel in a support region respectively. An intersection $(u, v, p_{xy})^\top$ of these constraint equations is expressed as

$$\begin{pmatrix} u \\ v \\ p_{xy} \end{pmatrix} = \begin{pmatrix} \frac{(\beta_2\phi_1 - \beta_1\phi_2)(\gamma_1 - \beta_3 - \gamma_3\beta_1) - (\beta_3 - \phi_1 - \beta_1\phi_3)(\gamma_1\beta_2 - \gamma_2\beta_1)}{(\alpha_1\beta_2 - \alpha_2\beta_1)(\gamma_1\beta_3 - \gamma_3\beta_1) - (\alpha_1\beta_3 - \alpha_3\beta_1)(\gamma_1\beta_3 - \gamma_3\beta_1)} \\ \frac{(\gamma_1\alpha_2 - \gamma_2\alpha_1)(\gamma_1 - \alpha_3 - \gamma_3\alpha_1) - (\phi_1 - \alpha_3 - \phi_3\alpha_1)(\gamma_1\alpha_2 - \gamma_2\alpha_1)}{(\beta_1\alpha_2 - \beta_2\alpha_1)(\gamma_1 - \alpha_3 - \gamma_3\alpha_1) - (\beta_1\alpha_3 - \beta_3\alpha_1)(\gamma_1 - \alpha_2 - \gamma_2\alpha_1)} \\ \frac{(\alpha_2\phi_1 - \alpha_1\phi_2)(\beta_1\alpha_3 - \beta_3\alpha_1) - (\phi_1 - \alpha_3 - \phi_3 - \alpha_1)(\beta_1 - \alpha_2 - \beta_2 - \alpha_1)}{(\gamma_1\alpha_2 - \gamma_2\alpha_1)((\beta_1\alpha_3 - \beta_3\alpha_1) - (\gamma_1 - \alpha_3 - \gamma_3 - \alpha_1)(\beta_1\alpha_2 - \beta_2\alpha_1)} \end{pmatrix}. \tag{5.13}$$

If the equation (5.10) is a constraint equation effected by noise, the spatial/temporal gradients in the image are changed intensely. Thus, (5.10) is replaced by

$$\alpha_1' u + \beta_1' v + \gamma_1 p_{xy} = \phi_1', \tag{5.14}$$

159

where α_1', β_1' or ϕ_1' are coefficients of equation (5.10) in case of not satisfying realizable conditions of the constraint equation respectively. Therefore the intersection $(u, v, p_{xy})^\top$ of the constraint equations is changed to

$$\left(\begin{array}{c} u' \\ v' \\ p_{xy}' \end{array} \right) = \left(\begin{array}{c} \frac{(\beta_2\phi_1' - \beta_1'\phi_2)(\gamma_1 - \beta_3 - \gamma_3\beta_1') - (\beta_3 - \phi_1' - \beta_1'\phi_3)(\gamma_1\beta_2 - \gamma_2\beta_1')}{(\alpha_1'\beta_2 - \alpha_2\beta_1')(\gamma_1\beta_3 - \gamma_3\beta_1') - (\alpha_1'\beta_3 - \alpha_3\beta_1')(\gamma_1\beta_3 - \gamma_3\beta_1')} \\ \frac{(\gamma_1\alpha_2 - \gamma_2\alpha_1')(\gamma_1 - \alpha_3 - \gamma_3\alpha_1') - (\phi_1' - \alpha_3 - \phi_3\alpha_1')(\gamma_1\alpha_2 - \gamma_2\alpha_1')}{(\beta_1'\alpha_2 - \beta_2\alpha_1')(\gamma_1 - \alpha_3 - \gamma_3\alpha_1') - (\beta_1'\alpha_3 - \beta_3\alpha_1')(\gamma_1 - \alpha_2 - \gamma_2\alpha_1')} \\ \frac{(\alpha_2\phi_1' - \alpha_1'\phi_2)(\beta_1'\alpha_3 - \beta_3\alpha_1') - (\phi_1' - \alpha_3 - \phi_3 - \alpha_1')(\beta_1' - \alpha_2 - \beta_2 - \alpha_1')}{(\gamma_1\alpha_2 - \gamma_2\alpha_1')((\beta_1'\alpha_3 - \beta_3\alpha_1') - (\gamma_1 - \alpha_3 - \gamma_3 - \alpha_1')(\beta_1'\alpha_2 - \beta_2\alpha_1')} \end{array} \right) . \qquad (5.15)$$

Then, I define a difference vector $(\Delta u, \Delta v, \Delta p_{xy})^\top$ as

$$\left(\begin{array}{c} \Delta u \\ \Delta v \\ \Delta p_{xy} \end{array} \right) = \left(\begin{array}{c} u - u' \\ v - v' \\ p_{xy} - p_{xy}' \end{array} \right) . \qquad (5.16)$$

Since $\alpha_1 \neq \alpha_1'$, $\beta_1 \neq \beta_1'$, $\gamma_1 \neq \gamma_1'$, the difference vector $(\Delta u, \Delta v, \Delta p_{xy})^\top$ is not zero vector. This means, if there is a constraint equation effected by noise in a support region, intersections of constraint equations are scattered.

I use voting process to estimate values of estimation parameters from scattered intersections of constraint equations by the factors of $(\mathbf{A})$, excluding intersections of constraint equations by the factors of $(\mathbf{B})$. By voting of intersections in the parameter space u-v-p_{xy}
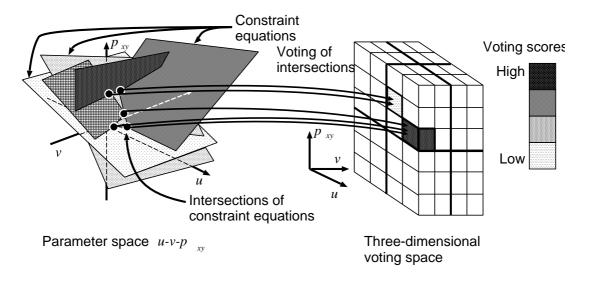
Figure 5.2: Voting process of intersections in parameter space u-v-p_{xy} to 3-dimensional voting space.

to the voting space, if scattered intersections of constraint equations by the factors of $(\mathbf{A})$ converge into a cell in voting space, the voting score in the cell will be the maximum voting score. Then we decide the coordinate of the maximum voting score as estimated parameters u, v and p_{xy}. By this process, we can expect to precisely estimate estimated parameters u and v excluding the intersections of constraint equations by the factors of $(\mathbf{B})$ (Figure 5.2). In case that intersections of constraint equations do not converge into a cell in voting space, There is a case that we cannot obtain the maximum voting score by

160

fluctuation of voting scores. To obtain the reasonable maximum voting score in case of fluctuation of voting scores, a method of voting process with a weighting function has been proposed. This method determines (u_{med}, v_{med}) as a velocity vector in the interest pixel in the support region by detecting the coordinate u_{med}, v_{med} and p_{xymed} of the maximum voting score in $f'(u_\alpha, v_\alpha, p_{xy\alpha})$ represented as

$$f'(u_\alpha, v_\alpha, p_{xy\alpha}) = \sum_{u=-V/2}^{V/2} \sum_{v=-V/2}^{V/2} \sum_{p_{xy}=-V_p/2}^{V_p/2} w(u - u_\alpha, v - v_\alpha, p_{xy} - p_{xy\alpha}) f(u, v, p_{xy}), \quad (5.17)$$

where V and V_p are size on axis u and v in the voting space and size on axis p_{xy} of the voting space respectively, u_α, v_α, $p_{xy\alpha}$ are interest coordinates in the voting space, W is a weighting function. I decide a weighting function as

$$w(u - u_\alpha, v - v_\alpha, p_{xy} - p_{xy\alpha}; \sigma, \sigma_p) = \frac{1}{(2\pi)^{3/2}\sqrt{\sigma}\sqrt{\sigma_p}} \exp\left\{-\frac{(u - u_\alpha)^2 + (v - v_\alpha)^2}{2\sigma^2} - \frac{(p - p_\alpha)^2}{2\sigma_p^2}\right\},$$
$$(5.18)$$

where σ and σ_p are a variance parameter on u and v axis in the voting space and a variance parameter on p_{xy} axis in the voting space respectively.
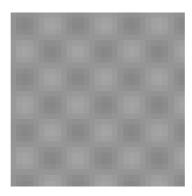
Figure 5.3: The model image used in the experiments.

5.4 Experiments for comparison of velocity vector estimation precision

To evaluate effectiveness of the proposed method quantitatively, I experiment on comparison of precision of velocity vectors in the proposed method and conventional methods.

In conventional methods, since they experimented using 2-dimensional steady flow, Thus, we experiment using 2-dimensional steady flow. By using steady flow, we regard gravity as zero because optical axis of a camera is parallel with gravity. Thus, we set X and Y to zero respectively. We set $\partial u/\partial t = \partial v/\partial t = 0$ because there is no change of stream line in time variant.

5.4.1 Experiments in synthetic image sequences

In this section, I quantitatively evaluate precision of velocity vector estimation by the proposed method and conventional methods in synthetic image sequences. I set an environment setting of the flow field 1 as a criterion (Figure 5.4). In the flow field 2, I changed quantity of inflow of the flow field 1 as shown in the Figure 5.6. In the flow field 3, I changed the position of the obstacle of the flow field 1 as shown in the Figure 5.8. Then, I generated flow fields shown in Figure 5.5, Figure 5.7 and Figure 5.9 by the numerical calculation of incompressible viscous based on the situations in inside regions surrounded by point lines in the Figure 5.4, Figure 5.6 or Figure 5.8. The values of ν, ρ and Reynolds number Re used in the numerical calculation are set to $1.004{\times}10^{-9}[\text{m}^2/\text{s}]$ and $1.0{\times}10^3[\text{kg/m}^3]$ and $Re = 25.0$ as the values of water respectively. As the first frame of each image sequences used in this experiments, I used images that the size is $20{\times}20[\text{pixels}]$ and the quantity level is $8[\text{bit/pixel}]$ and intensity is smooth temporally and spatially (Figure 5.3). As the second frame of each image sequence used in this experiments, I generated images based on the flow field in Figure 5.5, Figure 5.7 or Figure 5.9. I call the set of the first image and second image generated based on the each flow field as image 1, image 2 and image 3 respectively. Since each image dose not contain motion boundary, I do not consider boundary conditions. To quantitatively evaluate precision of velocity vectors, I use the mean of normalized error

$$\bar{e}_n = \frac{1}{MN} \sum_{x=0}^{M-1} \sum_{y=0}^{N-1} \frac{||\tilde{\boldsymbol{f}}_{xy} - \hat{\boldsymbol{f}}_{xy}||}{||\tilde{\boldsymbol{f}}_{xy}||}, \tag{5.19}$$

Table 5.1: The parameters used in each method.

Method	Values of parameters	
The proposed method	$V = 1.2 \times 10$	$V_p = 4.0 \times 10^9$
	$\sigma = 1.5 \times 10$	$\sigma_p = 2.0$
Nakajima	$\alpha_N = 1.0 \times 10^{-4}$	$\beta_N = 1.0 \times 10^{-4}$
Corpetti	$\alpha_C = 1.0 \times 10^{-2}$	$\beta_C = 1.0 \times 10^2$
Bereziat	$\alpha_B = 1.0 \times 10^{-3}$	

Table 5.2: The mean of normalized error $\bar{e}_n$ of each method in the model image 1.

Method	$\bar{e}_n$
The proposed method	4.15×10^{-1}
Nakajima	4.81×10^{-1}
Corpetti	5.15×10^{-1}
Bereziat	5.18×10^{-1}

Table 5.3: The mean of normalized error $\bar{e}_n$ of each method in the model image 2.

Method	$\bar{e}_n$
The proposed method	5.43×10^{-1}
Nakajima	5.79×10^{-1}
Corpetti	5.95×10^{-1}
Bereziat	6.04×10^{-1}

Table 5.4: The mean of normalized error $\bar{e}_n$ of each method in the model image 3.

Method	$\bar{e}_n$
The proposed method	4.16×10^{-1}
Nakajima	4.31×10^{-1}
Corpetti	4.43×10^{-1}
Bereziat	4.45×10^{-1}

where M and N are vertical and horizontal image size respectively, $\tilde{\boldsymbol{f}}_{xy}$ is an correct velocity vector on a pixel (x, y), $\hat{\boldsymbol{f}}_{xy}$ is an estimated velocity vector on a pixel (x, y). The parameters used in this experiments are shown in the Table 5.1. I decided the parameters to be the optimum experimentally. I set the size of support region to 9×9[pixels] and cell size V and V_p in the voting space to 1.0×10^{-2} and 1.0×10^{-1} respectively. As values in water, I set ν and ρ in Nakajima's method and the proposed method to 1.004×10^{-9} and 1.0×10^3 respectively. I set iterative calculation times for estimating velocity vectors in conventional methods to 5000 times.

Experimental results of from image 1 though image 3 are shown in from Table 5.2 through Table 5.4. Estimated flow fields in each image sequence are shown in from Figure 5.10 through Figure 5.21. In the experimental result of image1, by using the proposed method, I could obtain approximately 20% higher precision of velocity vector estimation in comparison with precision of conventional methods. I consider that the factors of improvement of precision of velocity vectors by using the proposed method are considering physical conditions of incompressible viscous fluid and excluding equations

(5.9) that deviate from premise condition of the theorem 2. On the other hand, in image 2 and image 3, the subtraction of precision of velocity vector estimation in the conventional methods and the proposed method kept no more than 7 %. I consider that the factor is, by asymmetry of the vortex in image 2 and image 3, declining of approximation precision in partial differential coefficients with respect to u and v of equation (5.9) based on theorem 2.
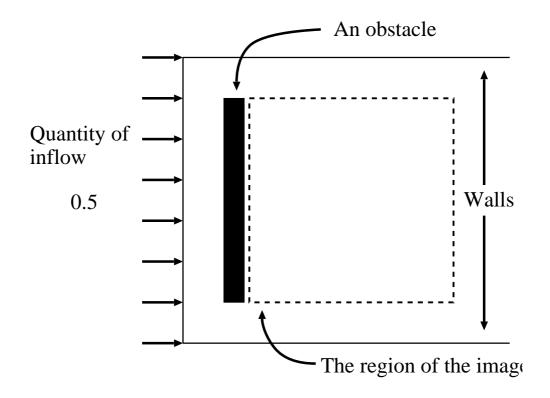
Figure 5.4: The setting condition for the flow field 1.
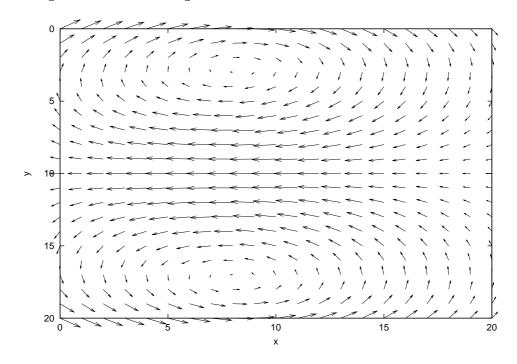
Figure 5.5: The generated flow field 1.
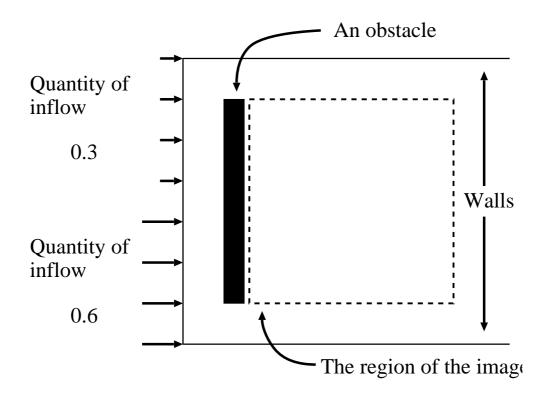
Figure 5.6: The setting condition for the flow field 2.
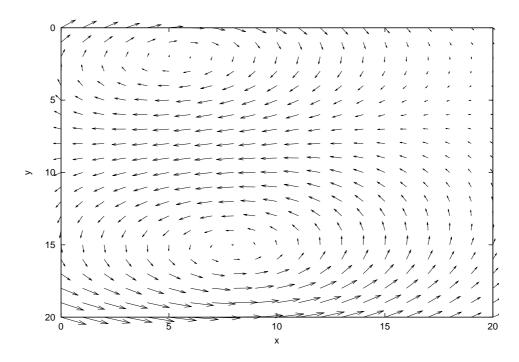
Figure 5.7: The generated flow field 2.
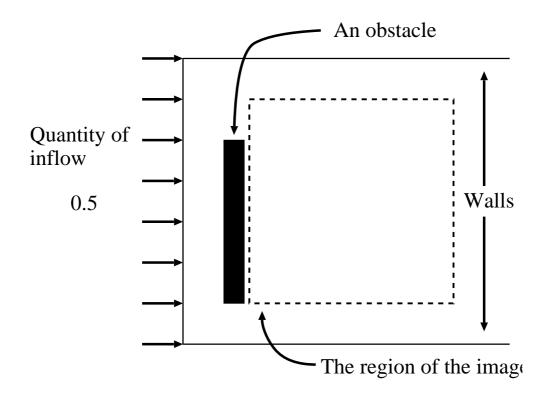
Figure 5.8: The setting condition for the flow field 3.
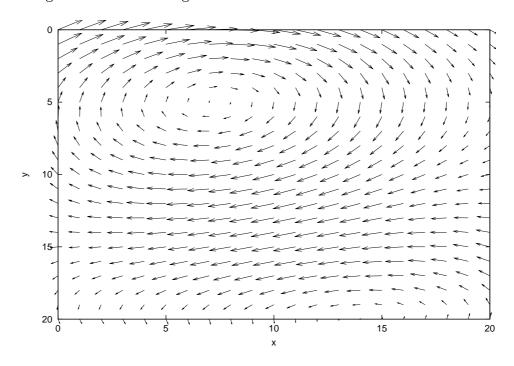
Figure 5.9: The generated flow field 3.
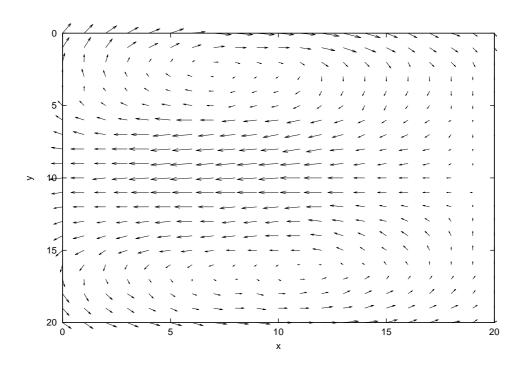
Figure 5.10: An estimated flow field by the proposed method in image 1.
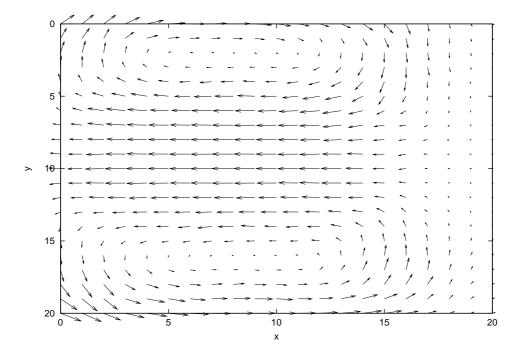
Figure 5.11: An estimated flow field by Nakajima's method in image 1.
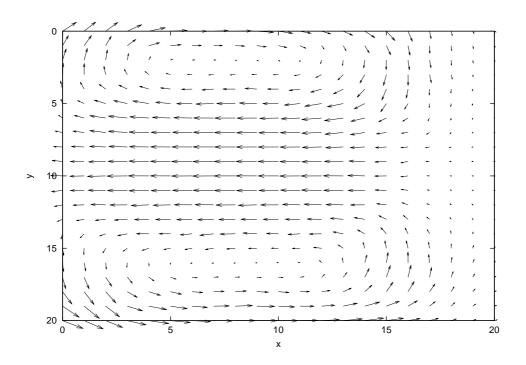
Figure 5.12: An estimated flow field by Corpetti's method in image 1.
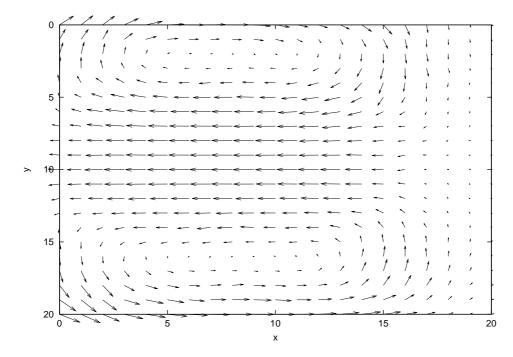
Figure 5.13: An estimated flow field by Bereziat's method in image 1.

169
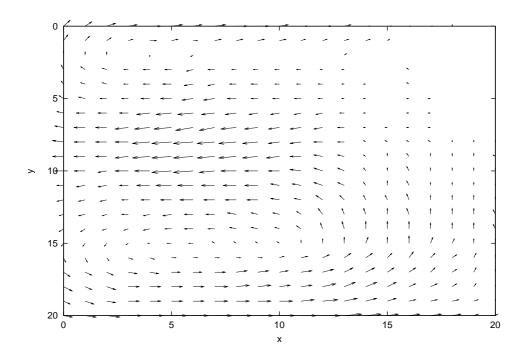
Figure 5.14: An estimated flow field by the proposed method in image 2.
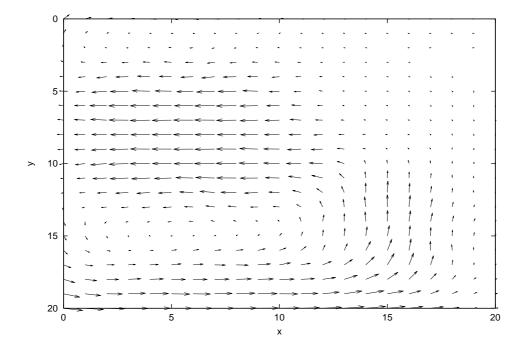
Figure 5.15: An estimated flow field by Nakajima's method in image 2.
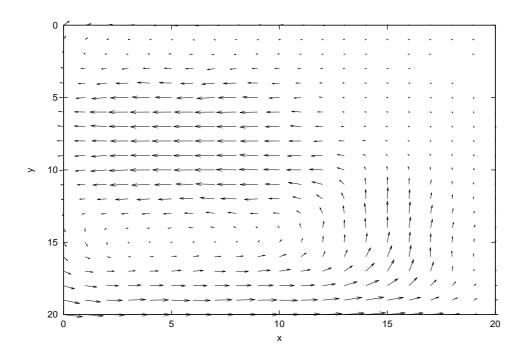
Figure 5.16: An estimated flow field by Corpetti's method in image 2.
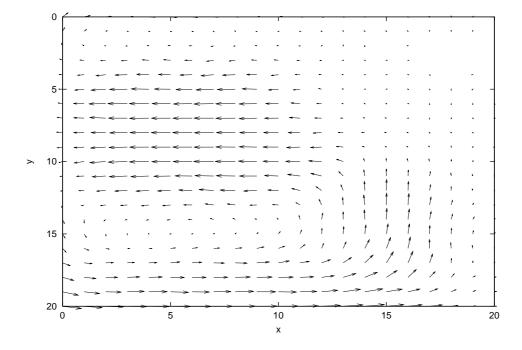
Figure 5.17: An estimated flow field by Bereziat's method in image 2.
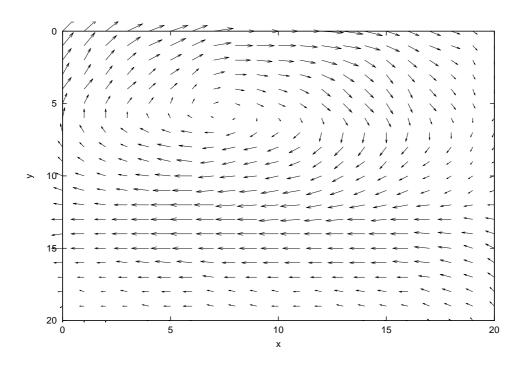
Figure 5.18: An estimated flow field by the proposed method in image 3.
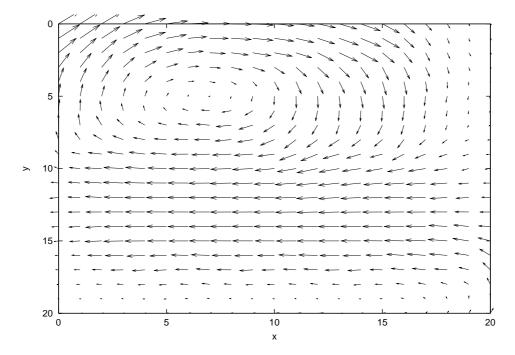
Figure 5.19: An estimated flow field by Nakajima's method in image 3.
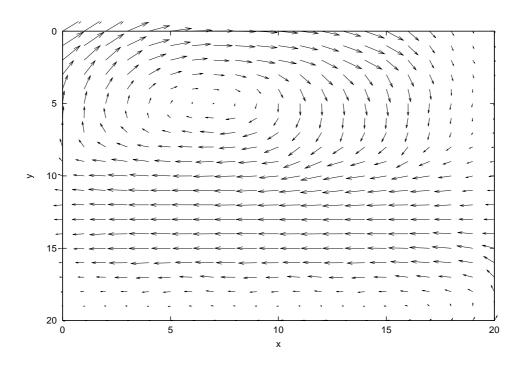
Figure 5.20: An estimated flow field by Corpetti's method in image 3.
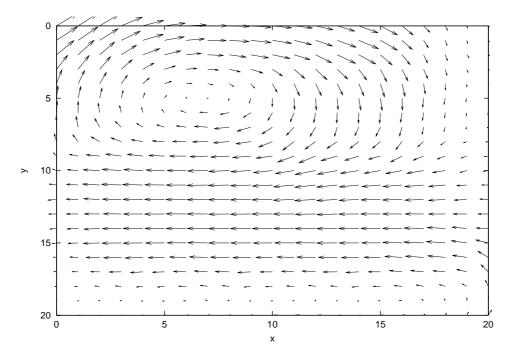
Figure 5.21: An estimated flow field by Bereziat's method in image 3.

5.4.2 Experiments in noisy image sequences

I quantitatively evaluate precision of velocity vector estimation by the proposed method and conventional methods in noisy image sequences.

In this experiments, I add Gaussian noise n whose probability distribution is given by

$$P(n) = \frac{1}{\sqrt{2\pi}\sigma}e^{-\frac{n^2}{2\sigma^2}} \tag{5.20}$$

to $I(x, y, t)$ and obtain

$$I'(x, y, t) = I(x, y, t) + n \tag{5.21}$$

where $I(x, y, t)$ denotes an intensity of the images which is used in the previous experiments. I use

$$PSNR[dB] = 20\log\frac{255}{\sigma} \tag{5.22}$$

to indicate the quantity of noise. I added the Gaussian noise to image 1, image 2 and image 3, then I call the images added Gaussian noise as image 4, image 5 and image 6 respectively. In this experiments, I use the same value of parameters in the methods as it used in the previous experiments.

Estimated flow fields in each image sequence are shown in from Figure 5.22 through Figure 5.33. The experimental result from in image 4 through in image 6 are shown from in Figure 5.34 through in Figure 5.36. I could obtain precision of velocity vector estimation higher than precision of conventional methods by using the proposed method. Especially, The more noise is added to the image, the more improvement of precision of velocity vector estimation is much better by using the proposed method. This factor is supposed that the proposed method has robustness against noise.
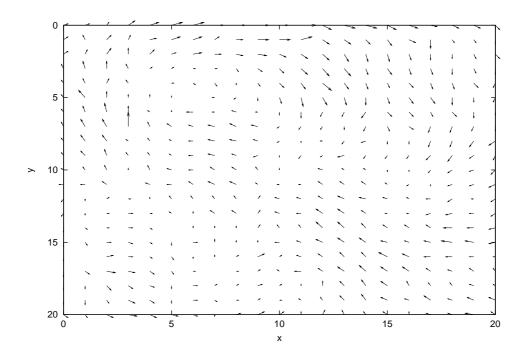
Figure 5.22: An estimated flow field by the proposed method in image 4 of 27.3[dB].
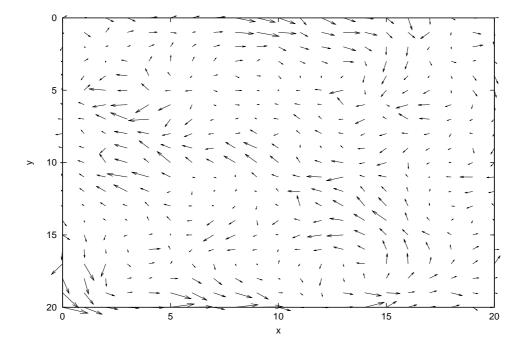
Figure 5.23: An estimated flow field by Nakajima's method in image 4 of 27.3[dB].

175
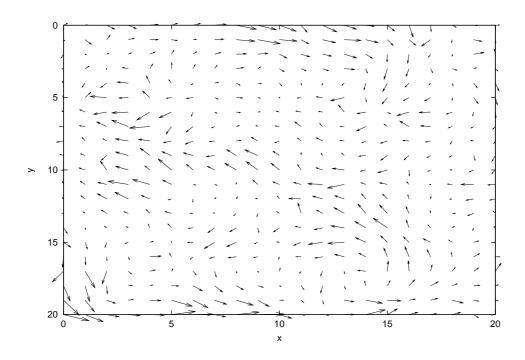
Figure 5.24: An estimated flow field by Corpetti's method in image 4 of 27.3[dB].
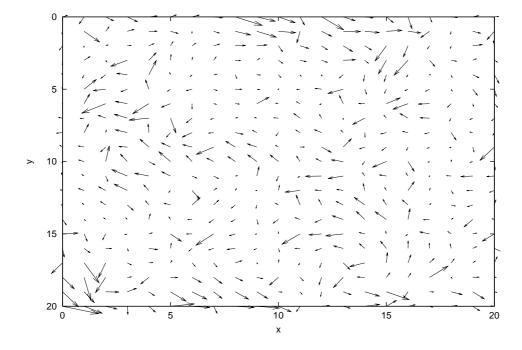
Figure 5.25: An estimated flow field by Bereziat's method in image 4 of 27.3[dB].

176
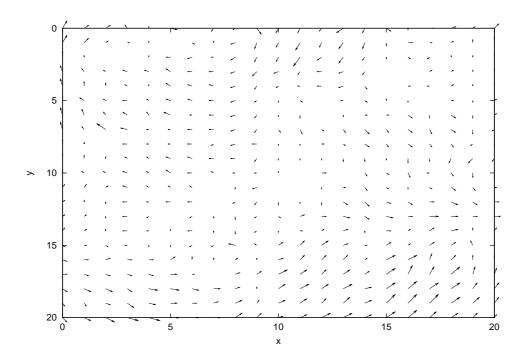
Figure 5.26: An estimated flow field by the proposed method in image 5 of 27.3[dB].
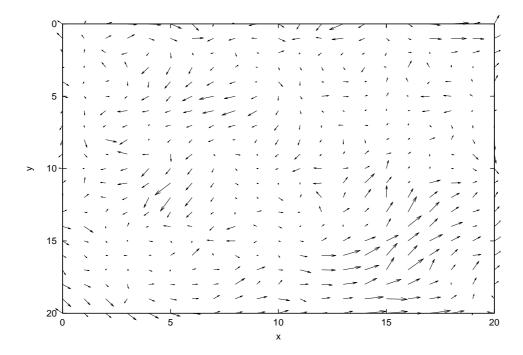
Figure 5.27: An estimated flow field by Nakajima's method in image 5 of 27.3[dB].
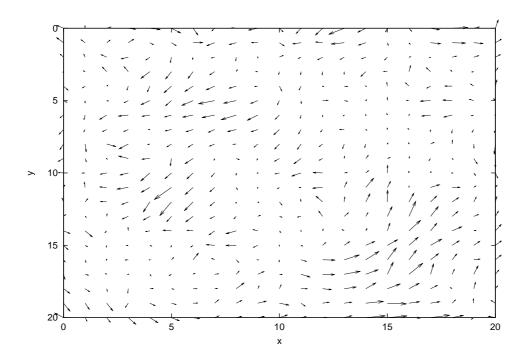
Figure 5.28: An estimated flow field by Corpetti's method in image 5 of 27.3[dB].
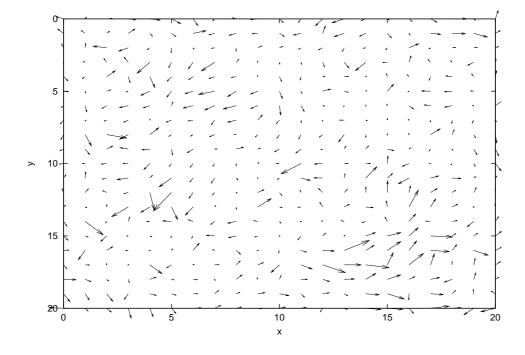
Figure 5.29: An estimated flow field by Bereziat's method in image 5 of 27.3[dB].

178
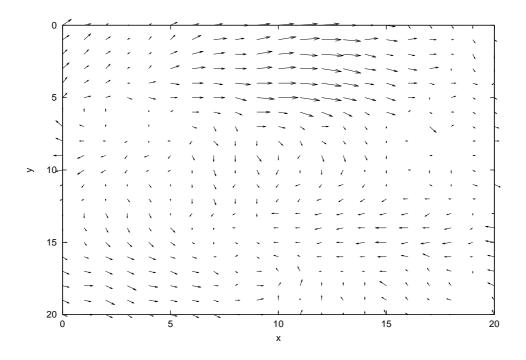
Figure 5.30: An estimated flow field by the proposed method in image 6 of 27.3[dB].
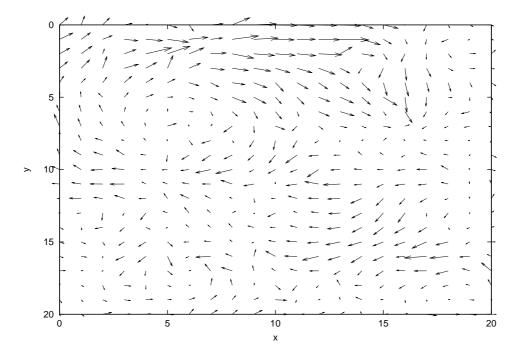
Figure 5.31: An estimated flow field by Nakajima's method in image 6 of 27.3[dB].

179
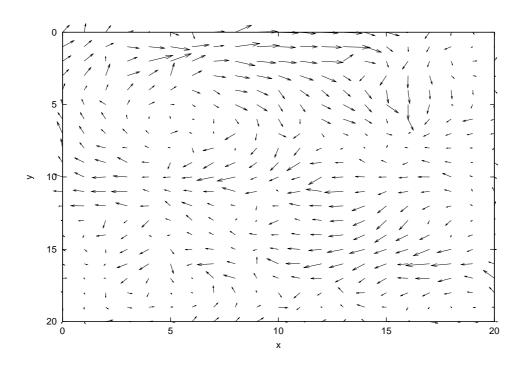
Figure 5.32: An estimated flow field by Corpetti's method in image 6 of 27.3[dB].
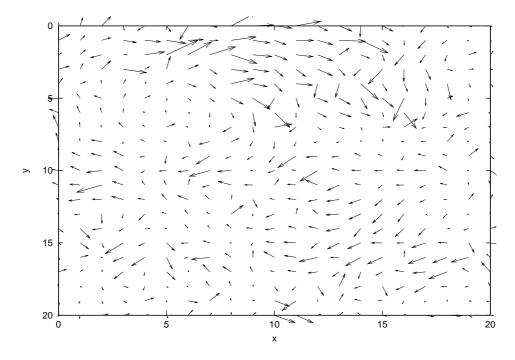
Figure 5.33: An estimated flow field by Bereziat's method in image 6 of 27.3[dB].
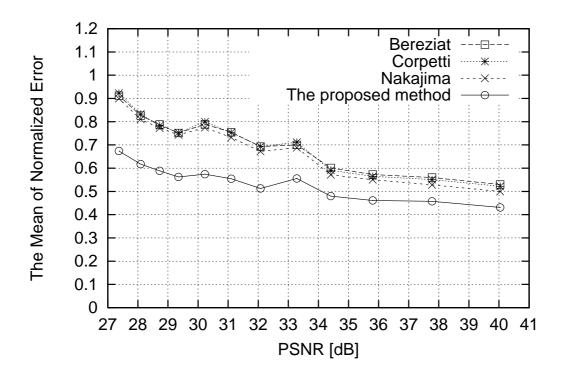
Figure 5.34: The mean of normalized error $\bar{e}_n$ of each method in noisy model image 4.
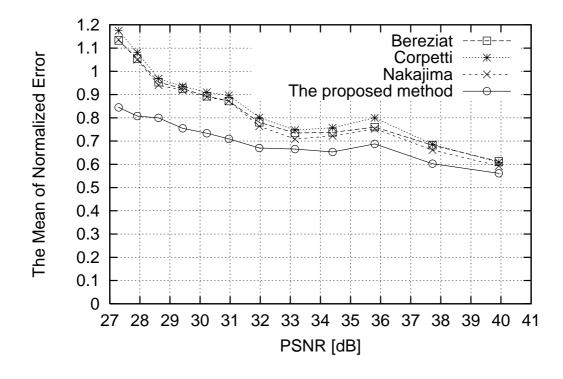
Figure 5.35: The mean of normalized error $\bar{e}_n$ of each method in noisy model image 5.
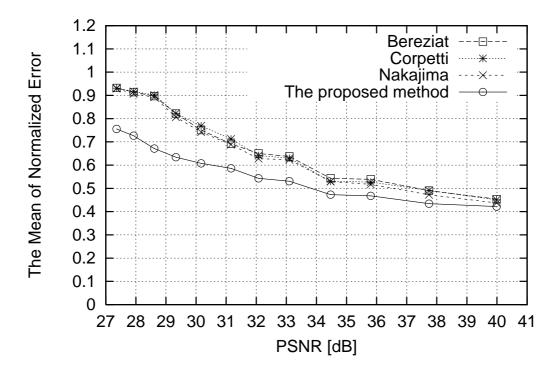
Figure 5.36: The mean of normalized error $\bar{e}_n$ of each method in noisy model image 6.

5.4.3   Experiment in an actual image sequence

In order to evaluate effectiveness of the proposed method, I experiment on comparison of velocity vector estimation precision of conventional methods and the proposed method in case of applying to an actual image sequence image sequences. I use temporal 2 frames (Figure 5.38) of an actual image sequence (Figure 5.37) for this experiment. The condition of the actual image sequence (Figure 5.37) is shown in Figure 5.39. The water flow in the actual image sequence is visiblized by using a dyestuff.

I set parameters in the proposed method and the conventional methods to the same parameter values shown in Table 5.1.

Estimated flow fields are shown in from Figure 5.40 though Figure 5.43.

From the result, we see that the result of velocity vector estimation by using the proposed method is the best. The main factor is supposed to exclude effectiveness of noise by velocity vector estimation method using a voting process with a weighting function.
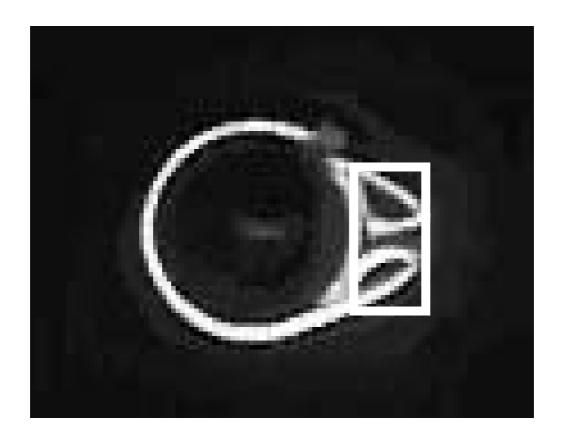
Figure 5.37: An actual image sequence used in this experiment ($Re = 25.0$).

Frame1   Frame2
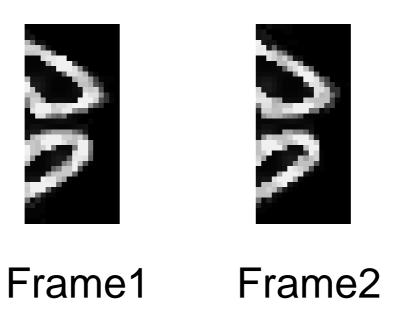
Figure 5.38: Temporal continuous 2 frames of the actual image sequence used in this experiment.
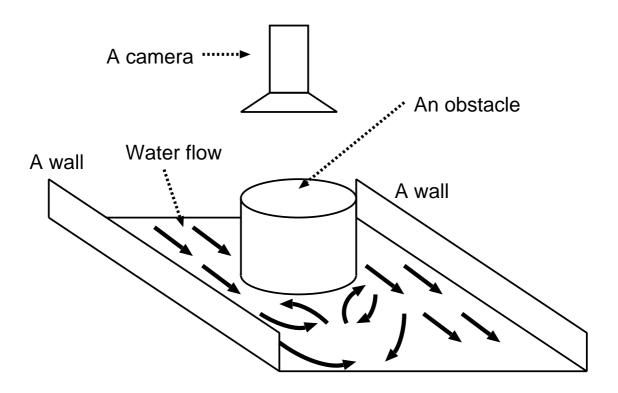
Figure 5.39: The condition in the actual image sequence used in this experiment.
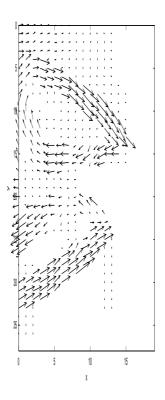
Figure 5.40: An estimated flow field by the proposed method.
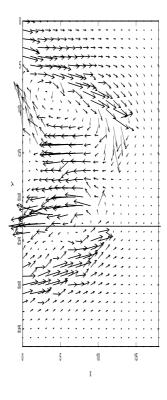

Figure 5.41: An estimated flow field by Nakajima's method.

186
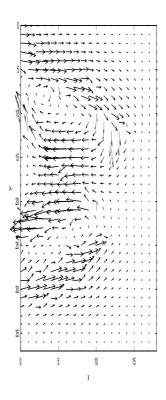
Figure 5.42: An estimated flow field by Corpetti's method
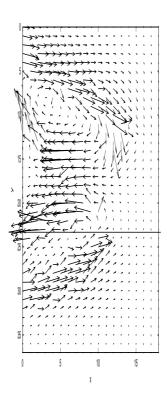
Figure 5.43: An estimated flow field by Bereziat's method

187

5.5   Summary

In order to precisely estimate velocity vectors in fluid analysis using actual image sequences, I derived a constraint equation of a velocity vector considering physical constraint of incompressible viscous fluid. Using theorem 1 and theorem 2, we decided the partial difference coefficients in the derived constraint equation of a velocity vector considering physical constraint of incompressible viscous fluid. We applied the constraint equation of a velocity vector determined partial differential coefficients to the method using voting process with a weighting function.

In order to quantitatively evaluate precision of velocity vector estimation, I experimented on comparison of precision velocity vector estimation by the proposed method and conventional methods in synthetic images, noisy images and an actual image sequence including an incompressible viscous fluid. From the experimental results in synthetic image sequences, I obtained precise precision of velocity vector estimation by using the proposed method. The factor is supposed to exclude intersections of constraint equations that do not satisfy the premise condition of the constraint equations. From the experimental results in noisy synthetic image sequences, by using the proposed method, I obtained approximately 25% higher precision of velocity vector estimation in the maximum than precision of velocity vector estimation in conventional methods. The factor is supposed to exclude intersections of constraint equations effected by noise. From the experimental results in an actual image sequence, I qualitatively obtained precise precision of velocity vector estimation in comparison with the conventional methods. In order to moreover obtain precise estimation results in the estimation of velocity vectors using the voting process, we have to investigate the optimum weighting function for each application in fluid analysis using image sequences.

For the future, I will evaluate effectiveness of the proposed method in unsteady vortex such as Kalman vortex. I will apply an incompressible viscous fluid velocity vector constraint equation determined coefficients by an intensity constraint to other robust estimations except the voting process with a weighting function to compare precision of velocity vector estimation in the proposed method and conventional methods in case of using an incompressible viscous fluid velocity vector constraint equation determined coefficients.

Chapter 6

Conclusions

6.1   Conclusions in this thesis

In actual image sequences, to solve the following important problems in optical flow estimation such as

- · Occlusion

- · Brightness change

- · Fluid analysis by using image sequences

we dealt with the problems as estimation problems of the most likelihood parameter of constraint equations that can be applied to estimate "actual motion of objects". As a method to estimate the most likelihood parameter of the constraint equations, we used a estimation method via voting process with a weighting function. Since each problem has a peculiar problem, I attempted to solve the peculiar problem by different approaches.

In following, I summarize the proposed methods for each problem and its effectiveness.

·Occlusion

In estimating velocity vectors, in order to exclude effectiveness of constraint equations effected by noise and in occlusion regions, I used an estimation method of velocity vectors via voting process with a weighting function. To separate different motions in regions of different motions, in the voting process, I set a condition to separate constraint equations in different motions. In occlusion regions, there is a limit of precision of velocity vector estimation in the estimation method of velocity vectors via voting process with a weighting function. For estimating velocity vectors in occlusion regions, I used extrapolation from estimated velocity vectors in assigned regions of occlusion regions. In experiments for evaluating effectiveness of the proposed method, we obtained following results.

- To evaluate effectiveness of the proposed method, I experimented on comparison of velocity vector estimation precision in conventional methods and the method via voting process with a weighting function in synthesis image sequences and noisy synthesis image sequences. From the results of the experiment, By using the method via the voting process, I obtained well results of velocity vector estimation precision in comparison with the conventional methods. The factor is supposed to get rid of

189

effectiveness of intersections of constraint equations effected by noise or in occlusion regions and separate different motions in regions including different motions.

- I experimented on comparison of velocity vector estimation precision in the method via voting process with a weighting function and in case of applying extrapolation in synthesis image sequences and noisy synthesis image sequences. From the results of the experiment, By applying extrapolation, I obtained well results of velocity vector estimation precision in occlusion regions in comparison with the method via the voting process. The factor is supposed to extrapolate velocity vectors in occlusion regions from estimated velocity vectors that have reliability in assigned regions of occlusion regions.

- Finally, I experimented on comparison of velocity vector estimation precision in conventional methods and the method via voting process with a weighting function in actual image sequences. By using the method via the voting process, I obtained well results of velocity vector estimation precision in comparison with the conventional methods. Similarly, I experimented on comparison of velocity vector estimation precision in the method via voting process with a weighting function and in case of applying extrapolation in actual image sequences. By applying extrapolation, I obtained well results of velocity vector estimation precision in comparison with the method via the voting process.

·**Brightness change**

By dealing with estimating velocity vectors in a situation of occurring brightness change as estimating the most likelihood parameter of constraint equations considering brightness change in a parameter space, I proposed a method that has all effective properties in the conventional methods considering brightness change. In order to estimate the most likelihood parameter in a parameter space, I expanded the parameter space to a 3-dimensional parameter space since a constraint equation considering brightness change has three parameters. I then estimated the parameters in the constraint equation by using a voting process with a weighting function in a 3-dimensional voting space. In experiments for evaluating effectiveness of the proposed method, we obtained following results.

- In order to evaluate that the proposed method has the all properties from property 1 through property 6, I first experimented on comparison of velocity vector estimation precision in following image sequence.

    - For evaluating property 1 and property 2 : Image sequences including effectiveness of different reflection rate on an object
    - For evaluating property 3 : Image sequences including effectiveness of shading on an object
    - For evaluating property 4 : Image sequences including effectiveness of intensity change of a light source
    - For evaluating property 5 : Image sequences including effectiveness of noise
    - For evaluating property 6 : Image sequences including effectiveness of regions where pattern changes intensely

From the results of the experiments, precision of velocity vector estimation by using the proposed method was well in comparison with the other methods. The factor is supposed that the proposed method has each property.

- I next experimented on comparison of velocity vector precision in image sequences that have factors of all properties. From the result of the experiment, precision of velocity vector estimation by using the proposed method was well in comparison with the other methods. The factor is supposed that the proposed method has all properties.

- I finally applied the proposed method and the conventional methods to actual image sequences that include translation, expansion, contraction or rotation respectively. From the result of the experiment, precision of velocity vector estimation by using the proposed method was qualitatively well in comparison with the other methods.

·Fluid analysis by using image sequences

In order to precisely estimate velocity vectors in fluid analysis using actual image sequences, I derived a constraint equation of velocity vectors considering physical constraint of incompressible viscous fluid. Using theorem 1 and theorem 2, we decided the partial difference coefficients in the derived constraint equation of velocity vectors considering physical constraint of incompressible viscous fluid. We applied the constraint equation of velocity vectors determined partial differential coefficients to the method using voting process with a weighting function. In experiments for evaluating effectiveness of the proposed method, we obtained following results.

- In order to quantitatively evaluate precision of velocity vector estimation in synthetic images including an incompressible viscous fluid, I experimented on comparison of precision of velocity vector estimation by the proposed method and conventional methods. From the experimental results in synthetic image sequences, I obtained precise precision of velocity vector estimation by using the proposed method. The factor is supposed to exclude intersections of constraint equations that do not satisfy the premise condition of the constraint equations.

- In order to quantitatively evaluate precision of velocity vector estimation in noisy synthetic images including an incompressible viscous fluid, I experimented on comparison of precision of velocity vector estimation by the proposed method and conventional methods. From the experimental results in noisy synthetic image sequences, I obtained precise precision of velocity vector estimation by using the proposed method. The factor is supposed to exclude intersections of constraint equations effected by noise.

- In order to qualitatively evaluate precision of velocity vector estimation in an actual image sequence, I experimented on comparison of precision of velocity vector estimation by the proposed method and conventional methods. From the experimental results in an actual image sequence, I qualitatively obtained precise precision of velocity vector estimation in comparison with the conventional methods.

By solving each problems using the proposed methods for solving each problem, I believe that could expand range of application in velocity vector estimation.

6.2 Future works

For the future, we will investigate following terms.

·Investigation of applicable range in the proposed methods

Each method for the problems must have applicable range. By applying the proposed method to various image sequences, I will investigate the applicable range in the proposed methods for each problem.

·Investigation of a relation between calculation time and precision of velocity vector estimation

The method using voting process with a weighting function has a property such that we can reduce calculation time for velocity vector estimation keeping robustness against noise. I will investigate a relation between calculation time and precision of velocity vector estimation.

·Application of the proposed method to other robust estimation methods

Based on a voting process with a weighting function, I proposed each method for the problems. As I mentioned in introduction, there are other robust estimation methods such as

· M estimation

· LMedS estimation

Attempting to apply the proposed method to the other robust estimations, I investigate properties of the proposed method in case of applying to the other robust estimations.

·Construction of a system for real time image sequences analysis using the proposed methods

From the results of investigation of range of application and the relation between calculation time and precision of velocity vector estimation in the method using voting process with a weighting function, we can obtain properties of the proposed method for each problem. Based on the properties, I will construct a system for real time image sequences analysis using the proposed methods for each problem.

·Application of the proposed methods to the applications based on velocity vector estimation

For example image composition, super resolution, structure estimation and so on, there are many applications based on velocity vector estimation. Attempting to apply the proposed method to the applications, I investigate effectiveness of the proposed method in case of applying to the applications.

Appendix A

Evaluation scales for evaluating estimation precision of optical flow

For evaluating estimation precision of optical flow, Various evaluation scales have been used in a different point of view. Each evaluation scale has a different property for evaluating optical flow. In this section, I mention about each evaluation scale minutely.

A.1 The mean of error

A evaluation scale for precision of optical flow called the mean of error is defined as

$$E_m = \frac{1}{M_c} \sum_{x,y \in M} ||\tilde{\boldsymbol{f}}(x,y) - \hat{\boldsymbol{f}}(x,y)||, \tag{A.1}$$

where M_c denotes the number of pixels in an image frame, M denotes a region of an image frame, $\tilde{\mathrm{f}}(x,y)$ denote a actual optical flow on the coordinates (x,y), $\hat{\mathrm{f}}(x,y)$ denotes a estimated optical flow on the coordinates (x,y). This evaluation scale is often used to evaluate precision of optical flow in an image sequence including non-moving regions. this evaluation scale is one of the most popular evaluation scale for evaluating estimation precision of optical flow.

A.2 The normalized mean of error

A evaluation scale for precision of optical flow called the normalized mean of error is defined as

$$E_n = \frac{1}{M_c} \sum_{x,y \in M} \frac{||\tilde{\boldsymbol{f}}(x,y) - \hat{\boldsymbol{f}}(x,y)||}{||\tilde{\boldsymbol{f}}(x,y)||}. \tag{A.2}$$

This evaluation scale is often used to evaluate precision of optical flow in an image sequence not including non-moving regions and in terms of evaluating errors against actual optical flow. this evaluation scale is one of the most popular evaluation scale for evaluating estimation precision of optical flow too.

A.3 $PSNR$

A evaluation scale for precision of optical flow called $PSNR$ is defined as

$$E_p = 20 \log \left\{ \frac{1}{M_c} \sum_{x,y \in M} \frac{255}{||\tilde{\boldsymbol{f}}(x,y) - \hat{\boldsymbol{f}}(x,y)||} \right\}. \tag{A.3}$$

This evaluation scale is often used to evaluate precision of optical flow as $PSNR$.

A.4 The mean of angle error

A evaluation scale for precision of optical flow called the mean of angle error is defined as

$$E_a = \frac{1}{M_c} \sum_{x,y \in M} \frac{\tilde{\boldsymbol{f}}(x,y) \cdot \hat{\boldsymbol{f}}(x,y)}{||\tilde{\boldsymbol{f}}(x,y)|| ||\hat{\boldsymbol{f}}(x,y)||}. \tag{A.4}$$

This evaluation scale is often used to evaluate precision of optical flow in terms of evaluating errors of angle against actual optical flow.

Appendix B

Theorems and derivation of partial differential coefficients of u and v with respect to x, y and t

B.1 Theorem 1 and its proof

Theorem 1 *If optical flow* $(u(x, y, t), v(x, y, t))^\top$ *and pressure* $p(x, y, t)$ *satisfy Navier-Storkes equation and* Δx, Δy *and* Δt *are* $\Delta x \to 0$, $\Delta y \to 0$ *and* $\Delta t \to 0$, *the following equations hold.*

$$u(x, y, t) = u(x + \Delta x, y + \Delta y, t + \Delta t) \tag{B.1}$$

$$v(x, y, t) = v(x + \Delta x, y + \Delta y, t + \Delta t) \tag{B.2}$$

$$t(x, y, t) = t(x + \Delta x, y + \Delta y, t + \Delta t) \tag{B.3}$$

$(Proof)$ If $(u(x, y, t), v(x, y, t))^\top$ and pressure $p(x, y, t)$ satisfy Navier-Storkes equation, $(u(x, y, t), v(x, y, t))^\top$ and pressure $p(x, y, t)$ can be possible to be done partial difference with respect to x, y, or t. Therefore, $(u(x, y, t), v(x, y, t))^\top$ and pressure $p(x, y, t)$ are continuous function with respect to x, y, or t. Thus,

$$\lim_{\substack{\Delta x \to 0 \\ \Delta y \to 0 \\ \Delta t \to 0}} u(x, y, t) = u(x + \Delta x, y + \Delta y, t + \Delta t) \tag{B.4}$$

$$\lim_{\substack{\Delta x \to 0 \\ \Delta y \to 0 \\ \Delta t \to 0}} v(x, y, t) = v(x + \Delta x, y + \Delta y, t + \Delta t) \tag{B.5}$$

$$\lim_{\substack{\Delta x \to 0 \\ \Delta y \to 0 \\ \Delta t \to 0}} p(x, y, t) = p(x + \Delta x, y + \Delta y, t + \Delta t) \tag{B.6}$$

Equation (B.1), (B.2) and (B.3) hold $(Q.E.D)$

B.2 Theorem 2 and its proof

Theorem 2 *In case that intensity constraints of optical flow have intersections, in parameter space u and v, on neighboring points $(x \pm \Delta x, y, t)$, $(x, y \pm \Delta y, t)$ or $(x, y, t \pm \Delta t)$ of the point (x, y, t) in an image coordinates (x, y) at time t of an image sequence, and in case that Δx, Δy, Δt are infinitesimal, difference of the points for u and v axis approximates difference of u and v in actual optical flow on (x, y, t) and neighboring point of (x, y, t).*

$(Proof)$ Let optical flow on coordinates (x, y) at time t in an image sequence be $(u(x, y, t)$, $v(x, y, t))^\top$ and Let intensities on a point (x_0, y_0, t_0) and neighboring point $(x_0 + \Delta x, y_0, t_0)$ and $(x_0 - \Delta x, y_0, t_0)$ be I, I_+ and I_- respectively on condition that I, I_+ and I_- are continuous functions with respect to x, y and t. intensity constraints of optical flow are represented as

$$\frac{\partial I}{\partial x} u(x_0, y_0, t_0) + \frac{\partial I}{\partial y} v(x_0, y_0, t_0) + \frac{\partial I}{\partial t} = 0 \tag{B.7}$$

$$\frac{\partial I_+}{\partial x} u(x_1, y_0, t_0) + \frac{\partial I_+}{\partial y} v(x_1, y_0, t_0) + \frac{\partial I_+}{\partial t} = 0 \tag{B.8}$$

$$\frac{\partial I_-}{\partial x} u(x_2, y_0, t_0) + \frac{\partial I_-}{\partial y} v(x_2, y_0, t_0) + \frac{\partial I_-}{\partial t} = 0 \tag{B.9}$$

where x_1 denotes $x_0 + \Delta x$, x_2 denotes $x_0 - \Delta x$. First, we express difference of intersections on the intensity constraint equation of optical flow in (x_0, y_0, t_0) and (x_1, y_0, t_0) or (x_0, y_0, t_0) and (x_2, y_0, t_0). Let intersections on the intensity constraint equation of optical flow in (x_0, y_0, t_0) and (x_1, y_0, t_0) be $(u_{+\Delta x}, v_{+\Delta x})^\top$. With respect to $u_{+\Delta x}$, $v_{+\Delta x}$, $(u(x_0, y_0, t_0), v(x_0, y_0, t_0))^\top$ and $(u(x_1, y_0, t_0), v(x_1, y_0, t_0))^\top$ in equation (B.7) and (B.8) are represented

$$u_{+\Delta x} = \frac{\frac{\partial I}{\partial y}\frac{\partial I_+}{\partial t} - \frac{\partial I}{\partial t}\frac{\partial I_+}{\partial y}}{\frac{\partial I}{\partial x}\frac{\partial I_+}{\partial y} - \frac{\partial I}{\partial y}\frac{\partial I_+}{\partial x}} \tag{B.10}$$

$$v_{+\Delta x} = \frac{\frac{\partial I}{\partial x}\frac{\partial I_+}{\partial t} - \frac{\partial I}{\partial t}\frac{\partial I_+}{\partial x}}{\frac{\partial I}{\partial y}\frac{\partial I_+}{\partial x} - \frac{\partial I}{\partial x}\frac{\partial I_+}{\partial y}}. \tag{B.11}$$

Let intersections on the intensity constraint equation of optical flow in (x_0, y_0, t_0) and (x_2, y_0, t_0) be $(u_{-\Delta x}, v_{-\Delta x})^\top$. With respect to $u_{-\Delta x}$, $v_{-\Delta x}$, $(u(x_0, y_0, t_0), v(x_0, y_0, t_0))^\top$ and $(u(x_2, y_0, t_0), v(x_2, y_0, t_0))^\top$ in equation (B.7) and (B.9) are represented

$$u_{-\Delta x} = \frac{\frac{\partial I}{\partial y}\frac{\partial I_-}{\partial t} - \frac{\partial I}{\partial t}\frac{\partial I_-}{\partial y}}{\frac{\partial I}{\partial x}\frac{\partial I_-}{\partial y} - \frac{\partial I}{\partial y}\frac{\partial I_-}{\partial x}}, \tag{B.12}$$

$$v_{-\Delta x} = \frac{\frac{\partial I}{\partial x}\frac{\partial I_-}{\partial t} - \frac{\partial I}{\partial t}\frac{\partial I_-}{\partial x}}{\frac{\partial I}{\partial y}\frac{\partial I_-}{\partial x} - \frac{\partial I}{\partial x}\frac{\partial I_-}{\partial y}}. \tag{B.13}$$

By equation(B.10) and (B.12), difference of intersections on the intensity constraint equations of optical flow in (x_0, y_0, t_0) and (x_1, y_0, t_0) or (x_0, y_0, t_0) and (x_2, y_0, t_0) represented

$$u_{+\Delta x} - u_{-\Delta x} \quad = \quad \frac{\frac{\partial I}{\partial y}\frac{\partial I_+}{\partial t} - \frac{\partial I}{\partial t}\frac{\partial I_+}{\partial y}}{\frac{\partial I}{\partial x}\frac{\partial I_+}{\partial y} - \frac{\partial I}{\partial y}\frac{\partial I_+}{\partial x}}$$

$$- \quad \frac{\frac{\partial I}{\partial y}\frac{\partial I_-}{\partial t} - \frac{\partial I}{\partial t}\frac{\partial I_-}{\partial y}}{\frac{\partial I}{\partial x}\frac{\partial I_-}{\partial y} - \frac{\partial I}{\partial y}\frac{\partial I_-}{\partial x}} \tag{B.14}$$

196

Similarly, by equation (B.11 and (B.13),

$$
\begin{aligned}
v_{+\Delta x} - v_{-\Delta x} \;=\;& \frac{\frac{\partial I}{\partial x}\frac{\partial I_+}{\partial t} - \frac{\partial I}{\partial t}\frac{\partial I_+}{\partial x}}{\frac{\partial I}{\partial y}\frac{\partial I_+}{\partial x} - \frac{\partial I}{\partial x}\frac{\partial I_+}{\partial y}} \\
&- \frac{\frac{\partial I}{\partial x}\frac{\partial I_-}{\partial t} - \frac{\partial I}{\partial t}\frac{\partial I_-}{\partial x}}{\frac{\partial I}{\partial y}\frac{\partial I_-}{\partial x} - \frac{\partial I}{\partial x}\frac{\partial I_-}{\partial y}}
\end{aligned}
\tag{B.15}
$$

on the condition that denominators from in equation (B.10) through (B.15) are not zero. Next, we express $(u(x_0, y_0, t_0), v(x_0, y_0, t_0))^\top$ and $(u(x_1, y_0, t_0), v(x_1, y_0, t_0))^\top$ to express difference of actual optical flow in (x_0, y_0, t_0) and (x_1, y_0, t_0). Since $(u(x_0, y_0, t_0), v(x_0, y_0, t_0))^\top$ are determined uniquely, we can express

$$
u(x_0, y_0, t_0) = \lim_{x_2 \to x_0} u_{-\Delta x},
\tag{B.16}
$$

$$
v(x_0, y_0, t_0) = \lim_{x_2 \to x_0} v_{-\Delta x}.
\tag{B.17}
$$

Similarly,

$$
u(x_1, y_0, t_0) = \lim_{x_0 \to x_1} u_{+\Delta x},
\tag{B.18}
$$

$$
v(x_1, y_0, t_0) = \lim_{x_0 \to x_1} v_{+\Delta x}.
\tag{B.19}
$$

However, equations from (B.16) though (B.19) are unsettled. Therefore, based on continuity of $u(x, y, t)$ and $v(x, y, t)$ with respect to x, y, t, we express the equations from (B.16) to (B.17) as approximate equations

$$
u(x_0, y_0, t_0) \simeq \lim_{x_2 \to x_0 + dx} u_{-\Delta x}
\tag{B.20}
$$

$$
v(x_0, y_0, t_0) \simeq \lim_{x_2 \to x_0 + dx} v_{-\Delta x}
\tag{B.21}
$$

$$
u(x_1, y, t) \simeq \lim_{x_0 \to x_1 + dx} u_{+\Delta x}
\tag{B.22}
$$

$$
v(x_1, y, t) \simeq \lim_{x_0 \to x_1 + dx} v_{+\Delta x}
\tag{B.23}
$$

where dx denotes infinitesimal value ($dx \neq 0$). Let Δx be dx and intensities in $(x_0 + dx, y, t)$ and $(x_1 + dx, y, t)$ be I_{+dx} and I_{-dx} respectively. By equation (B.20) and (B.22),

$$
\begin{aligned}
& u(x_1, y_0, t_0) - u(x_0, y_0, t_0) \\
\simeq\;& \lim_{x_0 \to x_1 + dx} u_{+\Delta x} - \lim_{x_2 \to x_0 + dx} u_{-\Delta x} \\
=\;& \frac{\frac{\partial I_{+dx}}{\partial y}\frac{\partial I_+}{\partial t} - \frac{\partial I_{+dx}}{\partial t}\frac{\partial I_+}{\partial y}}{\frac{\partial I_{+dx}}{\partial x}\frac{\partial I_+}{\partial y} - \frac{\partial I_{+dx}}{\partial y}\frac{\partial I_+}{\partial x}} \\
&- \frac{\frac{\partial I_{-dx}}{\partial y}\frac{\partial I_-}{\partial t} - \frac{\partial I_{-dx}}{\partial t}\frac{\partial I_-}{\partial y}}{\frac{\partial I_{-dx}}{\partial x}\frac{\partial I_-}{\partial y} - \frac{\partial I_{-dx}}{\partial y}\frac{\partial I_-}{\partial x}}.
\end{aligned}
\tag{B.24}
$$

By equation (B.21) and (B.23)

$$v(x_1, y_0, t_0) - v(x_0, y_0, t_0)$$

$$\simeq \lim_{x_0 \to x_1 + dx} v_{+\Delta x} - \lim_{x_2 \to x_0 + dx} v_{-\Delta x}$$

$$= \frac{\frac{\partial I_{+dx}}{\partial x} \frac{\partial I_+}{\partial t} - \frac{\partial I_{+dx}}{\partial t} \frac{\partial I_+}{\partial x}}{\frac{\partial I_{+dx}}{\partial y} \frac{\partial I_+}{\partial x} - \frac{\partial I_{+dx}}{\partial x} \frac{\partial I_+}{\partial y}}$$

$$- \frac{\frac{\partial I_{-dx}}{\partial x} \frac{\partial I_-}{\partial t} - \frac{\partial I_{-dx}}{\partial t} \frac{\partial I_-}{\partial x}}{\frac{\partial I_{-dx}}{\partial y} \frac{\partial I_-}{\partial x} - \frac{\partial I_{-dx}}{\partial x} \frac{\partial I_-}{\partial y}} .$$

$$(B.25)$$

On the condition that denominators in equation (B.24) and (B.25) are not zero. By equation (B.14) and (B.24) or equation (B.15) and (B.25), we can express

$$u(x_1, y_0, t_0) - u(x_0, y_0, t_0) \simeq u_{+\Delta x} - u_{-\Delta x}, \tag{B.26}$$

$$v(x_1, y_0, t_0) - v(x_0, y_0, t_0) \simeq v_{+\Delta x} - v_{-\Delta x}. \tag{B.27}$$

Thus, theorem 2 holds with respect to x. Similarly, theorem 2 holds with respect to y and t obviously. Therefore, theorem 2 holds. ($Q.E.D$)

B.3 Derivation of partial differential coefficients of u and v with respect to x, y and t

In case that theorem 2 holds, if we set

$$\frac{\partial u}{\partial x} = u(x_1, y_0, t_0) - u(x_0, y_0, t_0), \tag{B.28}$$

$$\frac{\partial v}{\partial x} = v(x_1, y_0, t_0) - v(x_0, y_0, t_0). \tag{B.29}$$

By equation (B.26) and (B.27), we can regard equation (B.28) and (B.29) as

$$\frac{\partial u}{\partial x} = u_{+\Delta x} - u_{-\Delta x}, \tag{B.30}$$

$$\frac{\partial v}{\partial x} = v_{+\Delta x} - v_{-\Delta x} \tag{B.31}$$

respectively. By using equation (B.30) and (B.31), we can directly determine the first order partial differential coefficients with respect to x from an image sequence. Let intersections on intensity constraint equations in (x_0, y_0, t_0) and $(x_0, y_0 + \Delta y, t_0)$ or (x_0, y_0, t_0) and $(x_0, y_0 - \Delta y, t_0)$ be $(u_{+\Delta y}, v_{+\Delta y})$ and $(u_{-\Delta y}, v_{-\Delta y})$ respectively. We can determine the first order partial differential coefficients with respect to y as

$$\frac{\partial u}{\partial y} = u_{+\Delta y} - u_{-\Delta y}, \tag{B.32}$$

$$\frac{\partial v}{\partial y} = v_{+\Delta y} - v_{-\Delta y} \tag{B.33}$$

from an image sequence. Similarly, let intersections on intensity constraint equations in (x_0, y_0, t_0) and $(x_0, y_0, t_0 + \Delta t)$ or (x_0, y_0, t_0) and $(x_0, y_0, t_0 - \Delta t)$ be $(u_{+\Delta t}, v_{+\Delta t})$ and $(u_{-\Delta t}, v_{-\Delta t})$ respectively. We can determine the first order partial differential coefficients with respect to t as

$$\frac{\partial u}{\partial t} = u_{+\Delta t} - u_{-\Delta t} \tag{B.34}$$

$$\frac{\partial v}{\partial t} = v_{+\Delta t} - v_{-\Delta t} \tag{B.35}$$

from an image sequence. Let intersections on intensity constraint equations of optical flow in$(x_0 - \Delta x, y_0, t_0)$ and $(x_0 - 2\Delta x, y_0, t_0)$ be $(u_{-2\Delta x}, v_{-2\Delta x})$. In case that we define second order partial differential coefficients of u and v with respect to x as

$$\frac{\partial^2 u}{\partial x^2} = \left(u_{+\Delta x} - u_{-\Delta x}\right) - \left(u_{-\Delta x} - u_{-2\Delta x}\right), \tag{B.36}$$

$$\frac{\partial^2 v}{\partial x^2} = \left(v_{+\Delta x} - v_{-\Delta x}\right) - \left(v_{-\Delta x} - v_{-2\Delta x}\right), \tag{B.37}$$

we can determine second order partial differential coefficients of u and v with respect to x by the first order partial differential coefficients of u and v with respect to x. Similarly, we can determine second order partial differential coefficients of u and v with respect to y or t as

$$\frac{\partial^2 u}{\partial y^2} = \left(u_{+\Delta y} - u_{-\Delta y}\right) - \left(u_{-\Delta y} - u_{-2\Delta y}\right), \tag{B.38}$$

$$\frac{\partial^2 v}{\partial y^2} = \left(v_{+\Delta y} - v_{-\Delta y}\right) - \left(v_{-\Delta y} - v_{-2\Delta y}\right), \tag{B.39}$$

$$\frac{\partial^2 u}{\partial t^2} = \left(u_{+\Delta t} - u_{-\Delta t}\right) - \left(u_{-\Delta t} - u_{-2\Delta t}\right), \tag{B.40}$$

$$\frac{\partial^2 v}{\partial t^2} = \left(v_{+\Delta t} - v_{-\Delta t}\right) - \left(v_{-\Delta t} - v_{-2\Delta t}\right), \tag{B.41}$$

if we can obtain the first order partial differential coefficients of u and v with respect to y or t.

Appendix C

Estimation of velocity vectors in image sequences taken by a digital video camera

In this section, I show results of estimation of velocity vectors in image sequences taken by a digital video camera.

First, I applied the proposed method for solving occlusion problem to an image sequence shown in Figure C.1 occurring occlusion. The situation of the image sequence is set as the situation of the image sequence shown in Figure 3.50.

Table C.1: Parameters in the proposed method for solving the occlusion problem

The threshold in the voting possible condition	30[intensity]
The size of the support region	11×11[pixels]
The size of a cell in the voting space	1.0×10^{-2}
The variance parameter in the weighting function σ	4

Table C.2: Parameters in the proposed method for solving the brightness change problem

The threshold in the voting possible condition	30[intensity]
The size of the support region	21×21[pixels]
The size of a cell in the voting space	1.0×10^{-2}
The variance parameter in the weighting function σ_{uv}	8
The variance parameter in the weighting function σ_w	8

This image sequence was taken by Sony Digital Handycam DCR-VX-1000 with DV codec. The size of the image sequence is 106×41[pixels], quantization level is 8[bit/pixel]. Parameters of the proposed method for solving occlusion problem is shown in Table C.1. I directly applied the proposed method for solving the occlusion problem to the image sequence shown in Figure C.1 taken by the digital video camera, therefore, Cross luminance obstruction dose not occur in the image sequence.

The result of estimation of velocity vectors in the image sequence is shown in Figure C.2. From the results, we could not precisely obtain precision of velocity vector estimation in comparison with in case of using the image sequence shown in Figure 3.50. Especially,

velocity vectors were not precisely estimated in boundary of the right object and inside of the right object. The image sequence shown in Figure 3.50 was taken each frame under the situation that objects were standed. On the contrary, the image sequence shown in Figure C.1 was taken under the situation that objects were moving. In case of taking image sequence by a digital video camera under the situation that objects are moving, there are cases that corrugated textures by interlace and motion blurs occur in each frame of the image sequence. Therefore, The factor of decrease of precision of velocity vector estimation is supposed the following causes, one is that we could not separate velocity vector constraint equations by the condition for separating each motion of object because intensities around boundaries of the objects were spatially smoothed by occurring of motion blurs. the other is that we could not obtain sufficient constraint equations satisfying realizable conditions of the constraint equation by effectiveness of corrugated texture by interlace. However, The result of estimated velocity vectors by the proposed method seems to be well in comparison with estimated velocity vectors by conventional methods shown in Figure C.3 or Figure C.4. I then applied the proposed method for solving the occlusion problem to an image sequence shown in Figure C.5 that includes objects moving faster than the objects in the image sequence shown in Figure C.1. The result of velocity vector estimation is shown in Figure C.6. In comparison with Figure C.2, I could not obtain well results. The factor is supposed that effectiveness of motion blur and corrugated textures by interlace increases as motion gets large.

Second, I applied the proposed method for solving brightness change problem to an image sequence shown in Figure C.7 occurring brightness change. The situation of the image sequence is set as the situation of the image sequence shown in Figure 4.63.
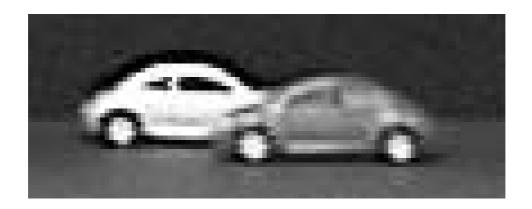
This image sequence was taken by Sony Digital Handycam DCR-VX-1000 with DV codec. The size of the image sequence is 111×56[pixels], quantization level is 8[bit/pixel]. Parameters of the proposed method for solving brightness change problem is shown in Table C.2. I directly applied the proposed method for solving the brightness change problem to the image sequence shown in Figure C.7 taken by the digital video camera, therefore, Cross luminance obstruction dose not occur in the image sequence.

The result of estimation of velocity vectors in the image sequence is shown in Figure C.8. From the results, we could not precisely obtain precision of velocity in comparison with in case of using the image sequence shown in Figure 4.63. Especially, velocity vectors were not precisely estimated in the boundary of the object and inside of the object. The image sequence shown in Figure 4.63 was taken each frame under the situation that the object was standed. On the contrary, the image sequence shown in Figure C.7 was taken under the situation that the object was moving. In case of taking image sequence by a digital video camera under the situation that objects are moving, there are a case that motion blurs and corrugated textures by interlace occur in each frame of the image sequence. Therefore, The factor of decrease of precision of velocity vector estimation is supposed the following causes, one is that we could not separate velocity vector constraint equations by the condition for separating each motion of object because intensities around boundaries of the objects were spatially smoothed by occurring of motion blurs. the other is that we could not obtain sufficient constraint equations satisfying realizable conditions of the constraint equation by effectiveness of corrugated texture by interlace. However, The result of estimated velocity vectors by the proposed method seems to be well in comparison with estimated velocity vectors by conventional methods shown in from Figure C.9 through Figure C.12. I then applied the proposed method for solving the brightness

201

change problem to an image sequence shown in Figure C.13 that includes objects moving faster than the objects in the image sequence shown in Figure C.7. The result of velocity vector estimation is shown in Figure C.14. In comparison with Figure C.8, I could not obtain well results. The factor is supposed that effectiveness of motion blur and corrugated textures by interlace increases as motion gets large.

In order to estimate velocity vector in image sequences taken by a digital video camera, we firstly have to exclude effectiveness of motion blurs. To exclude effectiveness of motion blurs, we should use a high-speed camera. We then have to exclude effectiveness of corrugated textures. To exclude effectiveness of corrugated textures, we firstly thin out the image sequences occurring corrugated textures to each even of odd line. Then, we interpolate the thined out lines in each frame of even line or frame of odd line. Finally, we should apply the proposed method to the interpolated image sequence.

Frame1

Frame2

Figure C.1: An image sequence occurring occlusion taken by a digital video camera.
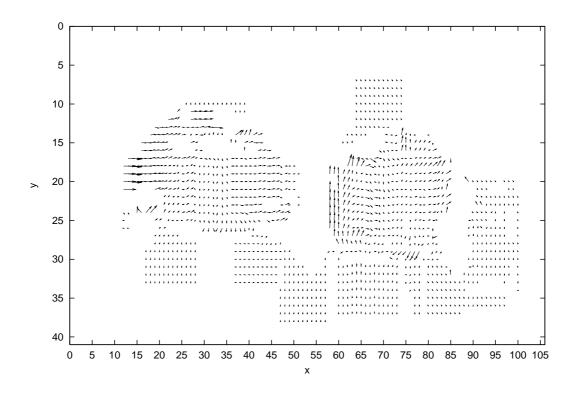
Figure C.2: Estimated velocity vectors by the proposed method for solving the occlusion problem in the image sequence occurring occlusion.
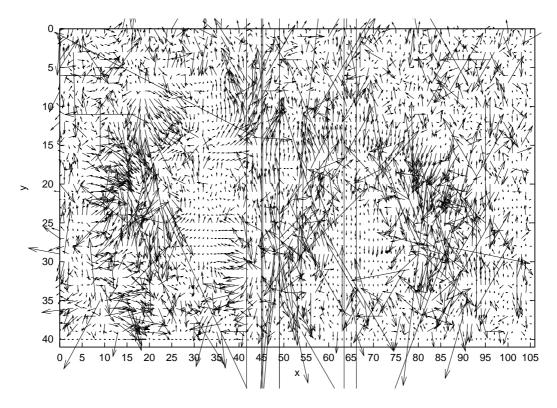
Figure C.3: Estimated velocity vectors by the global method in the image sequence occurring occlusion.
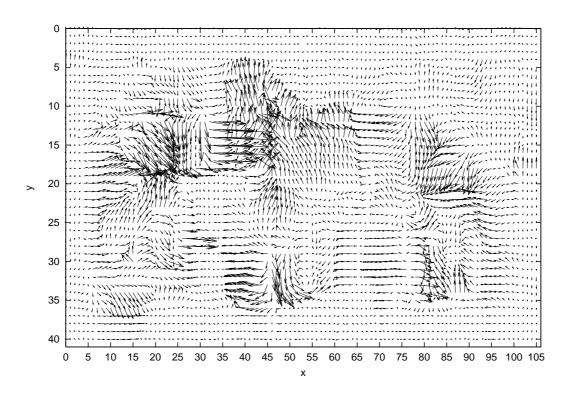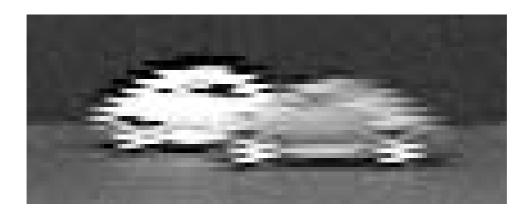
Figure C.4: Estimated velocity vectors by the local method in the image sequence occurring occlusion.

Frame1

Frame2

Figure C.5: An image sequence occurring occlusion taken by a digital video camera. The image sequence includes objects moving faster than the objects included in the image sequence of Figure C.1.

Figure C.6: Estimated velocity vectors by the proposed method for solving the occlusion problem in the image sequence shown in Figure C.5.

207

Frame1

Frame2

Figure C.7: An image sequence occurring brightness change taken by a digital video camera

Figure C.8: Estimated velocity vectors by the proposed method for solving the brightness change problem in the image sequence occurring brightness change.
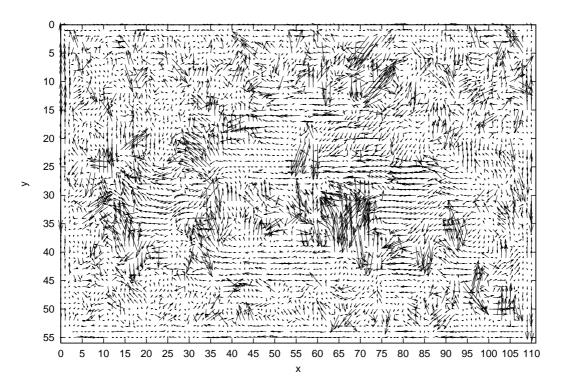
Figure C.9: Estimated velocity vectors by Cornelius's method in the image sequence occurring brightness change.
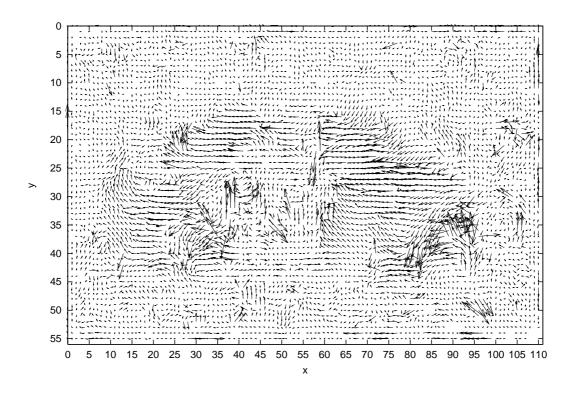
Figure C.10: Estimated velocity vectors by Nomura's method in the image sequence occurring brightness change.
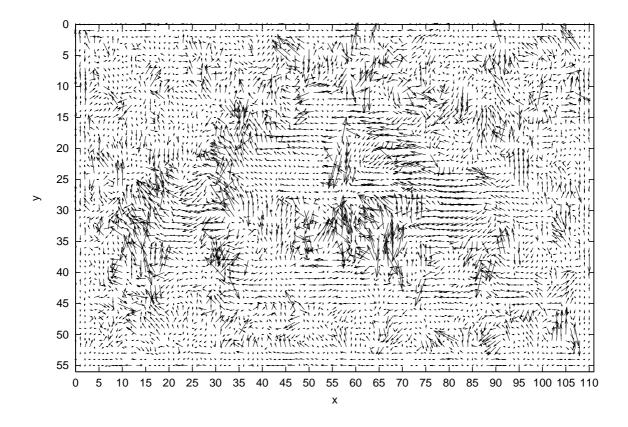
Figure C.11: Estimated velocity vectors by Mukawa's method in the image sequence occurring brightness change.
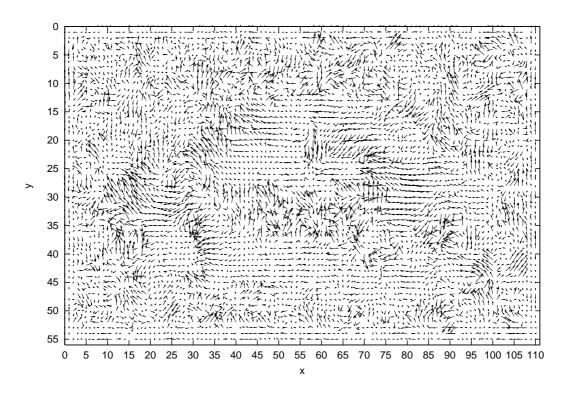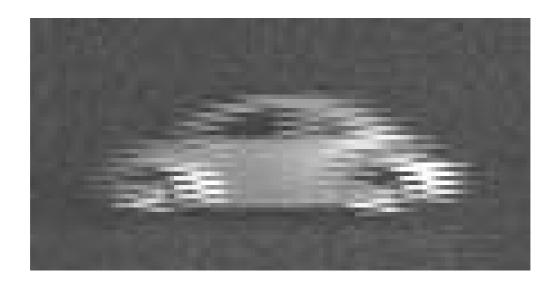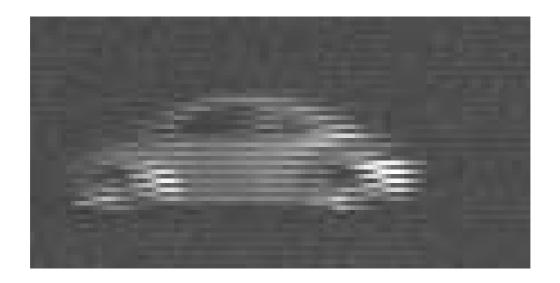
Figure C.12: Estimated velocity vectors by Negahdaripour's method in the image sequence occurring brightness change.

Frame1

Frame2

Figure C.13: An image sequence occurring brightness change taken by a digital video camera. The image sequence includes objects moving faster than the objects included in the image sequence of Figure C.7.
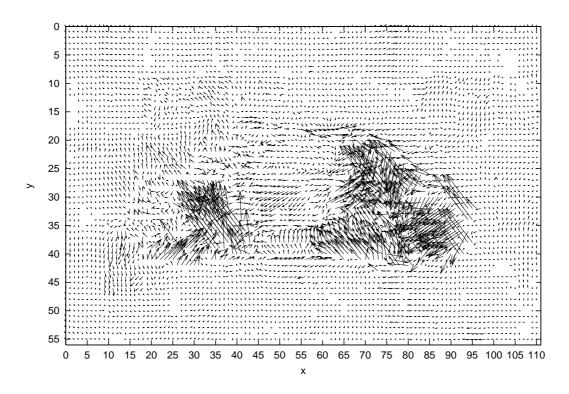
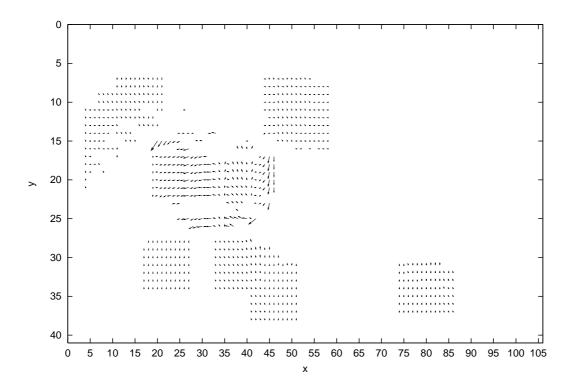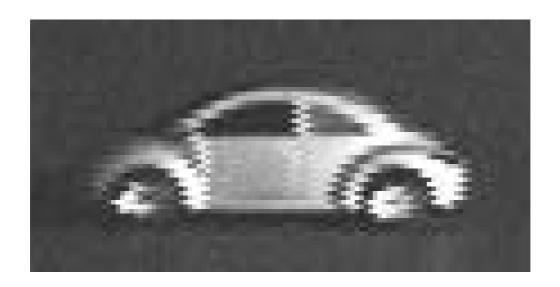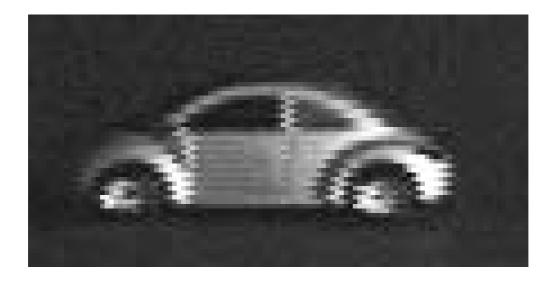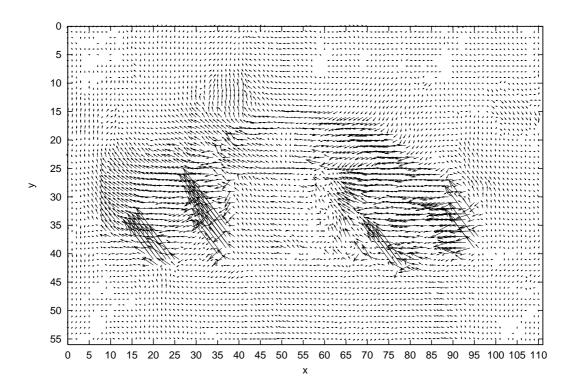Figure C.14: Estimated velocity vectors by the proposed method for solving the brightness change problem in the image sequence shown in Figure C.13.

Appendix D

Experiments for appropriateness of the proposed method for solving fluid analysis using image sequences

D.1 Experiments for appropriateness of using the continuous equation and Navier-Stokes equation in fluid analysis using image sequences

In order to show appropriateness of using the continuous equation and Navier-Stokes equation in fluid analysis using image sequences, I experimented on comparison of estimation precision of velocity vectors in case of using only an intensity constraint equation, using an intensity constraint equation and the continuous equation or using an intensity constraint equation, the continuous equation and Navier-Stokes equation. For this experiment, I used image sequences used in the experiments of chapter 5.

First, I experimented on comparison of estimation precision of velocity vectors in synthetic image sequences. The parameters of each method are shown in Table D.1. As evaluation scale, I used the mean of normalized error. The results of this experiment are shown in from Table D.2 through Table D.4.

Table D.1: The parameters used in each method.

Parameters	Values of parameters
V	1.2×10
V_p	4.0×10^9
σ	1.5×10
σ_p	2.0

From the results of this experiments, we obtained well results in case of using the method C in comparison with the other methods.

Finally, I experimented on comparison of estimation precision of velocity vectors in noisy synthetic image sequences. The parameters of each method are shown in Table D.1.

Table D.2: The mean of normalized error $\bar{e}_n$ of each method in the model image 1, A: a method using only an intensity constraint equation, B: a method using an intensity constraint equation and the continuous equation, C: a method using an intensity constraint equation, the continuous equation and Navier-Stokes equation.

Method	$\bar{e}_n$
A	7.98×10^{-1}
B	5.11×10^{-1}
C	4.15×10^{-1}

Table D.3: The mean of normalized error $\bar{e}_n$ of each method in the model image 2, A: a method using only an intensity constraint equation, B: a method using an intensity constraint equation and the continuous equation, C: a method using an intensity constraint equation, the continuous equation and Navier-Stokes equation.

Method	$\bar{e}_n$
A	8.23×10^{-1}
B	6.21×10^{-1}
C	5.43×10^{-1}

Table D.4: The mean of normalized error $\bar{e}_n$ of each method in the model image 3, A: a method using only an intensity constraint equation, B: a method using an intensity constraint equation and the continuous equation, C: a method using an intensity constraint equation, the continuous equation and Navier-Stokes equation.

Method	$\bar{e}_n$
A	8.12×10^{-1}
B	5.05×10^{-1}
C	4.16×10^{-1}

As evaluation scale, I used the mean of normalized error. The results of this experiment are shown in from Figure D.1 through Figure D.3.

From the results of this experiments, we obtained well results in case of using the method C in comparison with the other methods. Even though in noisy synthetic image sequences, the factor of the results in the synthetic and noisy synthetic image sequences is supposed following two causes. The one is to consider the continuous equation that is satisfied in incompressible viscous fluid since the image sequences used in the experiment are generated by numerical calculation of . The other is to consider a parameter of pressure since, according to Navier-Stokes equation, a velocity vector is constrainted by spatial change of the pressure.

D.2 Experiments on estimation precision of the parameter p_{xy} in the constraint equation considering physical condition of incompressible viscous fluid

I experimented on comparison of estimation precision of the parameter p_{xy} in the constraint equation considering physical condition of incompressible viscous fluid. For this experiment, I used image sequences used in the experiments of chapter 5.

First, I experimented on comparison of estimation precision of the parameter p_{xy} in synthetic image sequences. For comparison of estimation precision of the parameter p_{xy}, I used Nakajima's method which can estimate parameter p_{xy}. The parameters of each method are shown in Table D.5. As evaluation scale, I used the mean of normalized error

Table D.5: The parameters used in each method.

Method	Values of parameters	
The proposed method	$V = 1.2\times10$	$V_p = 4.0\times10^9$
	$\sigma = 1.5\times10$	$\sigma_p = 2.0$
Nakajima	$\alpha_N = 1.0\times10^{-4}$	$\beta_N = 1.0\times10^{-4}$

of p_{xy} which is defined as

$$\overline{p_{xy}} = \frac{1}{MN} \sum_{x=1}^{M} \sum_{y=1}^{N} \frac{|p_{cxy}(x,y) - p_{exy}(x,y)|}{|p_{cxy}(x,y)|} \tag{D.1}$$

where $p_{cxy}(x,y)$ denotes correct value of p_{xy} on a coordinate (x,y) in an image frame, $p_{exy}(x,y)$ denotes estimated value of p_{xy} on a coordinate (x,y) in an image frame, M and N denote size of image frame for x or y axis respectively. The results of this experiment are shown in Table D.6.

From the results in this experiment, we obtained estimation precision in approximately 50% against correct value of p_{xy}, and we obtained well results of estimation precision in comparison with Nakajima's method. Finally, I experimented on comparison of estimation precision of the parameter p_{xy}. The parameters of each method are shown in Table D.1. As evaluation scale, I used the mean of normalized error of p_{xy}. The results of this experiment are shown in from Table D.4 through Table D.6.

Table D.6: The mean of normalized error of p_{xy} in each image sequence.

Image names	$\overline{p_{xy}}$	
	The proposed method	Nakajima
Image 1	4.98×10^{-1}	5.42×10^{-1}
Image 2	5.11×10^{-1}	6.52×10^{-1}
Image 3	5.15×10^{-1}	5.25×10^{-1}

From the results in this experiment, we obtained well results of estimation precision in comparison with Nakajima's method. Decrease rate of estimation precision of $p_x y$ with respect to adding noise in the proposed method is less than that of Nakajima's method. The factor is supposed that the proposed method has robustness against noise.
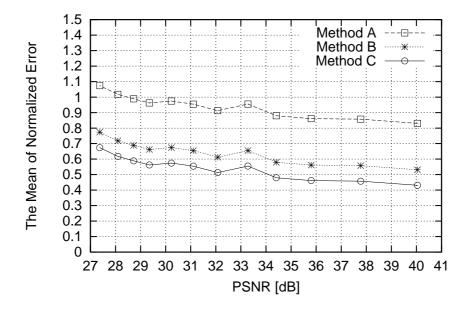
Figure D.1: The mean of normalized error of each method in image 4, A: a method using only an intensity constraint equation, B: a method using an intensity constraint equation and the continuous equation, C: a method using an intensity constraint equation, the continuous equation and Navier-Stokes equation.
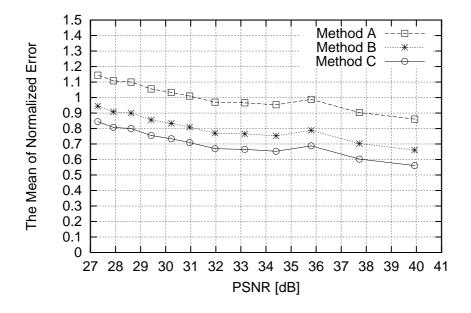
Figure D.2: The mean of normalized error of each method in image 5, A: a method using only an intensity constraint equation, B: a method using an intensity constraint equation and the continuous equation, C: a method using an intensity constraint equation, the continuous equation and Navier-Stokes equation.
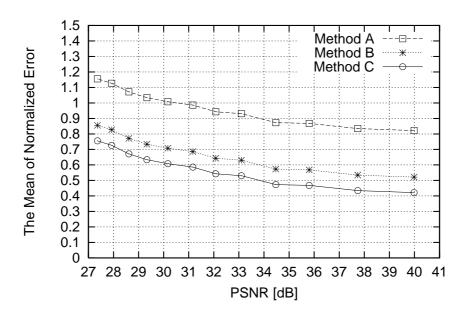
Figure D.3: The mean of normalized error of each method in image 6, A: a method using only an intensity constraint equation, B: a method using an intensity constraint equation and the continuous equation, C: a method using an intensity constraint equation, the continuous equation and Navier-Stokes equation.
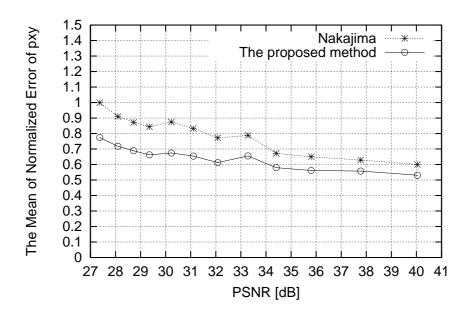
Figure D.4: The mean of normalized error of p_{xy} in Image 4.
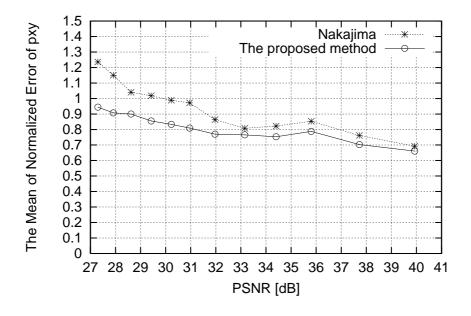
Figure D.5: The mean of normalized error of p_{xy} in Image 5.
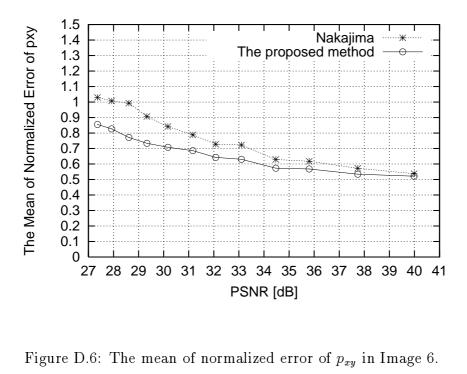
Figure D.6: The mean of normalized error of p_{xy} in Image 6.

Bibliography

[1] D. Marr, "Vision," W. H. Freeman and Company, 1982.

[2] T. Matsuyama, Y. Kuno, A. Imiya "Computer Vision -A reviwe of techniques and prospect of the future-", Shi-gijyutsu-communications, 1998.

[3] K. Toyama, J. Kramm, B. Brumitt and B. Meyeres, "Wallflower: Principles and Practice of Background maintenance," Proc. of ICCV, pp.255-261, 1999.

[4] T. Matsuyama, T. Wada, H. Habe and K. Tanahashi, "Background Subtraction under Varying Illumination," Trans. of IEICE, D-II, Vol. J84-D-II, No. 10, pp. 2201-2211, 2001.

[5] M. Kass, A. Witkin and D. Terzopoulos, "Snakes: Active Contour Models," Int. J. Conputer Vision, Vol. 1, No. 4, pp.321-331, 1988.

[6] Y. Matsuzawa and T. Abe, "Region Extraction Using Competition of Multiple Active Contour Models," Trans. of IEICE, D-II, Vol. J83-D-II, No. 4, pp. 1100-1109, 2000.

[7] B. K. P. Horn and B. G. Schunck, "Determining Optical Flow," Artificial Intelligence, Vol. 17, pp. 185-203, 1981.

[8] B. D. Lucas and T. Kanade, "An Iterative Image-Registration Technique with An Applicatoin to Stereo Vision," In DARPA Proc. of Image Understanding Workshop, pp. 121-130, 1981.

[9] N. Chiba, H. Kano, M. Minoh and M. Yasuda, "Feature-Basec Image Mosaicing," Trans. of IEICE, D-II, Vol. J82-D-II, No. 10, pp. 1581-1589, 1999.

[10] T. Yamamato and H. Hanaizumi, "An Automated Method for Registrantion of Remotely Sensed Image with Adaptive Generation of Corresponding Point Pairs to Local Disparities," Trans. of IEICE, B, Vol. J84-B, No. 9, pp. 1673-1682, 2001.

[11] R. R. Schultz and R. L. Stevenson, "Extraction of High-Resolution Frames from Video Sequences," Trans. Image Processing, Vol. 5, No. 6, pp. 996-1011, 1996.

[12] B. C. Tom and A. K. Katsaggelos, "Resolution Enhancement of Color Video," Proc. European Conf. on Signal Processing, pp. 145-148, 1996.

[13] S. Baker and T. Kanade, "Super-Resolution Optical Flow," CMU RI Technical Report, CMU-RI-TR-99-36, 1996.

[14] H. kawasaki, K. Ikeuchi and M. Sakauchi, "Super-Resolution of Omini Camera Image Using Spatio-Tamporal Analysis," Trans. of IEICE, D-II, Vol. J84-D-II, No. 8, pp. 1891-1902, 2001.

[15] A. N. Netravali, and J. D. Robbins, "Motion Compensated Television Cording - Part 1," Bell Syst. Tech. J., Vol. 58, pp. 631-670, 1979.

[16] K. A. Prabhu and A. N. Netravali, "Motion Compensated Composite Color Cording," IEEE Trans. Commun., Vol. COM-31, pp. 216-223, 1983.

[17] J. R. Jain and A. K. Jain, "Displacement Masurement and Its Application in Interframe Image Cording," IEEE Trans. Commun., Vol. COM-29, pp. 1799-1806, 1981.

[18] K. Matsuda, T. Tsuda, T. Ito and S. Make, "A New Motion Compensation Cording Scheme for Video Conference," Proc. ICC, pp. 234-237, 1984.

[19] K. Kamikura, H. Watanabe, N. Kobayashi, S. Ichinose and H. Yasuda, "Video Coding Using Global Motion and Brightness-Variation Compensation with Complexity Reduction," Trans. of IEICE, B, Vol. J82-B, No. 9, pp. 1676-1688, 1999.

[20] W. Nishii, Y. Yagi and M. Yachida, "Rolling and Swaying Motion Estimation for Mobile Robot by Using Omnidirectional Optical Flows," Trans. of IEICE, D-II, Vol. J80-D-II, No. 6, pp. 1512-1521, 1997.

[21] I. Mihara, Y. Yamauchi and M. Doi, "A Realtime Vision-Based Interface Using Motion Processor and Application to Robotics," Trans. of IEICE, D-II, Vol. J84-D-II, No. 9, pp. 2070-2078, 2001.

[22] K. Hata, T. Aoki and M. Etoh, "Estimation of Structure and Motion Parameters for a Roaming Robot that Scans the Space," Trans. of IEICE, D-II, Vol. J84-D-II, No. 3, pp. 448-458, 2001.

[23] T. Morita, K, "Motion Detection and Tracking Based on Local Correction Matching," Trans. of IEICE, D-II, Vol. J84-D-II, No. 2, pp. 299-309, 2001.

[24] S. Yamamoto, Y. Mae, Y. Shirai and J. Miura, "Realtime Multiple Object Tracking based on Optical Flows," IEEE Int. Conf. Robotics and Automation, pp. 2328-2333, 1995.

[25] D. W. Murray, P. F. McLauchlan, I. D. Reid and P. M. Sharkey, "Reactions to Peripheal Image motion Using a Head/Eye Platform," Proc. of ICCV, pp. 403-411, 1993.

[26] R. Okada, Y. Shirai, J. Miura and Y. Kuno, "Tracking a Person wiht 3-D Motion by Integrating Optical Flow and Depth," Trans. of IEICE, D-II, Vol. J82-D-II, No. 8, pp. 1252-1261, 1999.

[27] T. Hata, Y. Iwai and M. Yachida, "Robust Gesture Recognition by Using Image Motion and Data Compression," Trans. of IEICE, D-II, Vol. J81-D-II, No. 8, pp. 1727-1735, 1998.

[28] H. Tsujiai, "Dynamic Analysis fo Hands on a Keyboard Using Optical Flow," Trans. of IEICE, D-II, Vol. J81-D-II, No. 8, pp. 1796-1801, 1998.

[29] K. Mase, "Recognition of Facial Expression from Optical Flow," Trans. of IEICE, Vol. E74, No. 10, pp. 3474-3483, 1991.

[30] I. A. Essa and A. P. Pentland, "Facial Expression Recognition Using A Dynamic Model and Motion Energy," IEEE Proc. of 5th Int. Conf. on Computer Vision, pp. 360-367, 1995.

[31] I. A. Essa and A. P. Pentland, "Coding, Analysis, Interpertation, and Recognition of Facial Expressions," IEEE Trans. PAMI, Vol. 19, No. 7, pp. 757-763, 1997.

[32] M. J. Black and Y. Yacoob, "Recognizing Facial Expression in Image Sequences Using Local Parameterized Models of Image Motion," IEEE Trans. PAMI, Vol. 19, No. 7, pp. 757-763, 1997.

[33] N. Ohta and Y. Saito, "Accurate Shape Reconstruction by Optical Flow Re-Detection," Trans. of IEICE, D-II, Vol. J81-D-II, No. 5, pp. 1123-1131, 1998.

[34] N. Tagawa, T. Toriu, T. Endoh, T. Tanaka and T. Moriya, "Estimation of 3-D Shape and Motion from Optical Flow Based on Depth Model," Trans. of IEICE, D-II, Vol. J81-D-II, No. 8, pp. 1727-1735, 1998.

[35] K. Kanatani, N. Ohta and Y. Shimizu, "3-D Reconstruction from Uncalibrated-Camera Optical Flow and Its Reliability Evaluation," Trans. of IEICE, D-II, Vol. J84-D-II, No. 8, pp. 1665-1662, 2001.

[36] C. Tomasi and T. Kandade, "Shape and Motion from Image Streams under Orthography," IJCV, Vol. 9, No. 2, pp.137-154, 1992.

[37] C. J. Poelman and T. Kandade, "A Paraperspective Factorization Method for Shape and Motion Recovery," IEEE Trans. PAMI , Vol. 13, No. 3, pp.206-218, 1997.

[38] T. Kurata, J. Fujiki, M. Kourogi, K. Sakaue, "A Fast and Robust Approach Recovering Structure and Motion from Live Image Sequences," Trans. of IEICE, D-II, Vol. 84-D-II, No. 12, pp. 2515-2524, 2001.

[39] K. Hata, T. Aoki and M. Etou, "Estimation fo Structure and Motion Parameters for a Roaming Robot that Scans the Space," Trans of IEICE, D-II, Vol. 84-D-II, No. 3, pp.448-458, 2001.

[40] P. V. C. Hough, "Method and means for recognizing complex patterns," U. S. Patent No. 3069654, 1962.

[41] R.O. Duda and P. E. Hart, "Use of the Hough transformation to detect lines and curves in pictures," Comm. ACM, Vol. 15, No. 1, pp. 11-15, 1972.

[42] D. H. Ballard, "Generalizing the Hough transform to detect arbitary shapes," PR, Vol. 13 No. 2, pp. 111-122, 1981.

[43] Y. Lamdan and H. J. Wolfson, "Geometric hashing: a general and effecient medel-based recognition scheme," Proc. of ICCV, pp. 238-249, 1988.

[44] R. R. Schultz and R. L. Stevenson, "Extraction of High-Resolution Frames from Video Sequences," Trans. of Image Processing, Vol. 5, No. 6, pp. 996-1011, 1996.

[45] M. Shimizu and M. Okutomi, "Precise Sub-Pixel Estimation on Area-Based Matching," Trans. of IEICE, D-II, Vol. J84-D-II, No. 7, pp. 1409-1418, 2001.

[46] J. L. Barron, D. J. Fleet and S. S. Beauchemin, "Performance of Optical Flow," Int. Jour. of Computer Vision, Vol. 12, No. 1, pp. 185-203, 1994.

[47] S. S. Beauchemin, J. L. Barron, "The Computation of Optical Flow," ACM Computing Surveys, Vol. 27, No. 3, pp. 433-466, 1995.

[48] M. Chiba, S. Ozawa, "Detection of Optical Flow by Mode of Intersections of Constraint Equations," The Jour. of the Ins. of Tele. Eng. of Japan, Vol.45, No.10, pp.1199-1206, 1991.

[49] B. G. Schunck, "Image Flow Segmentation and Estimation by Constraint Line Clustering," IEEE Trans. of PAMI, Vol. 11, No. 10, pp. 1010-1027, 1989.

[50] M. Shizawa, K. Mase, "Multiple Optical Flow - Fundamental Constraint Equations and a Unified Computational Theory for Detecting Motion Transparency and Motion Boundaries," Trans. of IEICE, Vol.J76-D-II, No.5, pp.989-1005, 1993.

[51] A. Nomura, H. Miike and K. Koga, "Detection of Velocity Fileld from Sequantal Image under Temporally Variable Illumination," Trans. of IEICE, Vol.J76-D-II, No.9, pp.1977-1986, 1993

[52] N. Cornelius and T. Kanade, "Adapting Optical-Flow to Measure Object Motion in Reflectance and X-ray Image Sequences," ACM SIGGRAPH/SIGART interdisciplinary Workshop on Motion: Representation and Perception, 1983

[53] N. Mukawa, "Motion Field Estimation Based on Shading Model," Trans. of IEICE, Vol.J74-D-II, No.8, pp.1004-1011, 1991

[54] S. Negahdaripour and C. Yu, "A Generalized Brightness Change Model for Computing Optical Flow," Proc. of ICCV, pp.2-11, 1993.

[55] B. Lecordier, J. C. Lecordier and M. Trinite, "Iterative sub-pixel algorithm for the cross-correlation PIV measurements," Proc. 3rd International Workshop on PIV, pp. 37-43, 1999.

[56] A. Fincham and G. Delerce, "Advanced optimization of correlation imageing velocimetry algorithms," Proc. 3rd International Workshop on PIV, pp. 37-43, 1999.

[57] R. J. Adran, "Dynamic Range of Velocity and Spatial Resolution of Particle Image Velocimetry," Measurement Science and Technology, Vol. 8, No. 12, pp. 1393-1398, 1997.

[58] H. Huang, "An Extension of Digital PIV-Processing to Double-Exposed Images,"Experiments in Fluids. Vol. 24, No. 4, pp. 364-372, 1998.

[59] L. Lourenco and A. Krothapalli, "On the Accuracy of Velocity and Vorticity Measurements with PIV," Experiments in Fluids, Vol. 18, No. 6, pp.421-428, 1995.

225

[60] R. D. Keane, R. J. Adrian and Y. Zhang, "Super-Resolution Particle Imaging Velocimetry," Measurement Science and Technology, 6(6), pp. 754-768, 1995.

[61] D. Bereziat, I. Herlin, "A Generalized Optical Flow Constraint and its Physical Interpretation," Proc. of CVPR, Vol.2, pp.487-492, 2000.

[62] T. Corpetti, E. Memin, P. Perez, "Estimationg Fluid Optical Flow," Proc. of CVPR, Vol.3, pp.1033-1036, 2000.

[63] Y. Nakajima, H. Inomata, H. Nogawa, Y. Sato, S. Tamura, K. Okazaki and S. Torii, "Fluid Flow Computation Based on Physical Model," Trans. of IEICE, D-II, Vol. J81-D-II, No. 4, pp.602-610, 1998.

[64] S. Umeyama, "Dsicontinuity Extraction in Regularization Using Robust Statistics," Proc. of IEICE, PRMU95-217, pp. 9-16, 1996.

[65] S. Umeyama, "Multiple Optical Flow Estimation Based on The Robust Regression," Proc. of IEICE, PRMU96-108, pp.33-40, 1996.

[66] H. Imamura, Y. Kenmochi and K. Kotani, "Estimation of Optical Flow via Voting Process with Weight Function," Proc. of 2000 IEEE International Conference on System, Man, and Cybernetics, pp.1478-1483.

[67] J. D. Foley, A. van Dam, S. K. Feiner and J. F. Hughes, "Computer Graphics : Principle and Practice second edition", Addison-Wesley Publishing Company, Inc., 1990

Publications

[1] H. Imamura, Y. Kenmochi, K. Kotani, "Estimation of Optical Flow for Occlusion Using Extrapolation," Trans. of IEICE, D-II, Vol. J84-D-II, No. 8, pp. 1636-1644, 2001.

[2] H. Imamura, Y. Kenmochi, K. Kotani, "Estimation of Optical Flow for Brightness Change Using a Three-Dimensional Voting Space," Trans. of IEICE, D-II, Vol. J85-D-II, No. 1, pp. 12-22, 2002.

[3] H. Imamura, K. Kotani, "An Estimation Method of Optical Flow via Voting Process with a Weighting Function Using a Coefficients Determined Incompressible Viscous Fluid Optical Flow Constraint Equation," Trans. of IEICE, D-II (Submitted).

[4] H. Imamura, Y. Kenmochi, K. Kotani, "Estimation of Optical Flow for Occlusion Using Extrapolation," Proc. of IEEE International Conference on Image Processing, pp. 828-831, 2000.

[5] H. Imamura, Y. Kenmochi, K. Kotani, "Estimation of Optical Flow via Voting Process with Weight Function," Proc. of IEEE International Conference on System, Man, and Cybernetics, pp. 1478-1483, 2000.

[6] H. Imamura, Y. Kenmochi, K. Kotani, "Estimation of Optical Flow in a Three-Dimensional Voting Space for Brihtness Change," Proc. of International Conference on SPIE, Intelligent Robots and Computer Vision XIX: Algorithms, Techniques, and Active Vision, pp. 328-339, 2000.

[7] H. Imamura, Y. Kenmochi, K. Kotani, "Estimation of Optical Flow in Occluded and Appearance Region Using Flow Extrapolation," Proc. of IEICE, CS98-123, pp. 65-72, 1998.

[8] H. Imamura, Y. Kenmochi, K. Kotani, "Estimation of Optical Flow by 3-Dimensional Voting Process Considering Brightness-Change Situations," Proc. of IEICE, PRMU99-60, pp. 81-88, 1999.

[9] H. Imamura, Y. Kenmochi, K. Kotani, "Estimation of Optical Flow in Occluded Regions Using by Extrapolation," IMPS99, pp. 65-66, 1999.

[10] H. Imamura, Y. Kenmochi, K. Kotani, "Estimation of Optical Flow by Voting Using Weight Function," Proc. of IEICE, PRMU2000-18, pp. 47-54, 2000.

[11] H. Imamura, K. Kotani, "An Estimation Method of Optical Flow via Voting Process with a Weighting Function Using a Coefficients Determined Incompressible Viscous

Fluid Optical Flow Constraint Equation," JAIST Research Report, ISSN 0918-7553, IS-RR-2002-014, 2002.

[12] H. Imamura, K. Kotani, "A Statistical Method of Eye Action Classification aimed to Facial Components Analysis System," JAIST Research Report, IS-RR-2002-015, 2002.

[13] S. Hayashi, H. Imamura, Y. Kenmochi, K. Kotani, "Optical Flow estimation by Clustering of Intersections of Constraint Lines in a Velocity Space," Proc. of IEICE, CS2000-118, pp. 49-54, 2000.